Acetohydroxyacid synthase and its role in the biosynthetic pathway for branched-chain amino acids

Article *in* Amino Acids · October 2006

DOI: 10.1007/s00726-005-0297-3 · Source: PubMed

2 authors, including:

Ronald G Duggleby
The University of Queensland
199 PUBLICATIONS **8,346** CITATIONS

SEE PROFILE

Amino Acids (2006) 31: 173–210
DOI 10.1007/s00726-005-0297-3

Amino Acids
Printed in Austria

Acetohydroxyacid synthase and its role in the biosynthetic pathway for branched-chain amino acids

Review Article

J. A. McCourt and **R. G. Duggleby**

School of Molecular and Microbial Sciences, University of Queensland, Brisbane, Australia

Received December 1, 2005
Accepted December 9, 2005
Published online May 15, 2006;

Summary. The branched-chain amino acids are synthesized by plants, fungi and microorganisms, but not by animals. Therefore, the enzymes of this pathway are potential target sites for the development of antifungal agents, antimicrobials and herbicides. Most research has focused upon the first enzyme in this biosynthetic pathway, acetohydroxyacid synthase (AHAS) largely because it is the target site for many commercial herbicides. In this review we provide a brief overview of the important properties of each enzyme within the pathway and a detailed summary of the most recent AHAS research, against the perspective of work that has been carried out over the past 50 years.

Keywords: Acetohydroxyacid synthase – Acetolactate synthase – Branched-chain amino acids – Thiamin diphosphate – Flavin adenine dinucleotide – Herbicide – Inhibitor – Mechanism – Protein structure

Abbreviations: 2-IPMS, 2-isopropylmalate synthase; 2-KB, 2-ketobutyrate; 3-IPMD, 3-isopropylmalate dehydratase; 3-IPMDH, 3-isopropylmalate dehydrogenase; 3-IPMI, 3-isopropylmalate isomerase; Ac-ThDP, acetyl-ThDP; ADP, adenosine diphosphate; AHAS, acetohydroxyacid synthase; AHB, 2-aceto-2-hydroxybutyrate; AL, 2-acetolactate; ALS, acetolactate synthase; AMP, adenosine monophosphate; ATP, adenosine triphosphate; BCAA, branched-chain amino acid; BCAT, branched-chain aminotransferase; CE, chlorimuron ethyl; CoA, coenzyme A; CS, chlorsulfuron; CSU, catalytic subunit; DHAD, dihydroxyacid dehydratase; EDTA, ethylenediaminetetraacetic acid; FAD, flavin adenine dinucleotide; $FADH_2$, reduced FAD; HE-ThDP, hydroxyethyl-ThDP (carbanion); Hoe 704, 2-dimethylphosphinoyl-2-hydroxyacetic acid; IP, imazapyr; IpOHA, N-hydroxy-N-isopropyloxamate; IQ, imazaquin; IT, imazethapyr; KARI, ketol-acid reductoisomerase; L-ThDP, lactyl-ThDP; MM, metsulfuron methyl; $NAD(P)^+$, oxidized nicotinamide adenine dinucleotide (phosphate); NAD(P)H, reduced nicotinamide adenine dinucleotide (phosphate); *O*-IbOHA, *O*-isobutenyl oxalylhydroxamate; PAC, (*R*)-phenylacetyl carbinol; PDB, Protein Databank; PDC, pyruvate decarboxylase; POX, pyruvate oxidase; RSU, regulatory subunit; SM, sulfometuron methyl; TA, transaminase; TB, tribenuron methyl; TD, threonine deaminase; ThDP, thiamin diphosphate; TK, transketolase; TThDP, thiamin thiazolone diphosphate; U/mg, μmol product produced per minute per mg

1. Introduction to branched-chain amino acid synthesis

The branched-chain amino acids (BCAAs) are synthesized by plants, algae, fungi, bacteria and archaea, but not by animals. Therefore, the enzymes of the BCAA biosynthetic pathway (Fig. 1) are potential targets for the development of herbicides, fungicides, and antimicrobial compounds. Indeed, some of the most popular herbicides used worldwide over the past 20 years act by inhibiting the first common enzyme in the BCAA biosynthetic pathway, acetohydroxyacid synthase (AHAS, EC 2.2.1.6; formerly known as acetolactate synthase, ALS). Other enzymes that could potentially serve as excellent targets for the development of inhibitory compounds are threonine deaminase (TD, EC 4.3.1.19), ketol-acid reductoisomerase (KARI, EC 1.1.1.86) and dihydroxyacid dehydratase (DHAD, EC 4.2.1.9) because they are all unique to this pathway, are required for the synthesis of all three BCAAs and inhibition of their action would be detrimental to the organism.

Amongst these enzymes AHAS and KARI have attracted the most attention over the past ten years. KARI was reviewed fairly recently (Dumas et al., 2001) and here we will summarize briefly the main advances that have occurred since then. However, our main aim is to summarize the most recent AHAS research, with special emphasis on studies that have not been covered in detail in other reviews of this enzyme (Chipman et al., 1998; Duggleby and Pang, 2000; Chipman et al., 2005). To set

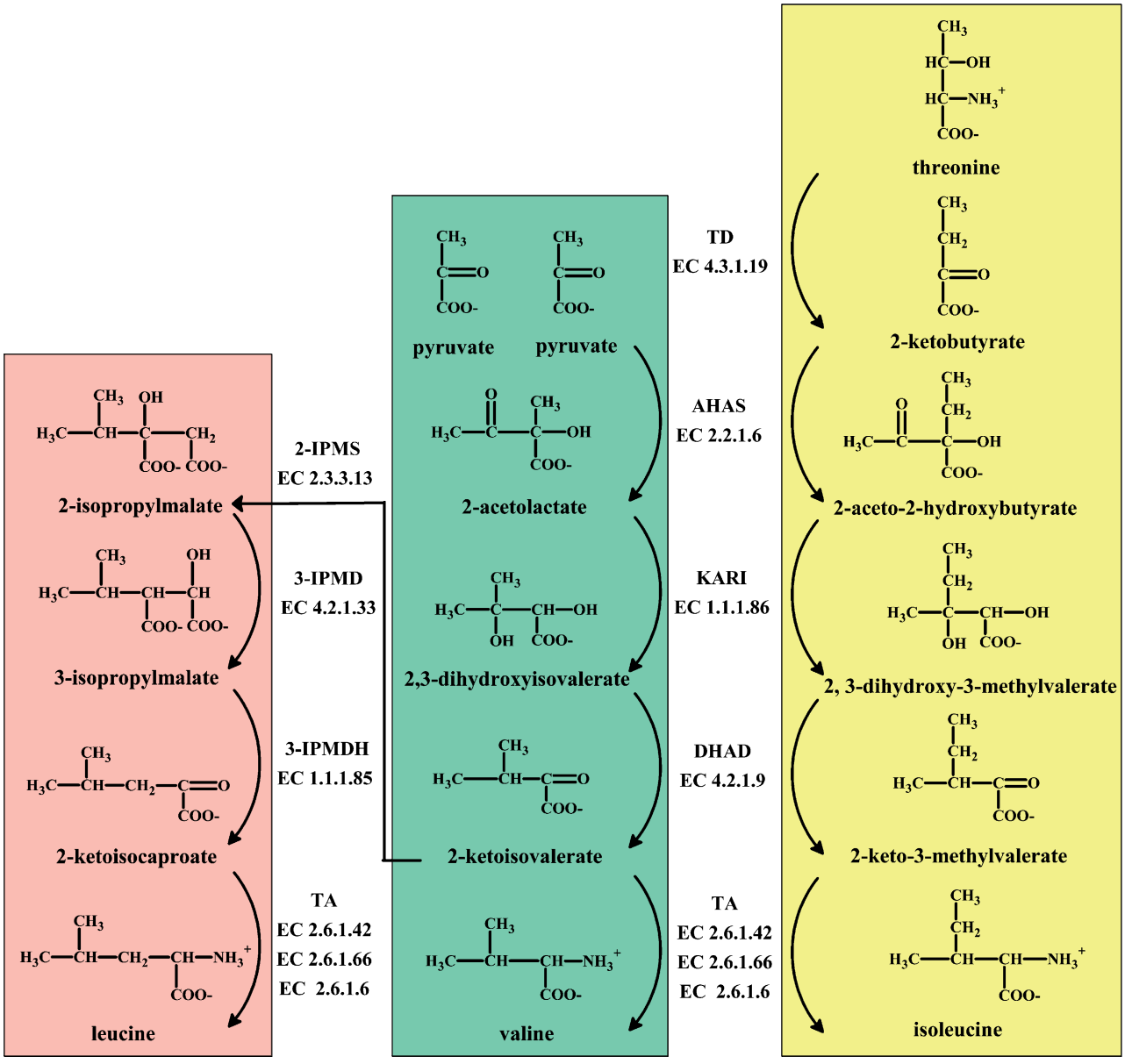

Fig. 1. The branched-chain amino acid biosynthesis pathway. TD, Threonine deaminase; AHAS, acetohydroxyacid synthase; KARI, ketol-acid reductoisomerase; DHAD, dihydroxyacid dehydratase; TA, transaminase; 2-IPMS, 2-isopropylmalate synthase; 3-IPMD, 3-isopropylmalate dehydratase; 3-IPMDH, 3-isopropylmalate dehydrogenase

the scene, we shall provide an overview of the reactions catalyzed and important properties of each enzyme in the BCAA synthesis pathway. These reactions are tightly regulated at many levels within the cell. However, aside from the regulation of AHAS by feedback inhibition, the details of the many mechanisms employed by a variety of organisms will not be covered in this article. For more information on this topic we refer you to Umbarger (1996), Duggleby and Pang (2000), and Kohlhaw (2003).

1.1 Threonine deaminase

The first enzyme in the pathway, TD is encoded by *ilv*A in bacteria and is required only for the synthesis of isoleucine. The function of TD is to provide a supply of 2-ketobutyrate (2-KB) which, unlike the precursor pyruvate that is required for the synthesis of valine and leucine, is not a central metabolite. The enzyme utilizes the cofactor pyridoxal-5′-phosphate for the deamination of L-threonine (Fig. 2). The crystal structure of tetrameric

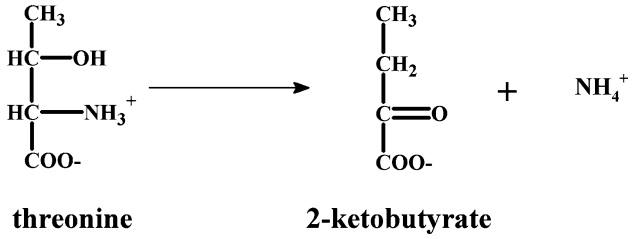

Fig. 2. Reaction catalysed by threonine deaminase

Escherichia coli TD has been determined to 2.8 Å in the absence of any effectors (Gallagher et al., 1998). The recombinant enzyme from *Arabidopsis thaliana* (mouse-ear cress) (Wessel et al., 2000), and native enzymes from *Candida maltosa* (Bode et al., 1986) and *Bacillus stearothermophilus* (Muramatsu and Nosoh 1976) have also been studied. *A. thaliana* TD exists as a tetramer composed of 59.6 kDa monomers (Halgand et al., 2002) with a specific activity and Michaelis constant for L-threonine at 25 °C of 400 μmol/min/mg (U/mg) and 7.65 mM, respectively (Wessel et al., 2000). Isoleucine causes its dissociation into dimers (Halgand et al., 2002) and inhibits the enzyme with a $K_{0.5}$ of 70 μM (Wessel et al., 2000). The inhibition by isoleucine can be reversed by the addition of valine which converts the enzyme back into tetramers (Halgand et al., 2002) and is presumed to induce a conformational change that disfavors isoleucine binding (Wessel et al., 2000).

1.2 Acetohydroxyacid synthase

Here we will give a brief introduction to AHAS before returning to consider it in greater detail in Section 2. AHAS, when present as a single isoform, is encoded by *ilv*BN in bacteria. It is the first common enzyme to the BCAA biosynthetic pathway and is capable of catalyzing the synthesis of either (2*S*)-acetolactate (AL) from two molecules of pyruvate or (2*S*)-2-aceto-2-hydroxybutyrate (AHB) from pyruvate and 2-KB (Fig. 3) (Umbarger and Brown, 1958; Radhakrishnan and Snell, 1960). The reaction, which is mediated by the cofactor thiamin diphosphate (ThDP, formerly known as thiamin pyrophosphate, TPP), involves the non-oxidative decarboxylation of pyruvate to yield CO_2 and the reactive resonating hydroxyethyl-ThDP (HE-THDP)/enamine-ThDP intermediate (Umbarger and Brown, 1958; Holzer et al., 1960; Tittmann et al., 2003). Condensation with the second 2-ketoacid gives rise to either of the two products. AHAS also requires a divalent metal such as Mg^{2+} (Umbarger and Brown, 1958), which serves to anchor ThDP to the enzyme, and a molecule of flavin adenine dinucleotide (FAD) that does not participate in the reaction (Størmer and Umbarger, 1964). AHASs contain two types of subunits, one for catalysis and another that mediates regulation of the enzyme via feedback inhibition by one or more of the BCAAs (Eoyang and Silverman, 1984; Weinstock et al., 1992). The catalytic subunit of *Saccharomyces cerevisiae* AHAS has been crystallized (Pang et al., 2001) and the structure solved in the absence of any inhibitors (Pang et al., 2002) and in the presence of sulfonylurea herbicides (Pang et al., 2003; McCourt et al., 2005). More recently, six crystal structures of *A. thaliana* AHAS in complex with five different sulfonylureas and one imidazolinone herbicide have been reported (McCourt et al., 2006). The active site of AHAS (Pang et al., 2002, 2003; McCourt et al., 2005, 2006), like almost all ThDP-dependent enzymes (Frank et al., 2004), is formed at the interface between two monomers and therefore the minimum quaternary structure for catalysis is a dimer. Although AHASs from plants and fungi are nuclear-encoded, a signal peptide directs the plant and fungal proteins to the chloroplast or mitochondria, respectively, where the transit peptide is then cleaved to yield the mature protein (Duggleby and Pang, 2000). Recombinant *A. thaliana* AHAS catalytic and regulatory subunits that are truncated to remove the N-terminal transit peptide, when expressed separately in *E. coli* and reconstituted, yield a tetramer of ~470 kDa with a specific activity of 14 U/mg (at 30 °C) and a Michaelis constant of 11.7 mM for pyruvate (Pang and Duggleby, 1999; Lee and Duggleby, 2001).

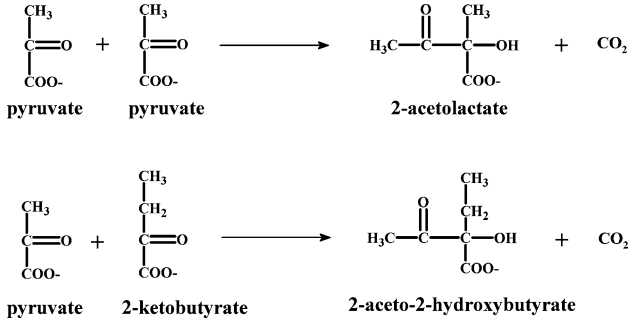

Fig. 3. Reactions catalysed by acetohydroxyacid synthase

1.3 Ketol-acid reductoisomerase

KARI, encoded by *ilv*C in bacteria, catalyses the conversion (Fig. 4) of either a molecule of AL to (2*R*)-2,3-dihydroxy-3-isovalerate leading to valine and leucine synthesis, or AHB to (2*R*,3*R*)-2,3-dihydroxy-3-methylvalerate, the precursor of isoleucine (Dumas et al., 2001). The reaction consists of two dissimilar steps involving

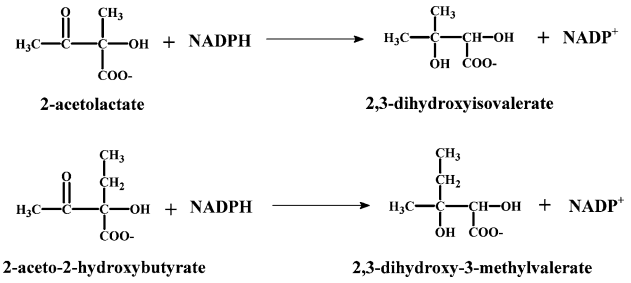

Fig. 4. Reactions catalysed by ketol-acid reductoisomerase

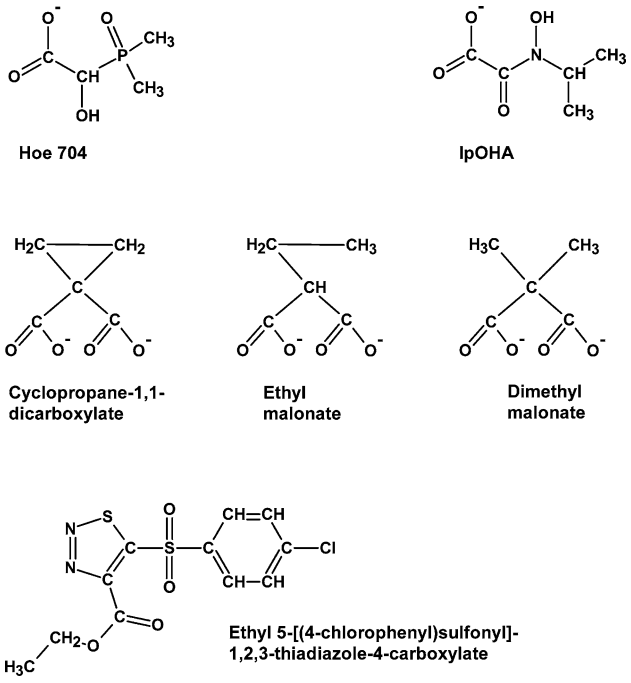

Fig. 5. Inhibitors of ketol-acid reductoisomerase

an alkyl migration (isomerization), which requires absolutely the presence of Mg^{2+}, followed by divalent metal ion dependent (Mg^{2+}, Mn^{2+}, or Co^{2+}) reduction of the proposed 2-ketoacid intermediate, with NADPH as the preferred electron donor (Dumas et al., 2001). KARI will also catalyze the reduction of several 2-ketoacids without the necessity of a prior isomerization (Tyagi et al., 2005b). Most studies of KARI have been performed on the enterobacterial and the *Spinacia oleracea* (spinach) enzymes, although purification of the enzyme from *Pseudomonas aeruginosa* (Eom et al., 2002), *Neurospora crassa* (Kiritani et al., 1966), *Hordeum vulgare* (barley) (Durner et al., 1993), *Triticum aestivum* (wheat) (Donadini and Copeland, 2000) and *Oryza sativa* (rice) (Lee et al., 2005) have been reported. Like AHAS, the eukaryotic enzyme has an N-terminal targeting peptide that directs it to the chloroplast in plants or mitochondria in fungi. After maturation of KARI by removal of this peptide, it has a subunit molecular weight of approximately 37 kDa for the fungal enzyme or 55 kDa for plant KARI. Enterobacterial KARI is similar in size to the plant enzyme while most other bacteria contain the smaller form.

Although specific activities and Michaelis constants for the substrates have been reported, meaningful comparison of the enzyme from different sources is difficult due to different reaction conditions and the strong pH dependence of these properties (Mrachko et al., 1992). In general, the enzyme shows as high or higher activity with AHB than with AL, K_m values for these substrates in the range 10^{-5} to 10^{-3} M, and K_m values for NADPH in the range 10^{-6} to 10^{-5} M. The K_m value for Mg^{2+} is much higher for *E. coli* KARI than it is for the *S. oleracea* enzyme, which is surprising since the active site geometry is very similar in the two proteins (see below). The enzyme is inhibited by products and substrate analogs and, in some bacteria, by BCAAs (Leyval et al., 2003). However, most attention has focused on potentially herbicidal compounds (Fig. 5) such as Hoe 704 (2-dimethylphosphinoyl-2-hydroxyacetic acid) (Schulz et al., 1988) and IpOHA (N-hydroxy-N-isopropyloxamate) (Aulabaugh and Schloss, 1990). These compounds are powerful inhibitors of the plant and bacterial enzymes but are not effective as herbicides. Cyclopropane-1,1-dicarboxylate and related compounds (Fig. 5) inhibit plant KARI in vitro (Lee et al., 2005) and in vivo (Gerwick et al., 1993) but do not appear to have been tested as herbicides. Similarly, the potent inhibition of plant KARI by thiadiazoles (Halgand et al., 1998) has not led to the development of effective herbicides.

The crystal structures of *S. oleracea* KARI in the presence of IpOHA (Biou et al., 1997) and with a reaction product (Thomazeau et al., 2000), as well as *P. aeruginosa* KARI (Ahn et al., 2003) and *E. coli* KARI (Tyagi et al., 2005a) in the absence of any effectors, have been determined. The *S. oleracea* enzyme is composed of an N-terminal domain of mixed α- and β-structure that resembles those found in other pyridine nucleotide dependent oxidoreductases, and an α-helical C-terminal domain with a previously unknown topology. The *E. coli* enzyme has a similar structure, and shows clear evidence that the C-terminal domain has been derived by duplication of 120–140 residues (Tyagi et al., 2005a). This agrees with the earlier work by Taylor (2000) who showed that the C-terminal domain of *S. oleracea* KARI contains a knot, and suggested that this unusual structure evolved by exchange of helices between the duplicated segments. Further confirmation of this duplication came from the

structure of the smaller *P. aeruginosa* KARI, which lacks the duplicated segment. The N-terminal domain is similar to that of the spinach enzyme but the C-terminal domain overlays with only half of the spinach KARI C-terminal domain. The other half is supplied by a second *P. aeruginosa* KARI monomer. Despite these different structural arrangements, the positions of eight active site residues are very similar across all three enzyme structures.

Mutagenesis of these eight active site residues (Tyagi et al., 2005b) in *E. coli* KARI has shown that several can be changed with little effect on the reductase, but any mutation that prevents the reductase also eliminates the isomerization reaction. This has been interpreted to mean that the isomerization is coupled to the reduction, without passing through a discrete 2-ketoacid intermediate. Measurement of the equilibrium constant for the isomerase shows that it heavily favors the initial substrate. Direct reduction of the isomerase transition state overcomes this unfavorable equilibrium and explains why these two very different activities must reside in a common active site.

1.4 Dihydroxyacid dehydratase

The dihydroxyacids produced by KARI are converted to 2-ketoacids (Fig. 6) by the action of DHAD, a product of the *ilv*D gene in bacteria. Dehydration of the vicinal diols, (2*R*)-2,3-dihydroxyisovalerate and (2*R*, 3*R*)-2,3-dihydroxy-3-methylvalerate to 2-ketoisovalerate and (3*S*)-2-keto-3-methylvalerate, respectively, occurs via an enol intermediate (Arfin, 1969; Hill et al., 1973) mediated by an iron-sulfur cluster (Flint and Emptage, 1988). The enzyme has been purified from *S. oleracea* (Flint and Emptage, 1988), *N. crassa* (Altmiller and Wagner, 1970), *E. coli* (Flint et al., 1993a) and *Methanococcus* sp. (Xing and Whitman, 1991). Very little is known about the exact mechanism of DHAD which involves a $[2Fe–2S]^{2+}$ cluster in *S. oleracea* DHAD (Flint and Emptage, 1988), but a $[4Fe–4S]^{2+}$ cluster in the *E. coli* enzyme (Flint et al., 1993a), rendering the *E. coli* enzyme oxygen sensitive (Flint et al., 1993a, b). It has been proposed that the reaction mechanism is similar to that of aconitase where the 3-hydroxyl group of the substrate binds one of the iron atoms, becoming activated for elimination (Flint et al., 1993a). DHAD from *S. oleracea* is a dimer of ~110 kDa with a specific activity of 486 U/mg and a K_m for racemic 2,3-dihydroxy-3-methylvalerate of 1.5 mM (Flint and Emptage, 1988). Valine and leucine, but not isoleucine, are very weak inhibitors of *Corynebacterium glutamicum* DHAD with IC_{50} values of 170 mM and 120 mM, respectively (Leyval et al., 2003).

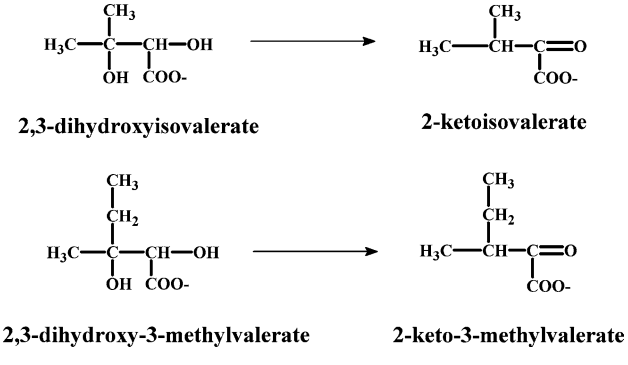

Fig. 6. Reactions catalysed by dihydroxyacid dehydratase

1.5 Transaminase

The final step for the synthesis of each of the three BCAAs is catalyzed by a transaminase (TA). Although several different transaminases may be capable of catalyzing the last reaction in the pathway, transaminase B, encoded by *ilv*E in bacteria (EC 2.6.1.42; also known as the branched-chain amino acid transaminase, BCAT) probably plays the major role in the cell. The reaction (Fig. 7) is mediated by pyridoxal-5′-phosphate and occurs in two steps. Upon binding to BCAT, glutamate donates an amino group via an aldimine-ketimine shift to give the pyridoxamine 5′-phosphate intermediate and the 2-ketoglutarate product. In the second step, pyridoxamine 5′-phosphate transfers its amino group to one of the two 2-ketoacid products of DHAD, or 2-ketoisocaproate from 3-isopropylmalate dehydrogenase (3-IPMDH), yielding the appropriate amino acid. Transaminases are widely distributed in nature and, unlike the other enzymes of BCAA biosynthesis, are found in animals where they participate in BCAA catabolism. Although the *Methanococcus aeolicus* enzyme has been purified and characterized (Xing and Whitman, 1992), there has been very little work reported on plant and fungal BCAT. The crystal structures of *Homo sapiens* BCAT in complex with pyridoxal-5′-phosphate (Yennawar et al., 2001) and with either the isoleucine ketimine or pyridoxamine 5′-phosphate (Yennawar et al., 2002), and *E. coli* BCAT in complex with pyridoxal-5′-phosphate (Okada et al., 1997) and either 4-methylvalerate or 2-methylleucine (Okada et al., 2001), glutamate or glutarate (Goto et al., 2003) have been solved. Interest in *H. sapiens* BCAT is largely centered upon the development of drugs to treat neurological disorders. One such drug, gabapentin (1-(aminomethyl)-cyclohexaneacetic acid), is currently used for the treatment of several neurological disorders including epilepsy (Andrews and Fischer, 1994).

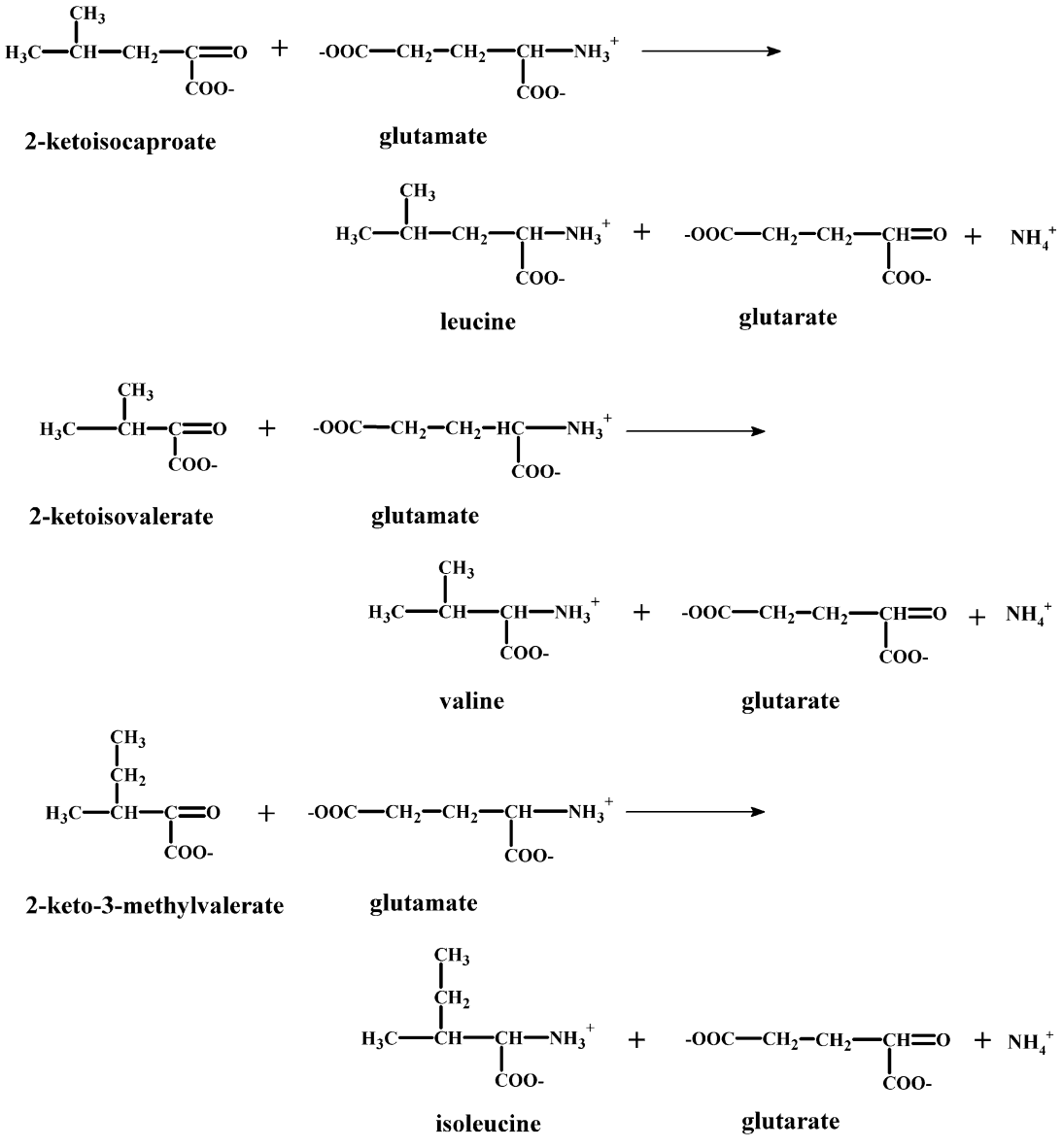

Fig. 7. Reactions catalysed by transaminases in the BCAA pathway

The first crystal structures of the oxidized and reduced states of cytosolic BCAT in complex with gabapentin were reported recently (Goto et al., 2005). The *E. coli* enzyme is a trimer of dimers (Goto et al., 2003) with specific activities in the presence of both 2-ketoglutarate and valine, isoleucine or leucine of 20.3, 30.5, and 27.7 U/mg and Michaelis constants of 3.13, 0.58, and 0.52 mM for these three amino acids, respectively (Lee-Peng et al., 1979).

1.6 2-Isopropylmalate synthase

The first enzyme in the pathway exclusively for leucine synthesis is 2-isopropylmalate synthase (2-IPMS, EC 2.3.3.13), encoded by *Leu*A in bacteria, which transfers an acetyl group from acetyl-CoA to 2-ketoisovalerate via an aldol condensation reaction to give (2*S*)-2-isopropylmalate and CoA. The reaction (Fig. 8) is almost identical to the first reaction of the citric acid cycle, catalyzed by citrate synthase. 2-IPMS has been isolated and characterized from *S. oleracea* (Hagelstein and Schulz, 1993), *S. cerevisiae* (Kohlhaw, 1988b), *C. glutamicum* (Pátek et al., 1994), and *Mycobacterium tuberculosis* (Koon et al., 2004a; Koon et al., 2004b), but not from archaea. The crystal structure of *M. tuberculosis* 2-IPMS in complex with the cofactor Zn^{2+} and 2-ketoisovalerate has been solved to 2.0 Å (Koon et al., 2004b). The *M. tuberculosis*

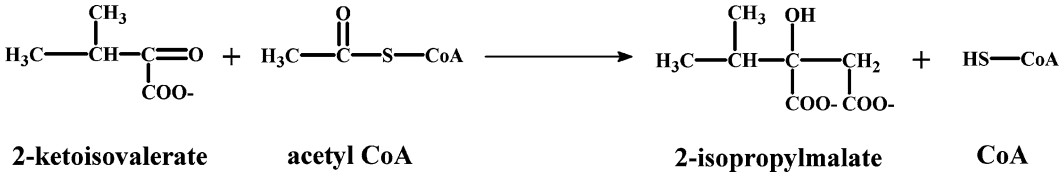

Fig. 8. Reaction catalysed by 2-isopropylmalate synthase

enzyme is a dimer of ~160 kDa with Michaelis constants of 25 μM (specific activity = 0.80 U/mg) for 2-ketoisovalerate and 240 μM (specific activity = 2.07 U/mg) for acetyl CoA (Chanchaem and Polittapongarnpim, 2002). Leucine acts as a slow, tight-binding inhibitor of the *M. tuberculosis* enzyme with an initial K_i of 17 μM and a final K_i^* of 3.6 μM (de Carvalho et al., 2005). Although there are currently no reports of any inhibitors that could potentially act as drugs or herbicides, the structure of the *M. tuberculosis* enzyme is expected to aid in the design of anti-tuberculosis agents (Koon et al., 2004b).

1.7 3-Isopropylmalate dehydratase

3-Isopropylmalate dehydratase (3-IPMD) (EC 4.2.1.33; also known as 3-isopropylmalate isomerase, 3-IPMI) catalyses the second reaction of the leucine synthesis pathway involving a hydroxyl transfer between adjacent carbon atoms of (2*S*)-2-isopropylmalate and (3*R*, 3*S*)-3-isopropylmalate (Fig. 9). The reaction is similar to that catalyzed by aconitase, involving a dehydration/rehydration via $[4Fe–4S]^{2+}$ cluster chemistry (Hawkes et al., 1993). The enzyme from *Salmonella typhimurium* is composed of two different subunits (~51 kDa and ~23.5 kDa) expressed from *Leu*CD in bacteria (Fultz and Kemper, 1981). Owing to its inherent instability (Gross et al., 1963; Burns et al., 1966; Satyanarayana et al., 1968; Bigelis and Umbarger, 1976; Fultz and Kemper, 1981; Kohlhaw, 1988a), very few studies have been performed on this enzyme, although the crystal structure, to 1.98 Å, of the *Pyrococcus horikosii* small subunit was reported recently (Yasutake et al., 2004). The purification of plant 3-IPMD has never been reported and most studies have been performed on the fungal enzyme (Gross et al., 1963; Satyanarayana et al., 1968; Gross, 1970; Bigelis and Umbarger, 1976; Kohlhaw, 1988a; Bode and Birnbaum, 1991) which, unlike those from bacteria (Fultz and Kemper, 1981) and archaea (Yasutake et al., 2004) is believed to consist of one subunit only (Bigelis and Umbarger, 1976; Kohlhaw, 1988a). The *S. cerevisiae* enzyme has a molecular mass of ~90 kDa, with a specific activity of 6.18 U/mg (at 30 °C), and a K_m for dimethylcitraconate of 216 μM (under low salt conditions) (Kohlhaw, 1988a). Although not available commercially, the compound 1-hydroxy-2-nitrocyclopentane-1-carboxylic acid is an inhibitor of 3-IPMD ($\sim K_i^{app} = 2$ nM) with herbicidal activity (Hawkes et al., 1993).

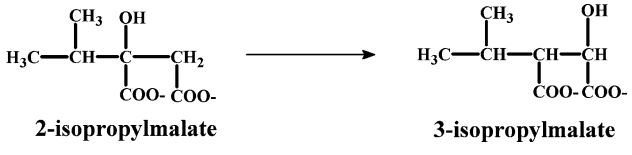

Fig. 9. Reaction catalysed by 3-isopropylmalate dehydratase

1.8 3-Isopropylmalate dehydrogenase

The third step in leucine biosynthesis is catalyzed by 3-isopropylmalate dehydrogenase (3-IPMDH; EC 1.1.1.85) and in bacteria it is encoded by *Leu*B. It is a bifunctional metal-dependent, decarboxylating dehydrogenase (Singh et al., 2005) like isocitrate dehydrogenase, the third enzyme of the citric acid cycle. The reaction (Fig. 10) is dependent upon oxidized nicotinamide adenine dinucleotide (NAD^+) and a divalent metal such as Mn^{2+} or Cd^{2+} (Hsu and Kohlhaw, 1980) and involves oxidative decarboxylation of (2*R*,3*S*)-3-isopropylmalate to (2*S*)-2-ketoisocaproate, also forming reduced nicotinamide adenine dinucleotide (NADH) and CO_2. 3-IPMDH has been purified and characterized from *Pisum sativum L.* (pea) (Wittenbach et al., 1994), *S. cerevisiae* (Hsu and Kohlhaw,

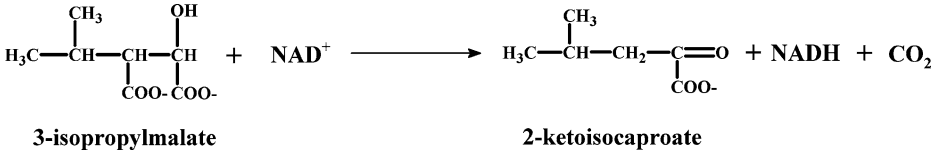

Fig. 10. Reaction catalysed by 3-isopropylmalate dehydrogenase

1980), *E. coli* (Wallon et al., 1997b), and *Thermus thermophilus* (Hayashi-Iwasaki and Oshima, 2000). *S. cerevisiae* 3-IPMDH exists in equilibrium as both monomers (~45 kDa) and dimers, has a K_m for 3-isopropylmalate of 23–42 μM, a K_m for NAD^+ of 54–150 μM, and a specific activity of 19.3 U/mg (Hsu and Kohlhaw, 1980). The crystal structures of 3-IPMDH from *M. tuberculosis* (Singh et al., 2005), *Bacillus coagulans* (Tsuchiya et al., 1997), *T. thermophilus* (Imada et al., 1991) *S. typhimurium* and *E. coli* (Wallon et al., 1997a) in the absence of effectors, from *T. thermophilus* in the presence of NAD^+ (Hurley and Dean, 1994) and of 3-IPMDH from *Thiobacillus ferrooxidans* (Imada et al., 1998) in the presence of 3-isopropylmalate have been determined. The compound *O*-isobutenyl oxalylhydroxamate (*O*-IbOHA), an IPMDH reaction intermediate analog, has been shown to inhibit *P. sativum* IPMDH with a K_i^{app} of 5 nM by competing with 3-isopropylmalate for the active site (Wittenbach et al., 1994). Application of *O*-IbOHA at rates of 110, 560, 940, and >4000 g/ha for *Zea mays* (maize), *Setaria faberi* (giant foxtail), *Ipomoea purpurea* (morning glory) and *Glycine max* (soybean), respectively, inhibits growth of the plants by 50% (Wittenbach et al., 1994). However, due to the short-term reversibility of inhibition, it is not expected that the compound would prove to be an effective herbicide.

2. AHAS

It has been almost 50 years since the discovery of AHAS and its role in BCAA biosynthesis (Umbarger and Brown, 1958). Since that time there has been a keen interest in AHAS. In particular, the enzyme's dependence upon a flavin cofactor in the absence of redox activity and the details of the ThDP-mediated reaction, the requirement for a regulatory subunit, and inhibition of AHAS by the sulfonylurea and imidazolinone herbicides have been topics of interest over the years. Here we review the purification, properties, and structure of AHAS, discuss what is known about the reactions catalyzed, and summarize the numerous studies concerning the regulation of AHAS activity by BCAAs. Finally, we take a look at the various inhibitors of AHAS, with an emphasis on the sulfonylyurea and imidazolinone herbicides.

2.1 Purification and characterization of AHAS

2.1.1 Bacterial AHAS

Bacterial AHAS has been characterized either in cellular extracts or as purified protein from both native and recombinant sources. The enzyme has been studied in several different organisms including *P. aeruginosa* (Arfin and Koziell, 1973a; catalytic and regulatory subunits of ~60 and ~15 kDa, Arfin and Koziell, 1973b), *E. coli* (isozyme I, 60.3 and 11.0 kDa; isozyme II, 59.0 and 9.5 kDa; isozyme III, 62.8 and 17.9 kDa; Grimminger and Umbarger, 1979; Barak et al., 1988; Hill et al., 1997), *S. typhimurium* (isozyme II, 59.4 and 9.4 kDa; Schloss et al., 1985), *Lactococcus lactis* (59.0 and 17.6 kDa; Snoep et al., 1992), *Serratia marcenscens* (~62 and ~35 kDa; Yang and Kim, 1993), *Leuconostoc lactis* (Carroll et al., 1995), *Leuconostoc mesenteroides* (~55 kDa; Phalip et al., 1995), *Streptomyces cinnamonensis* (65.5 and 19.0 kDa; Kopecký et al., 1999), *Mycobacterium avium* (65.9 and 18.1 kDa; Zohar et al., 2003), *C. glutamicum* (66.7 and 18.6 kDa; Leyval et al., 2003), *B. stearothermophilus* (62.3 and 18.6 kDa; Porat et al., 2004) and *M. tuberculosis* (65.9 and 18.1 kDa; Choi et al., 2005). However, the enterobacterial isozymes have drawn the most interest.

Størmer and Umbarger (1964) were the first to isolate AHAS from *S. typhimurium*. Eventually the three isozymes AHASI, AHASII, and AHASIII (encoded by *ilv*BN, *ilv*GM and *ilv*IH, respectively) were identified in enterobacteria (Guardiola et al., 1974; Grimminger and Umbarger, 1979). Grimminger and Umbarger (1979) first reported the purification of *E. coli* AHASI, however, at the time they did not realize the enzyme consists of two different polypeptides. Subsequently, both the catalytic and regulatory subunits of bacterial AHASI (Eoyang and Silverman, 1984), AHASII (Schloss et al., 1985) and AHASIII (Barak et al., 1988) were purified and characterized. The isozymes differ from one another in terms of their kinetic properties, substrate specificity, sensitivity to

Table 1. Properties of *E. coli* AHAS isozymes

Property[a]	AHASI	AHASII	AHASIII
SA (U/mg)	40[b]	52.7[c]	30[d]
K_m (mM)	1.5[e]	2.6[c]	11.5[f]
K_c ThDP (μM)	1.2[b]	1.1[c]	18[f]
K_c Mg^{2+} (μM)	60[b]	3.8[c]	3300[f]
K_c FAD (μM)	0.3[b]	0.2[c]	2.2[f]
K_i^{app} valine (μM)	100[b]	NI	12.7[f]
Regulatory subunit (kDa)	11.1[g]	9.5[h]	17.5[i]
Specificity ratio (*R*)	1[j]	185[j]	53[f]

[a] SA, specific activity. K_m, Michaelis constant for pyruvate. K_c, half-saturating concentrations of cofactors required for activation. K_i^{app}, concentration of valine required for 50% inhibition. [b] Grimminger and Umbarger (1979). [c] Hill and Duggleby (1998). [d] Weinstock et al. (1992). [e] Eoyang and Silverman (1988). [f] Vyazmensky et al. (1996). [g] Wek et al. (1985). [h] Lawther et al. (1987). [i] Squires et al. (1983). [j] Barak et al. (1987). NI, not inhibited

end-product inhibition, and the size of the regulatory subunit. Some of the properties of the *E. coli* isozymes are illustrated in Table 1.

Multiple AHAS isozymes within the enterobacteria enable the organism to cope with variable environments. One advantage of these multiple isoforms is that they have differences in their substrate preferences. This can be quantified using the specificity ratio (R, Eq. 1) (Barak et al., 1987), which varies substantially between isozymes.

$$R = \frac{(\text{AHB formed}/[\text{2-KB}])}{(\text{AL formed}/[\text{pyruvate}])} \quad (1)$$

Under normal growth conditions the cellular concentration of pyruvate is much greater than that of 2-KB so that a high R value is required for the synthesis of all three BCAAs. Thus AHASI, which has little preference for either substrate ($R = 1$) (Barak et al., 1987), is the most useful isozyme to the cell under conditions where the concentration of pyruvate is low (Dailey and Cronan, 1986) because it is able to sustain valine and leucine synthesis. For AHASII and AHASIII the R values have been estimated to be 185 (Barak et al., 1987) and 53 (Vyazmensky et al., 1996), respectively, indicating that both enzymes play an important role in the synthesis of isoleucine. However, AHASII is unlike the other two isozymes in that it requires absolutely the presence of the regulatory subunit for catalysis (Hill et al., 1997) and is completely insensitive to feedback inhibition by any of the BCAAs (Lawther et al., 1987). This way, in the presence of excess valine which inhibits AHASIII but not AHASII, the latter prevents cell death due to isoleucine starvation.

The crystal structure of bacterial AHAS has not yet been reported, although a homology model (Ibdah et al., 1996) for the catalytic subunit of *E. coli* AHASII has been constructed from the *Lactobacillus plantarum* pyruvate oxidase (POX) crystal structure (Müller and Schulz, 1993; Müller et al., 1994), an enzyme that is believed to be closely related to AHAS (Chang and Cronan, 1988). It would be interesting to obtain crystal structures of the catalytic and regulatory subunits of each isozyme, so that we could better understand why the sizes of the regulatory subunits vary, how the two subunits interact, the mechanism of feedback regulation and why AHASII is insensitive to inhibition by the BCAAs.

2.1.2 Archaeal AHAS

AHAS has been purified from a methanogen (*M. aeolicus*, Xing and Whitman, 1994), and an extreme halophile (*Haloferax volcanii*, Vyazmensky et al., 2000). Kinetically, the archaeal and bacterial AHAS are similar, although the archaeal enzymes have some unique properties. For example, *M. aeolicus* AHAS (~58 kDa) is oxygen sensitive and is the only AHAS that does not require FAD absolutely for catalysis; it can be substituted with flavin mononucleotide or riboflavin plus phosphate (Xing and Whitman, 1994). *H. volcanii* is a native inhabitant of the Dead Sea and therefore it is not surprising that AHAS from this organism (~50 kDa) cannot tolerate conditions of low salt and requires concentrations of greater than 3.5 M KCl for maximal activity (Vyazmensky et al., 2000). The only Kingdom for which an AHAS regulatory subunit has not been identified is the archaea. Even though an AHAS regulatory subunit could not be detected in either *M. aeolicus* and *H. volcanii* AHAS preparations, the enzymes are sensitive to feedback inhibition by BCAAs (Xing and Whitman, 1994; Vyazmensky et al., 2000). However, since all other AHASs consist of both catalytic and regulatory subunits, and the identification of a putative regulatory subunit gene for *M. aeolicus* has been reported (Bowen et al., 1997), it seems likely that archaeal AHAS regulatory subunits will be discovered.

2.1.3 Fungal AHAS

Fungal AHAS was first isolated from *N. crassa* and characterized by Glatzer et al. in 1972. Owing to the lability of the enzyme from the native source, subsequent characterization of the enzyme has been carried out on recombinant *S. cerevisiae* AHAS expressed in *E. coli* (Poulsen and Stougaard, 1989; Pang and Duggleby, 1999, 2001). Both the catalytic (*ilv*2, 74.8 kDa) and regulatory (*ilv*6, 34.1 kDa) subunits are nuclear-encoded (Polaina, 1984; Pang and Duggleby, 1999), mitochondrial-directed (Cassady et al., 1972) proteins that associate to form a heterotetramer (Pang and Duggleby, 1999). Unlike bacteria, fungi are not known to contain any isozymes and have only one copy of the AHAS gene. Fungal AHAS is inhibited by valine, but the enzyme can be reactivated by the addition of MgATP (Pang and Duggleby, 1999, 2001). The catalytic subunit of *S. cerevisiae* has been crystallized (Pang et al., 2001) and the structure solved in both the presence (Pang et al., 2003; McCourt et al., 2005) and absence (Pang et al., 2002) of a sulfonylurea herbicide. Details of these structures will be discussed throughout Sections 2.2 and 2.5.2.

2.1.4 Plant AHAS

Plant AHAS is nuclear encoded and contains a chloroplast-directing signal peptide at the N-terminus. The exact cleavage site of the transit peptide has not been determined

experimentally; however, several researchers (Wiersma et al., 1990; Rutledge et al., 1991; Chang and Duggleby, 1997) agree that the cleavage site is within a region shortly after the first 70–85 amino acids, depending on the plant species of interest. In the past, research on plant AHAS has been hindered due to its instability and low abundance in plants. Nevertheless, AHAS has been characterized, to some extent, from cellular extracts of *Brassica napus* (oilseed rape) (Bekkaoui et al., 1993) and *S. oleracea* (Delfourne et al., 1994) or purified from *T. aestivum* (57–58 kDa, Southan and Copeland, 1996), *H. vulgare* (58 kDa, Durner and Böger, 1988), and Z. *mays* (55 kDa, Singh et al., 1988; Mazur et al., 1987), to name a few. *E. coli* expression vectors have enabled the purification and characterization of *Nicotiana tabacum* (tobacco) (65 kDa, Chang et al., 1997), *A. thaliana* (65.1 kDa, Singh et al., 1991; Chang and Duggleby, 1997; Lee and Duggleby, 2001), *O. sativa* (69.3 kDa, unpublished) and *Nicotiana plumbaginifolia* (black-leaf tobacco) (65.1 kDa, Hershey et al., 1999) AHAS. Earlier, a homology model was constructed for the *A. thaliana* AHAS catalytic subunit (Ott et al., 1996) and more recently, crystallization of the *A. thaliana* AHAS catalytic subunit with a sulfonylurea herbicide (Pang et al., 2004b), and its structure (McCourt et al., 2006) in the presence of five sulfonylurea herbicides and one imidazolinone herbicide, have been reported. These structures will be discussed throughout Section 2.2 and 2.5.1. The first plant regulatory subunits, expressed as recombinant proteins, were only purified and characterized relatively recently (*N. plumbaginifolia*, 50.0 kDa, Hershey et al., 1999; *A. thaliana*, 53.0 kDa, Lee and Duggleby, 2001) and will be discussed at greater length in Section 2.4.

2.1.5 AHAS from other organisms

AHAS is also found in cyanobacteria (Forlani et al., 1991; Milano et al., 1992), green algae (Funke et al., 1999; Landstein et al., 1990) and red algae (Reith and Munholland, 1993) although it is poorly characterized and its purification has never been reported. Red algal AHAS is not nuclear-encoded like other AHASs; instead the genes reside within plastid DNA (Reith and Munholland, 1993). *Spirulina platensis* (cyanobacterium) and *Chlorella emersonii* (green alga) AHAS have been partially characterized (Riccardi et al., 1988; Forlani et al., 1991; Landstein et al., 1990). Two isoforms of ~600 and ~550 kDa have been detected for *S. platensis* AHAS (Forlani et al., 1991), whereas only one isoform was detected in *C. emersonii* (Landstein et al., 1990). *C. emersonii* AHAS, which is expressed in a heterotrophic medium, has a K_m for pyruvate of 9.1 mM, a preference for 2-KB over pyruvate ($R = 26$) and is inhibited 50% by 0.3 mM valine (Landstein et al., 1990). There is no confirmed report of AHAS from any animal species. A putative human AHAS gene (Joutel et al., 1996) was investigated by expressing the protein (Duggleby et al., 2000) but no enzymatic activity was detected. It now seems likely that the encoded protein is a 2-hydroxyphytanoyl CoA lyase (Foulon et al., 1999).

2.2 Structure of AHAS

The first X-ray crystal structure of AHAS, reported by Pang et al. in 2002, was of the *S. cerevisiae* catalytic subunit in complex with ThDP, Mg^{2+}, and FAD. Since that time, crystallization of the *A. thaliana* and *S. cerevisiae* AHAS catalytic subunits in the presence of all three cofactors and each of five sulfonylurea herbicides, as well as one imidazolinone herbicide for the *A. thaliana* enzyme, has been achieved and the structures have been determined (Pang et al., 2003; McCourt et al., 2005, 2006). Of these twelve structures, the imidazolinone-bound *A. thaliana* catalytic subunit (PDB code 1Z8N) is believed to be the most representative structure of catalytically active AHAS because: (a) the active site is not open to solvent; and (b) the ThDP cofactor is intact. These

Table 2. Equivalent residues in AHAS from *A. thaliana*, *E. coli* (isozyme II), and *S. cerevisiae*

A. thaliana	*E. coli* (Isozyme II)	*S. cerevisiae*
Gly121	Gly25	Gly116
Ala122	Ala26	Ala117
Glu144	Glu47	Glu139
Val196	Val99	Val191
Pro197	Ser100	Pro192
Arg199	Pro102	Thr193
Met200	Phe103	Ala195
Ala205	Ala107	Ala200
Phe206	Phe109	Phe201
Gln207	Gln110	Gln202
Lys256	Lys159	Lys251
Met351	Met250	Met354
Asp376	Asp275	Asp379
Arg377	Arg276	Arg380
Met570	Met460	Met582
Val571	Val461	Val583
Trp574	Trp464	Trp586
Ser653	Pro536	Gly657
Gly654	Gly658	Gly537

The active site and herbicide binding sites are made up of residues from two AHAS monomers. *A. thaliana* AHAS residues 121–256 are from one monomer and 351–654 are from the other

structural features will be discussed shortly. Therefore, unless otherwise noted, *A. thaliana* AHAS numbering will be used throughout the remainder of this review. As a reference, important equivalent residues in AHAS from two other organisms are provided in Table 2. Structural details of the herbicide binding site will be reserved for discussion throughout Section 2.5.2.

The DNA encoding the putative N-terminal transit sequence was removed for each of the recombinant enzymes used for crystallization (Pang et al., 2001, 2003, 2004b). This sequence was partly replaced with one encoding a 47 amino acid N-terminal histidine-tag to aid in purification of the yeast enzyme; however there is no electron density observed for the tag. For all of the structures solved, observable electron density commences after approximately the first 84 amino acids of the precursor protein. In addition, there is little or no electron density in the free yeast AHAS structure (PDB code 1JSC) for 19 amino acids linking two domains, for the stretch of amino acids from 568 to 583, and for the last 40 residues.

S. cerevisiae AHAS crystallizes as a dimer (Pang et al., 2002, 2003; McCourt et al., 2005), whereas the *A. thaliana* enzyme crystallizes as a tetramer (Fig. 11) (McCourt et al., 2006). The overall structure of AHAS resembles that of other ThDP-dependent enzymes (Müller and Schulz, 1993; Hasson et al., 1998; Caines et al., 2004; Pang et al., 2004a) in that the active site is formed at the interface between two monomers, each (Fig. 12) of which is composed of three domains; α (85–269), β (281–458), and γ (463–639). There is also a structured C-terminal tail (646–668) observed in each of the herbicide complexes which is not present in related ThDP-dependent enzymes. Two identical substrate access tunnels, which are located on opposite faces and composed of amino acids from both monomers, lead to the two active sites of a dimer. In the absence of an inhibitor this tunnel is not very well defined because residues 568 to 583, which have been termed the ''mobile loop'' (Pang et al., 2003), are in a position that leaves much of the active site exposed to solvent. Hence we refer to the conformation of the free yeast AHAS structure and herbicide-bound AHAS structures as ''open'' and ''closed'', respectively. It is believed that the closed conformation represents the catalytically active form of the enzyme (Pang et al., 2003).

FAD is bound tightly to the enzyme, in an elongated conformation, by seven hydrogen bonds to five amino acid residues and with 42 other close contacts (≤3.9 Å) to 16 other amino acid residues. Nine of these residues are completely conserved and seven are highly conserved across AHASs from 21 different species (McCourt et al., 2005; see also the alignment of AHAS catalytic subunits sequences in Duggleby and Pang, 2000). The FAD binding site is contained within a groove in the β domain of one monomer with the end of the adenine ring exposed to solvent and the isoalloxazine ring buried near the active site (Fig. 13). In comparison to the open form of AHAS, the isoalloxazine ring of the closed form is angled slightly more towards the active site, bringing the dimethylbenzene ring in closer proximity to the catalytic centre (C2 of ThDP; see Fig. 14a and Section 2.3.2). The isoalloxazine ring of FAD was originally modeled into the first two AHAS structures in a flat conformation (Pang et al., 2002, 2003). However, once higher resolution (2.19 Å) data was available, it became clear that there is actually a slight bend across the central N5–N10 axis, the same as that which is observed for the isoalloxazine ring of the closely related, redox-active *L. plantarum* POX (Müller et al., 1994; McCourt et al., 2005). The implications of this conformation of FAD with reference to an electron transfer side-reaction will be discussed in Section 2.3.6.

The electron density for ThDP is complete for the open conformation of *S. cerevisiae* AHAS (Pang et al., 2002), for one of two molecules in the asymmetric unit of the closed, chlorimuron ethyl-bound, *S. cerevisiae* AHAS structure (Pang et al., 2003), and for the closed conformation of *A. thaliana* AHAS in the presence of an imidazolinone. However, for all other sulfonylurea-AHAS complexes, the electron density for ThDP is fragmented. Possible reasons for destruction of this cofactor will be discussed in Section 2.5.1.

As in other ThDP-dependent enzymes, ThDP is bound to AHAS in a V-conformation, imposed in part by Met513, which protrudes between the pyrimidine and thiazolium rings. Residues from both monomers contribute to binding ThDP, therefore the prime symbol (′) will be used to differentiate residues of one monomer from residues of the other. The pyrimidine ring is held in place by ten hydrophobic contacts to Tyr118′, Pro170′ and Met513 and three hydrogen bonds. Two of these hydrogen bonds are between the 4′-amino group of ThDP and the side-chains of Glu144′ and Gln207′, while the other is between N1′ and the nitrogen atom of Gly120′; their importance and role in catalysis will be discussed in Section 2.3. The thiazolium ring and the C6 and C7 methylene groups are held in place through 14 hydrophobic contacts to Gly120′, Met513, Leu568, Met570, and Val571. The diphosphate moiety of ThDP is hydrogen bonded to one of the side-chain oxygen atoms of Asp538, the backbone atoms of Gln487, His488, Gly539, Ser540,

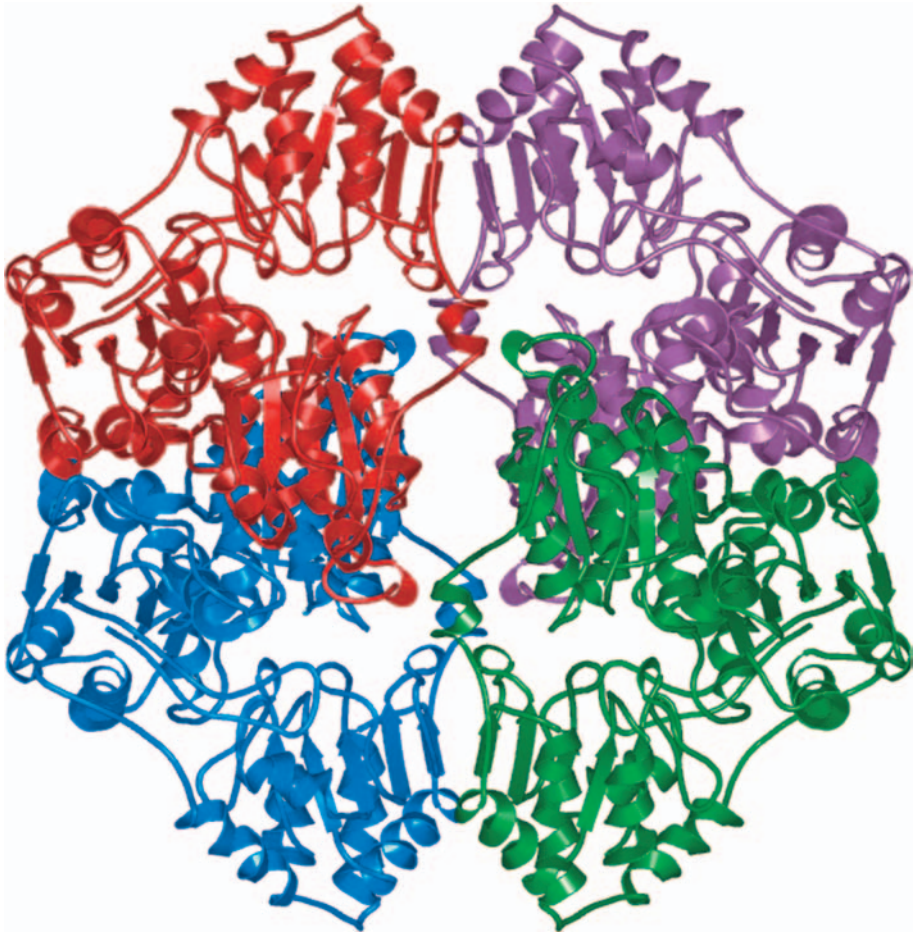

Fig. 11. Overall structure of *A. thaliana* AHAS. Each monomer has been coloured separately. The two functional dimers are shown in red/blue and green/purple

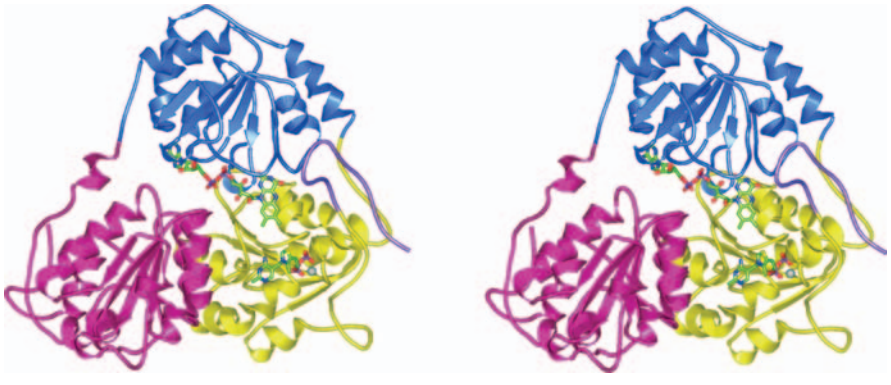

Fig. 12. Stereo representation of an *A. thaliana* AHAS monomer. The α, β, and γ domains are shown in pink, blue, and yellow, respectively. The C-terminal tail is highlighted in violet. ThDP and FAD are shown as sticks; carbon is green, nitrogen blue, oxygen red, sulfur yellow, and phosphorus magenta. The grey sphere is Mg^{2+}

His567, and Gly569 and is coordinated to Mg^{2+} via two of the diphosphate oxygen atoms. Mg^{2+} is also coordinated to the side-chains of Asp538 and Asn565, the backbone oxygen atom of His567 and to one water molecule in the herbicide bound structures. In the free yeast AHAS structure, an additional water molecule is ligated to Mg^{2+}

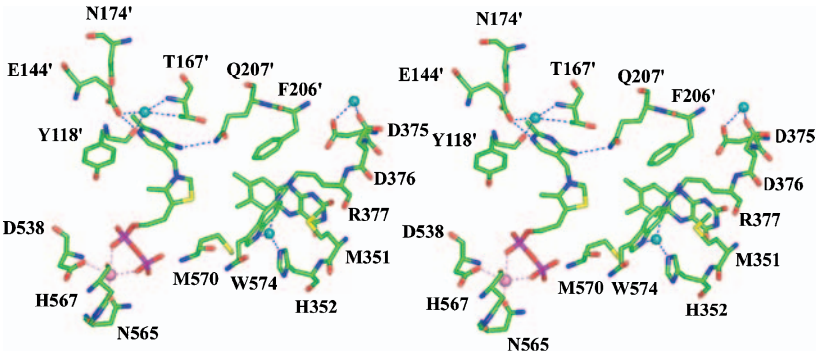

Fig. 13. Stereo representation of the active site residues within the *A. thaliana*-IQ complex. Residues that are believed to be essential for AHAS catalysis as well as nearby residues involved in hydrogen bonding (<3.2 Å; blue dashed lines) or Mg^{2+} coordination (pink dashed lines) are shown. Hydrogen bonds are indicated for water molecules (blue spheres) and side-chains only. The active site is formed at the dimer interface and the prime symbol (′) is used to distinguish residues from the two monomers. Carbon is green, nitrogen blue, oxygen red, sulfur yellow, phosphorus magenta, and Mg^{2+} is a pink sphere

(Pang et al., 2002), replacing His567, which is at the border of the mobile loop.

These recent crystal structures of AHAS have provided us with powerful information about the location and organization of the active site, and have also revealed the location of the binding sites for two different classes of herbicides. With this knowledge it will be possible to rationally design novel herbicides, create improved homology models for AHAS from other organisms such as that for *N. tabacum* AHAS (Le et al., 2004), and aid in the discovery of new antifungal and antimicrobial agents.

2.3 AHAS reactions and mechanism

2.3.1 Substrates

AHAS naturally catalyses the carboligation of an hydroxyethyl group, obtained by decarboxylation of pyruvate, with either another molecule of pyruvate to give AL, or with 2-KB to give AHB. However, the active site is quite indiscriminate and is capable of accepting a range of unnatural substrates including substrate homologs. In general, it seems that the first substrate binding site is rather specific for pyruvate. For example, it is possible for enterobacterial AHASI (Gollop et al., 1989) and AHASII (Schloss and Van Dyk, 1988) to combine two molecules of 2-KB to yield 2-ethyl-2-hydroxy-3-oxopentanoate although the rate of product formation is only 3% that of AHB. *E. coli* AHASIII is incapable of condensing two molecules of 2-KB and is also inhibited in the presence of glyoxylate, where the methyl group of pyruvate is replaced with hydrogen (Gollop et al., 1989). In this case it seems probable that glyoxylate undergoes decarboxylation but the resulting hydroxymethyl group is unable to be transferred to an acceptor, or released. The binding site for the second substrate is much less stringent than that for the first and can accept larger substrates than 2-KB. For example, *E. coli* AHASIII can combine pyruvate with 2-ketovalerate, a homolog of 2-KB consisting of a propyl rather than an ethyl substituent, to yield 2-aceto-2-hydroxyvalerate (Gollop et al., 1989).

Recently, it was realized that AHAS acts a proficient catalyst for the production of (*R*)-phenylacetylcarbinol (PAC), a precursor used in the pharmaceutical industry for the production of α- and β-adrenergic drugs (Engel et al., 2003) and other chiral hydroxyketones (Engel et al., 2004a). Although each of the three *E. coli* AHAS isozymes is able to catalyze the synthesis of PAC from pyruvate and benzaldehyde with a large enantiomeric excess of the (*R*) isomer, the specific activity of the reaction for *E. coli* AHASIII is much lower (0.21 U/mg) than that of AHASI and AHASII (3.3 U/mg) (Engel et al., 2003). Monosubstituted benzaldehydes with OH, CH_3, OCH_3, CN, or Cl in either the *meta* or *para* positions are also good substrates for AHAS and give rise to products with a high enantiomeric excess (Engel et al., 2004a). Interestingly, AHAS can also condense pyruvate with naphthaldehydes and pyridine carboxaldehydes with excellent conversion rates, as well as with furan, thiophene, and pyrrole carboxaldehydes, phenylacetaldehyde and cyclohexane carboxaldehyde, although the conversion rates using these substrates is poor. This gives rise to an enormous range of possibilities for the synthesis of chiral pharmaceutical precursors (Engel et al., 2004a). The use of *E. coli* AHASI for the production of PAC on an industrial scale has been proven to be efficient and a promising alternative to the current methods employed (Engel et al., 2005).

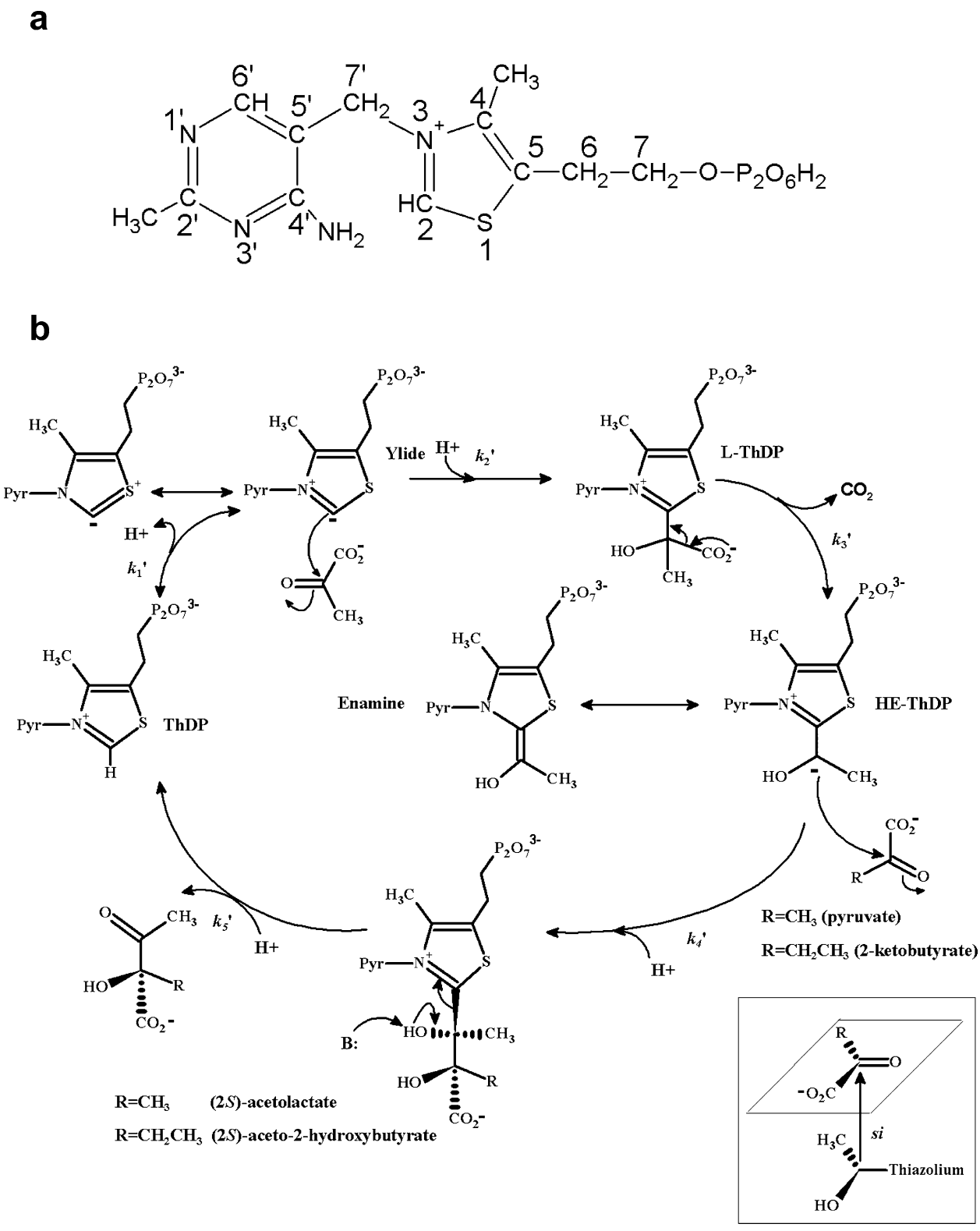

Fig. 14. **a** Structure of ThDP with the atoms numbered. **b** Catalytic cycle of AHAS. The box in the lower right hand corner indicates the geometry of the enamine that is required to give products of the (*S*) configuration

2.3.2 Catalytic mechanism

The catalytic mechanism of ThDP-dependent enzymes was first proposed by Breslow in 1958 and focused principally on the role of C2 (Fig. 14a). Since that time, a tremendous amount of effort has been expended to gain an understanding of the fine details underlying the mechanisms of individual enzymes. Although many of the acid and base groups involved in catalysis remain elusive, the powerful NMR technique developed by Tittmann et al. (2003) has enabled the identification and quantification of several different stable, covalent reaction intermediates of pyruvate decarboxylase (PDC), POX, transketolase (TK) and AHAS. With the knowledge of k_{cat}, this method can be utilized to calculate the net forward rate constants for the formation of these intermediates and has the potential to be applied to all ThDP-dependent enzymes under steady state conditions.

The catalytic cycle of AHAS is depicted in Fig. 14b. AHAS is believed to be activated in the same way as other ThDP-dependent enzymes (Bar-Ilan et al., 2001) in which Glu144, which is highly conserved among AHASs and other ThDP-dependent enzymes, protonates the N1′ atom of the pyrimidine ring (Kern et al., 1997) and induces formation of the 1′,4′-iminotautomer (Jordan et al., 2002, 2003; Nemeria et al., 2004). This highly basic 4′-imino group is in close proximity (~3.3 Å for the *A. thaliana* AHAS-IQ complex) to the C2 catalytic centre of ThDP as a result of the cofactor's V-conformation (Dyda et al., 1993; McCourt et al., 2006). Abstraction of the C2 proton by the 1′,4′-iminotautomer generates the highly reactive ylide required for catalysis (Jordan and Mariam, 1978; Kern et al., 1997; Lie et al., 2005). The *E. coli* AHASII Glu144Gln (Glu47 in *E. coli* AHAS II) mutant shows a 40-fold lower C2 proton exchange rate over the wildtype ($8\,s^{-1}$ *versus* $332\,s^{-1}$ at 37 °C) (Bar-Ilan et al., 2001), as expected from this scheme.

The activation of ThDP by this family of enzymes has drawn a large amount of interest over the years because the enzyme environment accelerates both the rates of formation of the ylide (by a factor of 1.2×10^5 for *Z. mobilis* PDC at pH 6.0) (Kern et al., 1997) and the decarboxylation of pyruvate by several orders of magnitude over ThDP alone in solution (by a factor of 3×10^{12} at pH 6.2 for *Saccharomyces carlsbergensis* PDC) (Alvarez et al., 1991). How this is accomplished, in the face of a pK_a for C2H dissociation that has been calculated to be as high as 17–19 for the free cofactor in water (Washabaugh and Jencks, 1988), is still controversial. It has been suggested that ThDP-dependent enzymes achieve these accelerated rates by stabilization of the reactive zwitterionic intermediates via the combined effect of an apolar active site with a low dielectric constant and formation of the 1′,4′-iminotautomer that decreases the pK_a for deprotonation (Jordan et al., 1999; Zhang et al., 2005). However, at least for formation of the ylide, Tittmann et al. (2005a) argue that the process is under kinetic control wherein deprotonation/reprotonation of C2 is simply due to fast proton shuttling as a consequence of the V-conformation of ThDP.

In the second step of the catalytic cycle of AHAS, the nucleophilic ylide attacks a molecule of pyruvate to give lactyl-ThDP (L-ThDP). The net forward rate constants (k_x') that have been calculated (Tittmann et al., 2003) for each of the covalent intermediates from *E. coli* AHASII indicate that the formation of L-ThDP is the principal rate-limiting step ($k_2' = 24\,s^{-1}$ in the presence of pyruvate or $21\,s^{-1}$ in the presence of pyruvate and 2-KB) for the overall reaction ($k_{cat} = 20\,s^{-1}$ for either AL or AHB formation) (Tittmann et al., 2003). This is an interesting property of AHAS because it is not observed in other ThDP-dependent enzymes where later steps are rate limiting (Chipman et al., 2005). In the third step, L-ThDP is decarboxylated ($k_3' = 530\,s^{-1}$ in the presence of pyruvate or $399\,s^{-1}$ with both pyruvate and 2-KB) to give the resonating HE-ThDP/enamine intermediate. Since 2-KB does not participate in the reaction until a later stage, a rate constant that is lower in the presence of both substrates than with pyruvate alone is unexpected (McCourt and Duggleby, 2005). One possible explanation for this, advanced by Duggleby et al. (2004) on entirely separate grounds, is that the second substrate is bound in the active site at an early stage of the catalytic cycle and is held in a ''waiting room'' until HE-ThDP is formed. In this way the enzyme would avoid opening of the active site to admit the second substrate midway through the catalytic cycle. Otherwise, doing so would expose HE-ThDP to solvent and possibly result in conversion to acetaldehyde and ThDP. Herbicidal inhibitors of AHAS (see Section 2.5), benzaldehyde or other aromatic aldehydes, when present, can also occupy the waiting room.

While these first three steps are common among other ThDP-dependent pyruvate utilizing enzymes PDC, POX, the E1 component of pyruvate dehydrogenase, and pyruvate:ferridoxin oxidoreductases, the fate of the HE-ThDP intermediate for AHAS is quite different. Rather than the protonation or oxidation of this intermediate, HE-ThDP reacts with a second ketoacid ($k_4' = 1060\,s^{-1}$ for pyruvate or $>2000\,s^{-1}$ for 2-KB) after which the product is released. The reaction catalyzed by AHAS is enantiospe-

cific so that both products are of the (*S*) isomer (Crout et al., 1990). This implies that the HE-ThDP/enamine intermediate must attack the second ketoacid from the *si* face of the molecule (Fig. 14b). We have also indicated the stereochemistry of the acetolactyl- or acetohydroxybutyryl-ThDP adduct in Fig. 14b although the second chiral centre proximal to C2 is yet to be confirmed. However, the results of mutagenesis studies by Chipman and coworkers repeatedly suggest the configuration shown (Engel et al., 2004b and D. M. Chipman, personal communication).

2.3.3 Substrate preference

As mentioned previously, depending on the organism of origin, AHAS favors one 2-ketoacid over the other. For example, *E. coli* AHASII is much more likely to combine the HE-ThDP intermediate with 2-KB than with pyruvate ($R = 56$; Tittmann et al., 2005b). Interestingly, mutation of Trp574 (Trp464 in *E. coli* AHASII) to leucine virtually abolishes this substrate preference ($R = 1.3$; Ibdah et al., 1996). Thus, although it was shown that Trp574 plays an integral role in selecting the second substrate, the way in which the enzyme accomplishes this task was unclear. In their recent paper, based on the kinetic analysis of a series of *E. coli* AHASII mutants, Tittmann et al. (2005b) have shown that the formation of AHB is more highly committed ($k_5' => 2000\ s^{-1}$) than AL ($k_5' = 176\ s^{-1}$) and have suggested that the preference for 2-KB can be attributed to this property. That is, if a second molecule of pyruvate binds to HE-ThDP it is more likely to be released than 2-KB, which would then give 2-KB another chance to react and form AHB.

2.3.4 Residues involved in catalysis

Although the crystal structure of AHAS in complex with reaction intermediates, substrates or products has not yet been reported, mutagenesis studies on *E. coli* AHASII by Chipman and coworkers (Ibdah et al., 1996; Bar-Ilan et al., 2001; Engel et al., 2003, 2004b; Tittmann et al., 2005b) and *N. tabacum* AHAS by the Choi/Yoon group (Chong et al., 1999; Shin et al., 2000; Oh et al., 2001; Yoon et al., 2002; Le et al., 2005) have provided evidence for the involvement of several residues in catalysis. A representation of the proposed active site of *E. coli* AHASII with HE-ThDP and 2-KB has been offered by Engel et al. (2004b). The studies by Chipman and coworkers indicate that in addition to Phe206 and Met351, Arg377 is critical for the recognition of both pyruvate and 2-KB, but not for benzaldehyde. Therefore, they reason that the cationic side-chain of Arg377 interacts with the carboxylate group of the ketoacid while Phe206 and Met351, which are flanking Arg377 in space, are probably important for maintaining the correct orientation for ionic interaction. The importance of Arg377 in catalysis has also been demonstrated for *N. tabacum* AHAS (Le et al., 2005). Chipman's group also suggest additional roles for Gln207, which they believe may be involved in proton transfer to the carbonyl oxygen of the second substrate, and the positive dipole on the nitrogen atom of Gly121 which might be responsible for stabilizing the negative charge on the carbonyl oxygen (Engel et al., 2004b). As discussed previously, Trp574 is involved in recognition of the second substrate and Met570, which is close to Trp574 in space, might also aid in binding the second substrate (Engel et al., 2004b).

2.3.5 Unconventional ThDP intermediates

Some bacteria contain an FAD-independent form of the enzyme, now referred to as ALS, which catalyses the same reaction as AHAS although it displays a very high preference for pyruvate as the second substrate. It also has a much higher specific activity than any AHAS. Determination of the crystal structure of ALS (Pang et al., 2004a) has revealed some unusual features of the ThDP cofactor that may be related to its high activity. The thiazolium ring in ThDP is shown conventionally with N3 carrying a positive charge and connected to C2 by a double bond (Fig. 15, **Ia**), which would make N3 planar. However, in ALS the N3 to C7′ bond is clearly not in the same plane as the thiazolium ring, with N3 being pyramidal. This implies that there is no double bond to C2; this could occur if the positive charge migrates to C2 (Fig. 15, **Ib**) or S1 (Fig. 15, **Ic**). There is a good precedent for charge migration in the crystal structure of free ThDP (Pletcher and Sax, 1972) where the thiazolium ring is comprised of a mixture of five resonance forms, with a 25% contribution from form **Ic** (Fig. 15). It would only require a small distorting force applied by the protein to make this the predominant form.

In the same paper by Pang et al. (2004a), the crystal structure of ALS is solved with a bound hydroxyethyl group, obtained by incubation with pyruvate. This intermediate is also unconventional, with a tricyclic structure (Fig. 15, **IIIb**) formed by reaction of the 4′-NH_2 with C2. This structure is similar to dihydrothiachrome diphosphate except for the extra substituent on C2. There is strong evidence for the formation of the tricyclic dihydrothia-

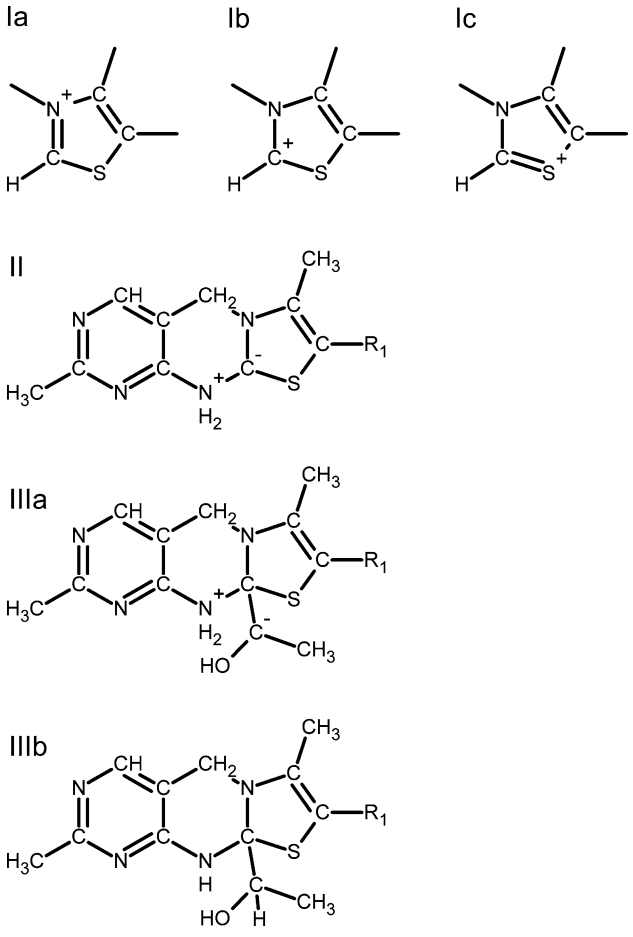

Fig. 15. Forms of ThDP in the catalytic cycle of acetolactate synthase. The conventional representation of the thiazolium ring (**Ia**) has the positive charge on N3 but this charge may migrate to C2 (**Ib**) or S1 (**Ic**). After proton dissociation, the tricyclic **II** is formed and reacts with pyruvate to give the enamine shown previously in Fig 14b. Reaction with the second molecule of pyruvate requires the tricyclic α-carbanion (**IIIa**) but this may be diverted into the side product **IIIb** by an intramolecular proton transfer

chrome from thiamin under mild conditions (Washabaugh et al., 1993), and its oxidation yields thiochrome (Barger et al., 1935), the fluorescent compound that is used frequently for estimating thiamin and its derivatives.

Pang et al. (2004a) propose that after proton dissociation from the resonating **Ib** and **Ic**, the highly reactive tricyclic **II** is formed and reacts with the first pyruvate. This then decarboxylates to give the relatively non-reactive enamine shown earlier (Fig. 14b). Because this is stable, the enzyme can pause midway through the catalytic cycle and allow the active site to release CO_2 and admit the second molecule of pyruvate. The tricyclic α-carbanion (**IIIa**) then forms, ready to react with the second pyruvate. It is **IIIa** that is the true reaction intermediate but during the prolonged incubation that occurs in a crystallization experiment, the added pyruvate is completely depleted and the accumulated **IIIa** is converted to **IIIb**.

2.3.6 Side-reactions catalyzed by AHAS

Not surprisingly, the highly reactive HE-ThDP AHAS intermediate is susceptible to combining with other electrophiles that can access the active site. In 1991 Abell and Schloss discovered a side-reaction catalyzed by *S. typhimurium* AHASII in which molecular oxygen reacts with HE-ThDP to form hydroperoxide-HE-ThDP. Over time, the hydroperoxide intermediate decomposes to peracetic acid and ThDP and the peracetic acid eventually decays to acetate and oxygen (Fig. 16). In the presence of pyruvate this reaction proceeds at 0.26 U/mg, which is approximately 1% the rate of AL production. Similarly, when 2-KB serves as the substrate, oxygenase activity drops to 0.02 U/mg, which is approximately 1% the rate of production of 2-propio-2-hydroxybutyrate. Oxygenase activity has also been reported for *H. vulgare* AHAS; the specific activity is 0.075 U/mg (Durner et al., 1994).

FAD was first recognized as a cofactor for *S. typhimurium* AHAS by Størmer and Umbarger (1964). Subsequent studies confirmed that FAD was a cofactor for *P. aeruginosa*, *E. coli* and *Z. mays* AHAS (Arfin and Koziell, 1973; Grimminger and Umbarger, 1979; Muhitch et al., 1987). To date, with the exception of *M. aeolicus* AHAS which can substitute flavin mononucleotide or riboflavin plus phosphate in place of FAD (Xing and Whitman, 1994), all reports of characterized AHASs confirm that FAD is required absolutely for catalysis. This requirement for FAD is unusual because, as demonstrated using a variety of experiments, the catalytic mechanism of AHAS does not involve electron transfer. First of all, reconstitution of AHAS with flavin analogs, including 5-deaza-5-carba FAD or 8-demethyl-8-chloro-FAD, has little effect on AHAS activity (Schloss, 1991); second, replacement of FAD with photoreduced FAD ($FADH_2$) gives 110% the activity of the native enzyme (Schloss, 1991); and third, ALS is capable of AL synthesis from two molecules of pyruvate in the absence of FAD. Mandelonitrile lyase (EC 4.1.2.10) is another example of an enzyme that requires FAD but does not catalyze a redox reaction (Hu and Poulton, 1999). In an interesting parallel to AHAS, tartronate-semialdehyde synthase (EC 4.1.1.47, also known as glyoxylate carboligase) requires FAD for the condensation of two molecules of glyoxylate (the lower homolog of pyruvate) (Cromartie and Walsh, 1976) and oxalyl-coenzyme A decarboxylase (EC 4.1.1.8), a homologous ThDP-dependent enzyme,

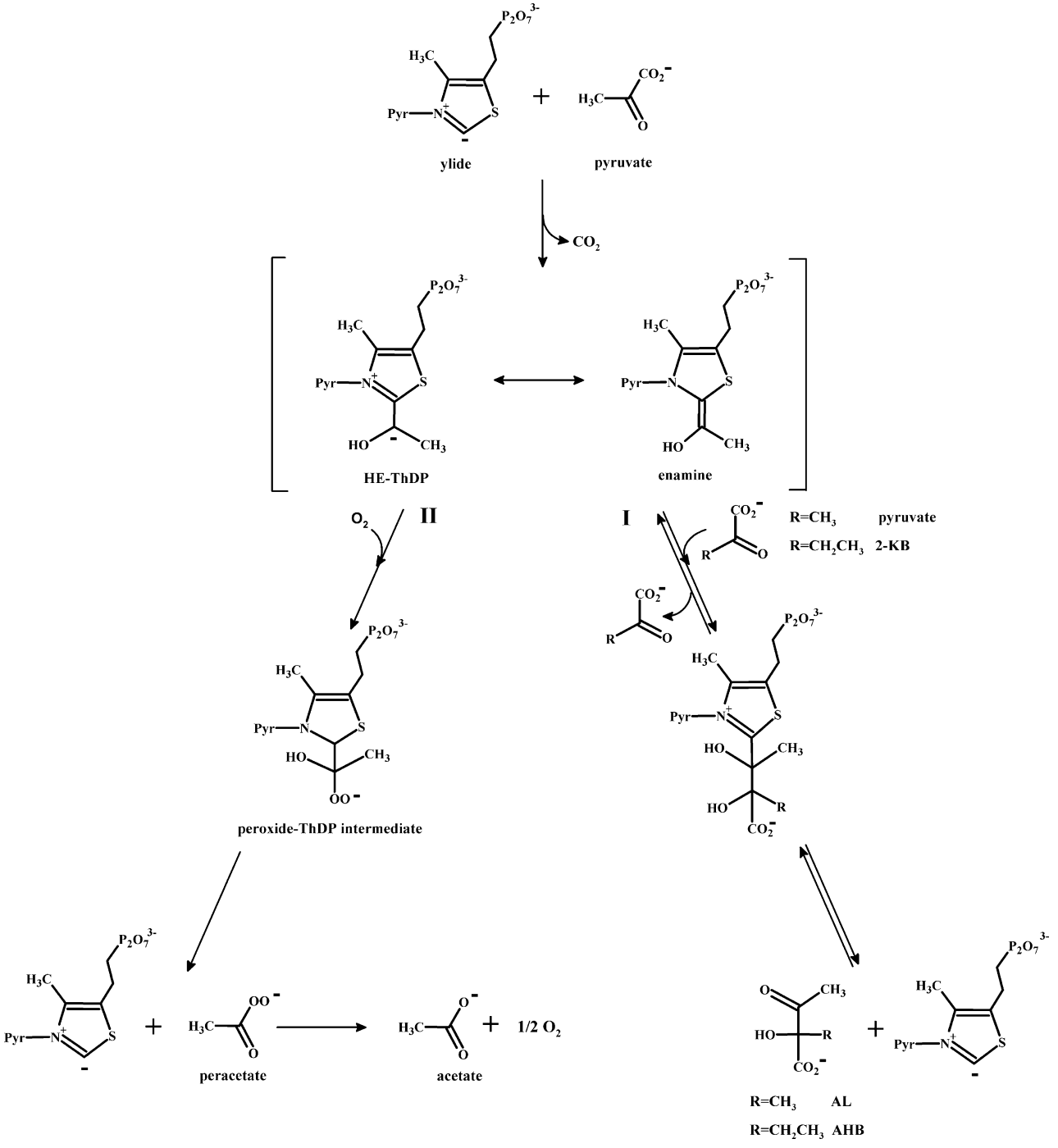

Fig. 16. Oxygenase side-reaction of bacterial AHAS. "Pyr" denotes the pyrimidine ring of ThDP. Following formation of the HE-ThDP/enamine intermediate, normal AHAS catalysis proceeds by route **I**. In an aerobic environment the enzyme will also catalyse an oxygenase side-reaction, route **II**

binds ADP in a similar region to FAD in AHAS (Berthold et al., 2005).

In 1988, Schloss and Aulabaugh reported that during the course of AHAS catalysis, there is a loss of FAD absorbance at 450 nm. In the light of mounting evidence against an FAD-mediated redox reaction in AHAS, at this time they suggested that the phenomenon was due to the catalytically non-productive nucleophilic attack of HE-ThDP on FAD. Recently, a more in-depth analysis of this observation led by Tittmann and coworkers uncovered an FAD-mediated side reaction catalyzed by the *E. coli* AHAS isozymes (Tittmann et al., 2004).

The *E. coli* AHASII side-reaction was investigated under both anaerobic and aerobic conditions. Each of the reductive and oxidative half reactions were characterized independently using pre-steady state and steady state kinetics by means of time-resolved spectroscopy. The reductive half reaction in the presence of pyruvate consists mainly of three phases over a period of 500 seconds. The pre-steady state phase (<20 s) in which there is a burst of FAD reduction ($k'_{obs} = 0.45\ s^{-1}$) represents all of the catalytic steps that lead up to, and including, the formation of HE-ThDP is then followed by the steady state phase (<100 s) where the rates of FAD reduction ($k'_{red} = 0.2\ s^{-1}$) and oxidation ($k'_{ox} = 0.25\ s^{-1}$) are approximately equal. Eventually, as dissolved oxygen is consumed, the equilibrium shifts toward FAD reduction and all the FAD is reduced over approximately the last 400 seconds. As expected, under anaerobic conditions, the rate of reduction is slightly faster ($k' = 1\ s^{-1}$) and is completed after 100 s. Although the precise mechanism of the electron transfer reaction is not known, it has been confirmed that HE-ThDP serves as the electron donor and is oxidized to acetyl-ThDP (Ac-ThDP) (Tittmann et al., 2004).

The AHAS side-reaction is reminiscent of the reaction catalyzed by the membrane-associated POX in which the HE-ThDP intermediate transfers two electrons to FAD to give Ac-ThDP. For *E. coli* POX, Ac-ThDP is hydrolyzed to give acetate and uses ubiquinone-8 as a final electron acceptor in vivo (Tittmann et al., 2000). Based on the many similarities between AHAS and POX including their common cofactors (FAD, ThDP, Mg^{2+}), substrate (pyruvate), product (CO_2), the capacity of AHAS to bind ubiquinones (Schloss et al., 1988) and the ability of POX to synthesize AL (Chang and Cronan, 1988), it has been proposed that POX and AHAS share a common ancestor (Grabau and Cronan, 1986; Chang and Cronan, 1988; Schloss et al., 1988). In addition, the arrangement of cofactors within *L. plantarum* POX and AHAS are almost identical. It is most interesting to note that in both structures the isoalloxazine ring is bent 15° across the N5–N10 axis, a conformation that is expected to favor reduced FAD (Müller et al., 1994; McCourt et al., 2005). Since the AHAS side-reaction is not productive, FAD is probably a remnant of the POX-like ancestor that has been retained to avoid solvent-mediated protonation of the reactive intermediate and to maintain the correct conformation of the enzyme. The existence of the FAD-independent ALS shows that these functions of FAD can be carried out by the protein alone. Indeed, ALS is significantly more efficient than any FAD-dependent AHAS.

2.4 Regulation of AHAS activity by feedback inhibition

Depending on the organism, several mechanisms have evolved for the intracellular regulation of BCAA synthesis. However, one way in which all organisms control this biochemical pathway is by feedback inhibition of AHAS by one or more of valine, leucine or isoleucine. Although it was known that valine is an inhibitor of *E. coli* AHAS as early as 1958, when AHAS was first characterized (Umbarger and Brown, 1958), the molecular mechanism of this inhibition was not clear. An important step towards its elucidation came when the first DNA sequence of an AHAS operon was determined (*ilv*IH encoding *E. coli* AHASIII; Squires et al., 1983), which showed that AHAS is actually composed of two different polypeptides. Shortly thereafter, the genes encoding AHASI (*ilv*BN; Wek et al., 1985) and AHASII (*ilv*GM; Lawther et al., 1981) from *E. coli* were also sequenced and shown to encode a small polypeptide downstream from the gene encoding AHAS. The first successful purification that demonstrated the presence of two AHAS subunits was reported by Eoyang and Silverman in 1984 for *E. coli* AHASI, and they later established that, in addition to activating the large subunit, the small subunit confers sensitivity to valine (Eoyang and Silverman, 1986). Separate purification and reconstitution of the large and small subunits of *E. coli* AHASIII finally confirmed that the large subunit alone is weakly active, but cannot bind valine, whereas the small subunit by itself is inactive and binds valine with a dissociation constant of 0.2 mM (Vyazmensky et al., 1996). To date, the only exception known is for enterobacterial AHASII, which requires absolutely both subunits for catalytic activity but is not feedback inhibited by any BCAAs (Blatt et al., 1972; Hill et al., 1997). Hence the larger subunit is now referred to as the ‘‘catalytic subunit’’ (CSU) while the smaller subunit is best described as the ‘‘regulatory subunit’’ (RSU). This terminology is particularly fitting for the plant regulatory subunits, which are almost as large as the catalytic subunits.

As mentioned previously, with the exception of enterobacterial AHASII, it has been shown that AHASs from enterobacteria (Umbarger and Brown, 1958; Bauerle et al., 1964; Grimminger and Umbarger, 1979), other Gram negative bacteria (Arfin and Koziell, 1973a; Yang and Kim, 1993), Gram positive bacteria (Eggeling et al., 1987, Leyval et al., 2003), archaea (Xing and Whitman, 1994; Vyazmensky et al., 2000), fungi (Magee and deRobichon-Szulmajster, 1968; Pang and Duggleby, 1999), unicellular green alga (Landstein et al., 1990) and plants (Singh et al.,

1988; Lee and Duggleby, 2001) are all feedback regulated by one or more of valine, leucine or isoleucine. However, prior to the discovery of putative plant and algal genes, which were shown to have significant homology to genes encoding bacterial RSUs (Duggleby, 1997), there was confusion as to whether or not eukaryotic RSUs exist. This is because the purification of both AHAS subunits from a eukaryotic source has never been successful (Durner and Böger, 1988; Singh et al., 1988; Southan and Copeland, 1996). Evidence in favor of the existence of eukaryotic RSUs (Singh and Shaner, 1995; Duggleby, 1997) included observations that crude extracts (Magee and deRobichon-Szulmajster, 1968; Southan and Copeland, 1996), but not homogeneous preparations (Poulsen and Stougaard, 1989; Southan and Copeland, 1996; Chang et al., 1997), of eukaryotic AHAS are inhibited by one or more BCAAs. In addition, in some cases there have been subtle differences in the properties of the purified enzyme, such as the K_m for pyruvate, pH optimum, and specific activity compared to those of the cellular extract (Magee and deRobichon-Szulmajster, 1968; Poulsen and Stougaard, 1989; Singh et al., 1992). One interpretation of these changed properties is that eukaryotic RSUs are lost during the purification process. Finally, in 1999 the first two eukaryotic RSUs were cloned, expressed in *E. coli*, and purified to homogeneity (*S. cerevisiae* RSU, Pang and Duggleby, 1999; *N. plumbaginifolia* RSU, Hershey et al., 1999). Reconstitution of the yeast CSU with its RSU resulted in stimulation of its activity (7–10 fold) and conferred sensitivity to BCAAs (Pang and Duggleby, 1999). In contrast, for reasons still unknown, although the plant RSU was capable of enhancing the activity of the catalytic subunit, it failed to confer sensitivity to the BCAAs (Hershey et al., 1999). However, later work with the subunits of *A. thaliana* AHAS demonstrated reconstitution of a fully functional enzyme that is sensitive to inhibition by all three BCAAs (Lee and Duggleby, 2001).

It is now widely believed that all organisms express an AHAS RSU (Duggleby and Pang, 2000) and the genes from at least 30 species among four Kingdoms have been identified (Lee and Duggleby, 2002). In several cases the protein has been purified either alone or in combination with the catalytic subunit and characterized (Table 3). If the CSU is expressed separately from the RSU the two subunits can later be reconstituted as the holoenzyme, usually by mixing the two subunits together and incubating for a short period of time. However, the expression of soluble eukaryotic AHAS subunits usually requires that at least part of the N-terminal transit sequence be removed.

Table 3. Purified AHAS catalytic and regulatory subunits

Purified enzyme	Catalytic subunit		Regulatory subunit	
	kDa	gi number	kDa	gi number
E. coli I[a]	60.3	124373	11.0	17380389
E. coli II[b]	59.0	12518626	9.5	12518627
E. coli III[c]	62.8	2507470	17.9	13359538
S. typhimurium II[d]	59.0	16422469	9.4	16422470
S. marcenscens[e]	~62	–	~35	–
S. cinnamonensis[f]	65.5	55540777	19.0	5733116
M. tuberculosis[g]	65.9	61226663	18.1	54041388
M. avium[h]	65.9	2501328	18.1	2501329
C. glutamicum[i]	66.7	62390158	18.6	21324040
B. stearothermophilus[j]	62.3	19918932	18.6	19918933
L. lactis[k]	59.0	15673206	17.6	12724195
P. aeruginosa[l]	~60		~15	
S. cerevisiae[m]	74.8	6323755	34.1	1907135
N. plumbaginifolia[n]	65.1	–	50.0	5931761
A. thaliana[o]	72.4	124372	53.0	30685070
O. sativa (unpublished)	69.3	60116604	52.0	50910330

Molecular weights have been calculated for the full-length gene product from the sequences listed in the public database. In cases where the sequence is not available in the database, the molecular weight has been provided by the author(s) in the listed references. [a] Eoyang and Silverman (1984). [b] Hill et al. (1997). [c] Vyazmensky et al. (1996). [d] Schloss et al. (1985). [e] Yang and Kim (1993), the enzyme was purified from the native, rather than from a recombinant source. [f] Kopecký et al. (1999). [g] Choi et al. (2005). [h] Zohar et al. (2003). [i] Elišáková et al. (2005). [j] Porat et al. (2004). [k] Snoep et al. (1992). [l] Arfin and Koziell (1973b). [m] Pang and Duggleby (1999). [n] Hershey et al. (1999). [o] Lee and Duggleby (2001)

Thus, 54 amino acids were removed from the CSU and 40 amino acids from the RSU of *S. cerevisiae* AHAS (Pang and Duggleby, 1999). Similarly, 86 amino acids were removed from the CSU (Chang and Duggleby, 1997), and 70 amino acids from the RSU of *A. thaliana* AHAS (Lee and Duggleby, 2001). Nevertheless, both prokaryotic and N-terminal truncated eukaryotic CSUs are generally much more soluble (10–40 mg/ml), than the RSUs (Vyazmensky et al., 1996; Hill et al., 1997; Pang and Duggleby, 1999; Lee and Duggleby, 2001; Choi et al., 2005; typically <2 mg/ml, authors' observation).

Reconstitution of the CSU with the RSU will greatly enhance the specific activity of the enzyme (Vyazmensky et al., 1996; Pang and Duggleby, 1999; Hershey et al., 1999; Lee and Duggleby, 2001; Porat et al., 2004; Choi et al., 2005). Moreover, reconstitution for all but AHASII from *E. coli* (Hill et al., 1997) where the process is highly cooperative, is rapid, efficient and follows simple hyperbolic saturation kinetics (Weinstock et al., 1992; Vyazmensky et al., 1996; Pang and Duggleby, 1999; Lee and Duggleby, 2001; Porat et al., 2004; Choi et al., 2005). The dissociation constants for the reconstituted enzyme (100 nM for *E. coli* AHASIII, Mendel et al.,

2001; 70 nM for *S. cerevisiae* AHAS, Pang and Duggleby, 1999; 167 nM for *A. thaliana* AHAS, Lee and Duggleby, 2001) indicate a tight association between the two subunits. As stated previously, in most cases reconstitution is achieved simply by mixing an excess of the RSU with the CSU (Weinstock et al., 1992; Vyazmensky et al., 1996; Hill et al., 1997; Hershey et al., 1999). However, unusual conditions are required for reconstitution of *S. cerevisiae* AHAS subunits, for which an extremely high concentration of phosphate (optimal at approximately 1 M) is necessary (Pang and Duggleby, 1999). The high salt concentration may be mimicking the mitochondrial environment in which the enzyme resides (Duggleby and Pang, 2000). In some cases it is possible to activate the CSU from one organism by reconstitution with the RSU from another (*N. plumbaginifolia* RSU with the *A. thaliana* CSU, Hershey et al., 1999; *S. cerevisiae* RSU with the *A. thaliana* CSU, Pang and Duggleby, 2001; *E. coli* AHASIII RSU with *B. stearothermophilus* CSU, Porat et al., 2004). However, given the different properties of the bacterial isozymes, it is not surprising that the *E. coli* AHASI RSU cannot be substituted for the *E. coli* AHASIII RSU (Weinstock et al., 1992).

Inhibition of AHAS by the BCAAs is complicated and, despite the numerous studies conducted over the past 50 years, it is not well understood. The inhibition has been reported to be noncompetitive (Bauerle et al., 1964; Magee and deRobichon-Szulmajster, 1968; Glatzer et al., 1972; Takenaka and Kuwana, 1972; Arfin and Koziell, 1973a; Oda et al., 1982; Proteau and Silver, 1991) and competitive (Xing and Whitman, 1994) with respect to pyruvate. Furthermore, the inhibition is incomplete so that even at saturating concentrations of these amino acids, anywhere from 11% to 87% of the activity still remains even in the presence of the best inhibitor (Table 4). This latter observation may be an indication that the BCAAs act to alter the conformation of the CSU so that the enzyme has a lower specific activity. It has also been reported that the extent of inhibition by the BCAAs is pH dependent (Magee and deRobichon-Szulmajster, 1968; Miflin, 1971; Arfin and Koziell, 1973a; Vyazmensky et al., 1996; Durner and Böger, 1990); for example at pH 8.5 the K_i^{app} for valine of *E. coli* AHASIII is lower (6 μM) than at pH 7.6 (12.7 μM) even though the extent of inhibition is lowered from 87% (at pH 7.6) to 71% (pH 8.5) (Vyazmensky et al., 1996).

Most studies have shown that AHAS is inhibited by all three BCAAs with valine being the most potent inhibitor, followed by isoleucine, then leucine (Table 4) (Arfin and Koziell, 1973a; Barak et al., 1988; Yang and Kim, 1993; Pang and Duggleby, 2001; Leyval et al., 2003; Choi et al., 2005). However, it must be emphasized that the most

Table 4. Inhibition of AHAS by valine, leucine, and isoleucine

Enzyme	Val		Leu		Ile	
	K_i^{app} (mM)	%	K_i^{app} (mM)	%	K_i^{app} (mM)	%
E. coli III	0.0127[a]	87[a]	ND	35[b]	ND	70[b]
C. glutamicum[c]	0.9[d]		6[d]		3.1[d]	
P. aeruginosa[c]	0.0044	28	1.8	34	0.270	29
S. marcenscens[f]	0.1[d]		~1[d]		~1[d]	
M. aeolicus[g]	0.3		0.4		ND	
M. avium[h]	0.056		ND		ND	
M. tuberculosis[j]	16.3	40	very weak		ND	
B. stearothermophilus[j]	0.004[k]	40[k]	ND		ND	
S. cerevisiae[l]	0.142	78	NI	NI	ND	13
A. thaliana[m]	0.231	36	0.336	49	1.38	27
H. vulgare[n]	2.3[d]	30	0.525[d]	41	ND	16
E. gracilis[o]	0.280	89	ND	23	ND	32
C. emersonii[p]	0.4[d]	~65	ND	~35	ND	~15
H. vulgare[q]	ND	~35	ND	~35	ND	~15
Z. mays[r]	ND	34	ND	34	ND	16
H. volcanii[s]	ND	50	ND	ND	weak	ND

% refers to % inhibition at saturating concentrations of BCAAs. ND, not determined. NI, not inhibited by this amino acid. [a] Vyazmensky et al. (1996). [b] Barak et al. (1988). [c] Leyval et al. (2003). [d] Indicates an IC_{50} value. [e] Arfin and Koziell (1973). [f] Yang and Kim (1993). [g] Xing and Whitman (1994). [h] Zohar et al. (2003). [i] Choi et al. (2005). [j] Porat et al. (2004). [k] indicates that the value was determined at non-saturating concentrations of pyruvate. [l] Pang and Duggleby (2001). [m] Lee and Duggleby (2001). [n] Miflin (1971). [o] Oda et al. (1982). [p] Landstein et al. (1990). [q] Durner and Böger (1990). [r] Singh et al. (1988). [s] Vyazmensky et al. (2000)

potent amino acid inhibitors (with the lowest K_i^{app} or IC_{50} value) are not necessarily the best inhibitors (those with the highest percentage of inhibition). For example, while it was demonstrated for the *P. aeruginosa* enzyme that the K_i^{app} values for isoleucine and leucine are 60-fold and 400-fold higher than that for valine, all three amino acids inhibit the enzyme to approximately the same extent (Table 4) (Arfin and Koziell, 1973a). Similarly, for the *A. thaliana* enzyme, even though the K_i^{app} value for valine is slightly lower than for leucine, it is leucine that gives the greatest inhibition at saturation (Table 4) (Lee and Duggleby, 2001). Furthermore, combinations of BCAAs have a synergistic effect on some AHASs (Miflin, 1971; Arfin and Koziell, 1973a; Singh et al., 1988; Lee and Duggleby, 2001). The most detailed study of the synergistic effect was performed using the *A. thaliana* enzyme (Lee and Duggleby, 2001). They showed that inhibition by leucine in combination with isoleucine ($K_i^{app} = 194\,\mu M$, 61% inhibition) or valine ($K_i^{app} = 12.3\,\mu M$, 65% inhibition) is each more potent and extensive than for any one amino acid alone (e.g. valine, $K_i^{app} = 231\,\mu M$, 36% inhibition). No synergy was observed between valine and isoleucine. Further investigation of the synergy between leucine and valine revealed that the addition of 5 μM and 20 μM valine lowered the K_i^{app} for leucine from 313 μM to 44.9 μM and 2.6 μM, respectively. Similarly, increasing the concentration of leucine in the presence of valine decreases the K_i^{app} value for valine. Therefore, it was suggested that there are two distinct binding sites, one for leucine and one for valine or isoleucine, on the RSU of *A. thaliana* AHAS.

The inhibition of fungal AHAS by valine can be fully reversed by the addition of ATP (Takenaka and Kuwana, 1972; Pang and Duggleby, 1999; Pang and Duggleby, 2001). ATP cannot be replaced by other nucleotide triphosphates, adenine diphosphate (ADP) or adenine monophosphate (AMP), although replacement with a non-hydrolysable form of ATP indicates that reversal of inhibition is not mediated by phosphorylation (Pang and Duggleby, 2001). It has been demonstrated that ATP, as its Mg^{2+} complex, binds to the *S. cerevisiae* RSU alone ($K_d = 0.2\,mM$) and it is likely that this binding site is contained within a 50 amino acid insert that is specific to fungal RSUs (Lee and Duggleby, 2006). The activation by ATP is very complex and depends on the concentration of valine present in the reaction (Pang and Duggleby, 2001). This additional method of regulation within the BCAA synthetic pathway may offer an alternative to the valine insensitive AHASII isozyme utilized by the enterobacteria.

There are several mutations that are known to confer resistance to valine (Bourgin et al., 1985; Relton et al., 1986; Rasinathabapathi et al., 1990; Subramanian et al., 1991; Wu et al., 1994; Vyazmensky et al., 1996; Kopecký et al., 1999). The molecular basis for valine resistance in *E. coli* AHASIII and *S. cinnamonensis* AHAS has been determined to be the result of a single amino acid substitution in the RSU (Vyazmensky et al., 1996; Kopecký et al., 1999), although there is at least one case in which a mutation within the CSU, Ser217Leu, confers valine resistance (Hervieu and Vaucheret, 1996). Interestingly, the mutation that was described for *E. coli* AHASIII, Gly14Asp, (Vyazmensky et al., 1996) was also identified in *S. cinnamonensis* AHAS (Kopecký et al., 1999) and shown to align with a glutamate residue in the valine-insensitive *E. coli* AHASII (Vyazmensky et al., 1996).

Unfortunately, neither solution nor crystal structures of an AHAS RSU have been reported. Nevertheless, the alignment (Fig. 17) and comparison of various RSU amino acid sequences with other proteins has provided some possible insight into the three-dimensional structure. In general, most bacterial RSUs are similar to *E. coli* AHASIII. Upon the identification of the first plant RSUs a few years ago (Hershey et al., 1999; Lee and Duggleby, 2001), it was realized that the plant RSU sequences contain a pair of repeats ~180 amino acids in length (Lee and Duggleby, 2001; Mendel et al., 2001). Each of these repeats resembles the full sequence of bacterial RSUs, lending further support for the presence of two amino acid binding sites. Lee and Duggleby (2001) tested the role of the repeats of the *A. thaliana* RSU by expressing each separately. Both truncated proteins were capable of activating the CSU, and the N-terminal repeat conferred sensitivity to leucine, but not valine or isoleucine. These results indicate the existence of a binding site that is specific for leucine on the first repeat of the *A. thaliana* RSU. The CSU reconstituted with the second repeat is insensitive to BCAAs but it is possible that the N-terminal fusion tag, which was added to facilitate purification, altered the properties of the protein and interfered with its ability to bind valine or isoleucine.

Homology models of the *A. thaliana* RSU and the *E. coli* AHASIII RSU have been constructed by Lee and Duggleby (2001) and Mendel et al. (2001), respectively. The model proposed by Lee and Duggleby is based on its similarity to the regulatory domain of *E. coli* TD, which is also regulated by two BCAAs (activated by valine, inhibited by isoleucine), and consists of a pair of repeats with some sequence identity to the *A. thaliana* RSU. The model of Mendel et al. (2001) is based on the similarity

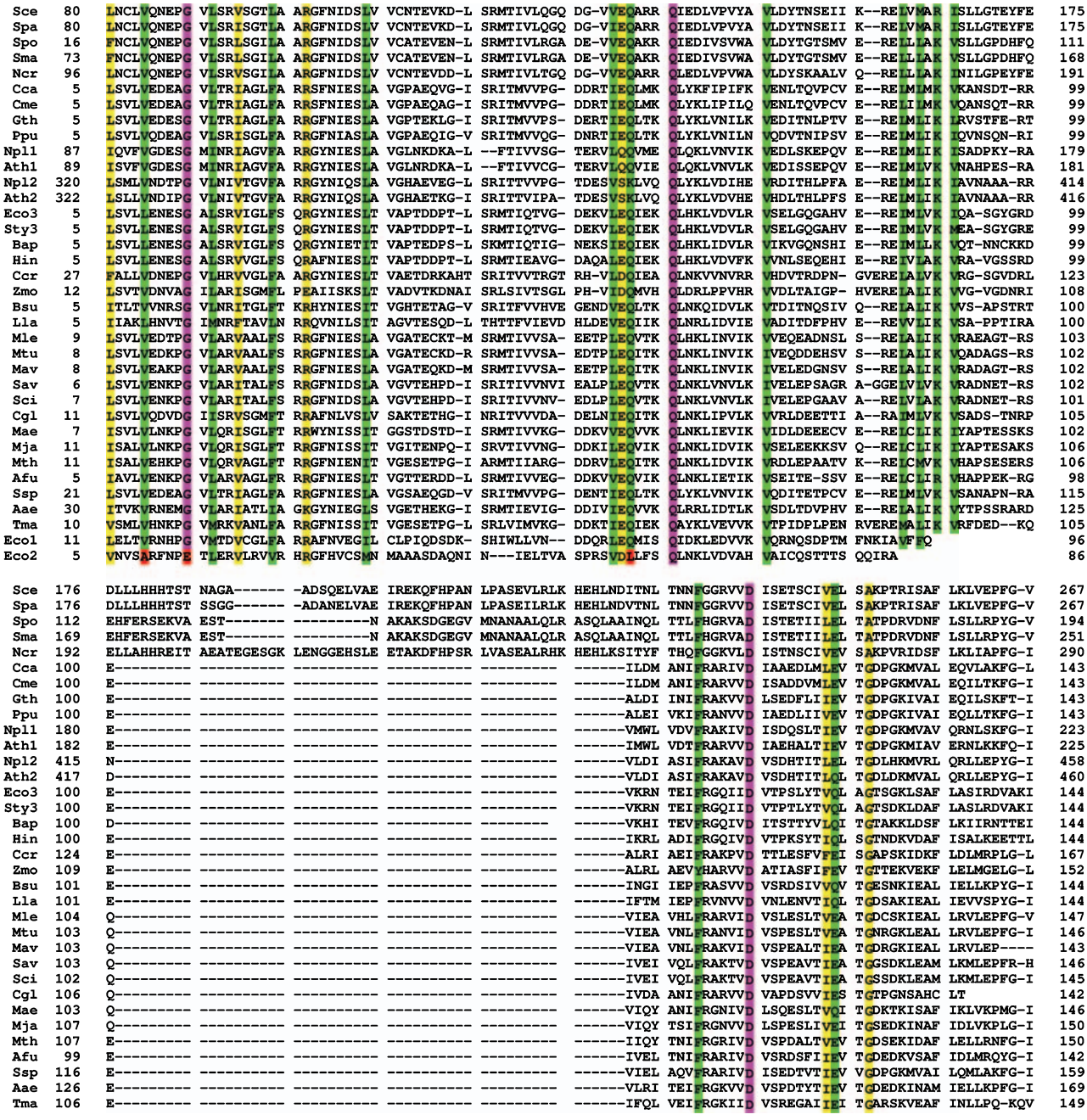

Fig. 17. Alignment of the core region of known and putative AHAS regulatory subunit protein sequences. Sequences were aligned using the Pileup program (Feng and Doolittle, 1987). Sequences shown are for fungi (Sce, *Saccharomyces cerevisiae*; Spa, *Saccharomyces pastorianus*; Spo, *Schizosaccharomyces pombe*; Sma, *Schizosaccharomyces malidevorans*; Ncr, *Neurospora crassa*), algae (Cca, *Cyanidium caldarium*; Cme, *Cyanidioschyzon merolae*; Gth, *Guillardia theta*; Ppu, *Porphyra purpurea*), plants (Npl1, *Nicotiana plumbaginifolia* repeat 1; Npl2, *N. plumbaginifolia* repeat 2; Ath1 *Arabidopsis thaliana* repeat 1; Ath1 *Arabidopsis thaliana* repeat 2), eubacteria (Eco1, *Escherichia coli* isozyme I; Eco2, *E. coli* isozyme II; Eco3, *E. coli* isozyme III; Sty3, *Salmonella typhimurium* isozyme III; Bap, *Buchnera aphidicola*; Hin, *Haemophilus influenzae*; Ccr, *Caulobacter crescentus*; Zmo, *Zymomonas mobilis*; Bsu, *Bacillus subtilis*; Lla, *Lactococcus lactis*; Mle, *Mycobacterium leprae*; Mtu, *Mycobacterium tuberculosis*; Mav, *Mycobacterium avium*; Sav, *Streptomyces avermitilis*; Sci, *Streptomyces cinnamonensis*; Cgl, *Corynebacterium glutamicum*; Ssp, *Synechocystis* sp; Aae, *Aquifex aeolicus*; Tma, *Thermotoga maritima*), and archaea (Mae, *Methanococcus aeolicus*; Mja, *Methanococcus jannaschii*; Mth, *Methanobacterium thermoautotrophicum*; Afu, *Archaeoglobus fulgidus*). Residues highlighted in pink are identical in all sequences, residues belonging to the strong conservation group (STA, NEQK, NHQK, NDEQ, QHRK, MILV, MILF, HY, FYW) are highlighted in green, and residues in the weaker conservation group (CSA, ATV, SAG, STNK, STPA, SGND, SNDEQK, NDEQHK, NEQHRK, FVLIM, HFY, HY, FYW) are highlighted in yellow. The three non-conserved residues of *E. coli* isozyme II are highlighted in red (A9, E14 and L58)

between the N-terminal half of *E. coli* AHASIII RSU and the C-terminal regulatory domain of 3-phosphoglycerate dehydrogenase. One of the main differences between these two models is that the former has two BCAA binding sites with different specificities at the interface between the two repeats within an RSU, while the latter has two identical binding sites at the interface between a pair of RSU monomers. Lee and Duggleby (2002) tested their model by mutating four residues in each repeat of the *A. thaliana* RSU and testing the effect of BCAAs on these mutants. All of the mutants were able to activate the CSU, but the response to the BCAAs was complicated and difficult to interpret. Mutagenesis studies have also supported the model of Mendel et al. (2001). Later, Mendel et al. (2003) determined that while the N-terminal domain (first 76 amino acids) of *E. coli* AHASIII was capable of activating the CSU, the entire subunit was required for valine binding and inhibition.

Which of these two models is correct, if either, will only be settled when the structure of an RSU is determined. However, the crystallization of an RSU has never been reported. Understanding the assembly of the complete enzyme, activation of the CSU by the RSU, and transmission of regulatory signals from the RSU to the CSU are fascinating problems that will not be resolved until the structure of the entire complex can be determined.

2.5 AHAS inhibitors

2.5.1 Herbicidal AHAS inhibitors on the market

Five major classes of herbicides that target AHAS are marketed in various countries throughout the world. These include the sulfonylaminocarbonyltriazolinones, triazolopyrimidines, pyrimidinylsalicylic acids (also known as pyrimidinyloxybenzoic acids and pyrimidinylthiobenzoic acids), sulfonylureas and the imidazolinones. In each case the herbicide is a time-dependent and potent inhibitor of AHAS (Geier et al., 2001; Gerwick et al., 1990; Shimizu et al., 1994a; LaRossa and Schloss, 1984; Shaner et al., 1984). Our discussion of these herbicides will be limited to the latter four classes because, as far as we are aware, although the sulfonylaminocarbonyltriazolinones are currently available for use in crops (flucarbazone marketed by Bayer CropScience as Everest™ and propoxycarbazone marketed as Attribut™/Olympus™), the interaction of these herbicides with AHAS has yet to be studied on a molecular level. One example of this herbicide class, flucarbazone, is shown in Fig. 18.

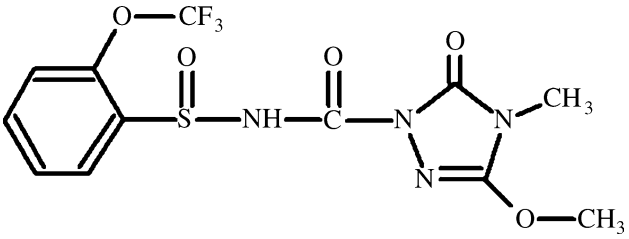

Fig. 18. Flucarbazone (Everest™), a sulfonylaminocarbonyltriazolinone

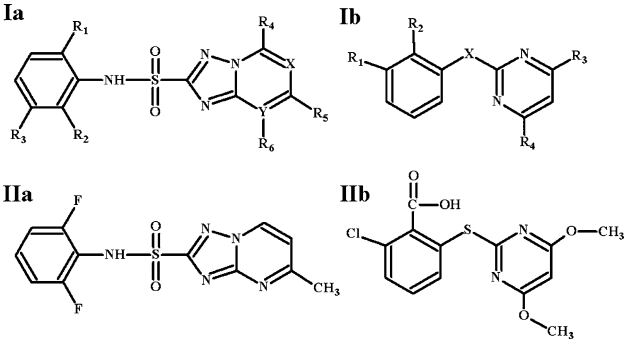

Fig. 19. The general structure for the triazolopyrimidines (**Ia**) and the pyrimidinylsalicylic acids (**Ib**), with the specific examples of one member of each family, flumetsulam (**IIa**) and pyrithiobac (**IIb**)

The triazolopyrimidines (Fig. 19, **Ia**) were invented in the late 1980's, by Dow Elanco (Gerwick et al., 1990), and are now manufactured by Dow Agrosciences. Flumetsulam was the first triazolopyrimidine on the market in the 1990's, sold as Broadstrike™ (Fig. 19, **Ib**). Post emergent application of flumetsulam at 9 g/ha controls >80% of broad-leafed weeds such as *Abutilon theophrasti* (velvetleaf) (Kleschick et al., 1992). In general, triazolopyrimidines consist of a di- or tri-substituted aromatic ring linked by a short bridge to a substituted triazolopyrimidine ring system (Fig. 19, **Ia**). R_1 and R_2 substituents are usually electron withdrawing groups such as Cl (diclosulam), F (flumetsulam), or CF_3 (penoxsulam), while R_3 and R_5 may be combinations of either CH_3, CF_3, OCH_3, H, or F. If Y = CH, R_6 is usually F or OCH_3; R_4 may be OCH_3, OCH_2CH_3, or H. One member of this class was shown to be a mixed inhibitor of *Catharanthus roseus* (vinca) AHAS with an I_{50} of 48.3 nM (Babczinski and Zelinski, 1991). Alternatively, the aromatic ring may be replaced with a quinoline ring to give ''quinoline-linked triazolopyrimidines'' which are also potent inhibitors of AHAS ($IC_{50} < 100$ nM) (Namgoong et al., 1999).

The pyrimidinylsalicylic acids (Fig. 19, **Ib**) were developed in the late 1980's by chemists at Kumiai Chemical Industry Co. Ltd., Ihara Chemical Industry Co. Ltd and co-developed by DuPont (Shimizu et al., 1994a).

Pyrithiobac (Fig. 19, **IIb**) was first registered in 1995 with the tradename Staple^{TM} for weed management within *Gossypium hirsutum* (cotton) crops in the United States of America, and can be applied post-emergence at a rate of 70 g/ha. The general structure of this class of herbicide (Fig. 19, **Ib**) consists of a di-substituted pyrimidine ring linked by either a sulfur atom (pyrimidinylthiobenzoic acid) or an oxygen atom (pyrimidinyloxybenzoic acid) to a substituted benzene ring. Most commonly, substituents R_3 and R_4 are methoxy groups, R_2 is a carboxyl group, and R_1 substitutions can vary from a single chlorine atom (pyrithiobac, Fig. 19, **IIb**) to a large aromatic ring (bispyribac). Inhibition of plant AHAS by the pyrimidinylsalicylic acids is potent and of the noncompetitive type with respect to pyruvate ($K_{is} = 5.0$ nM, $K_{ii} = 22$ nM for pyrithiobac inhibition of *P. sativum* AHAS) (Shimizu et al., 1994b).

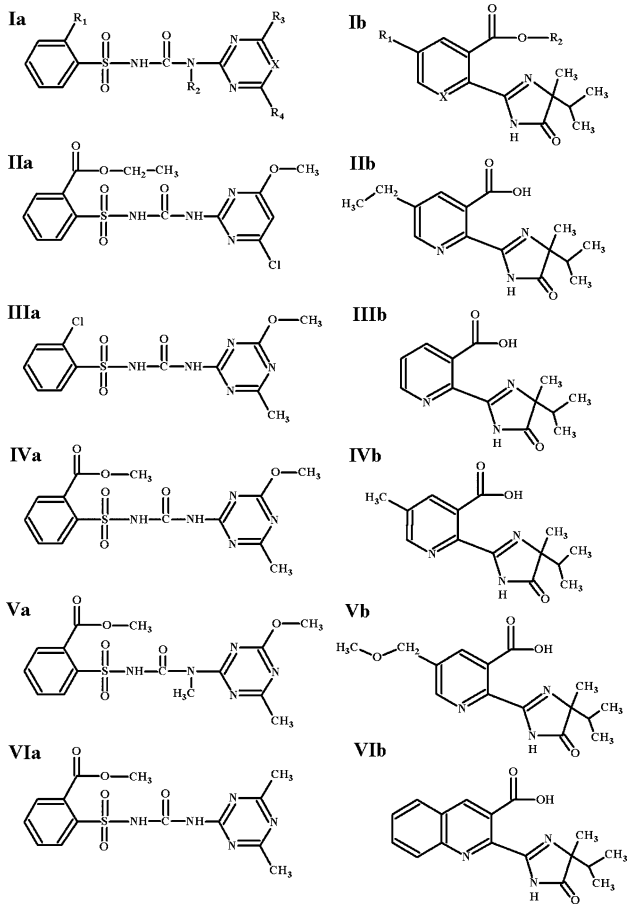

Fig. 20. The general structures for the sulfonylureas (**Ia**) and imidazolinones (**Ib**) are illustrated. Examples of sulfonylureas include chlorimuron ethyl (CE, **IIa**), chlorsulfuron (CS, **IIIa**), metsulfuron methyl (MM, **IVa**), tribenuron methyl (TB, **Va**), and sulfometuron methyl (SM, **VIa**). Imazethapyr (IT, **IIb**), imazapyr (IP, **IIIb**), imazapic (**IVb**), imazamox (**Vb**), and imazaquin (IQ, **VIb**) are examples of imidazolinones

The most popular herbicidal AHAS inhibitors currently on the market for broad spectrum weed control in major crops are the sulfonylureas and imidazolinones (Fig. 20) because they are highly selective, potent, and nontoxic to animals (Shaner and Singh, 1997). The sulfonylureas were developed in the late 1970's by Dr. George Levitt of DuPont (Levitt, 1978; Bhardwaj, 2006) and the imidazolinones in the early 1980's by Dr. Marinus Los of American Cyanamid (now part of BASF) (Los, 1984). However, neither class of herbicide was developed specifically to inhibit AHAS. In fact it was not until 1984, which was two years after the introduction of the first sulfonylurea, chlorsulfuron (CS, sold as Glean^{TM}), that AHAS was determined to be the site action for the sulfonylureas (Ray, 1984; LaRossa and Schloss, 1984; Chaleff and Mauvais, 1984). In the same year, but two years before the introduction of imazaquin (IQ, sold as Scepter^{TM}) as the first commercial imidazolinone herbicide, it was shown that the imidazolinones also act by inhibiting AHAS (Shaner et al., 1984). Owing to the low application rates of the sulfonylureas and imidazolinones (5–100 g/ha), their introduction to the market has decreased the total amount of herbicide applied to crops every year by more than 200 million pounds (Bhardwaj, 2006).

One of the most attractive features of the sulfonylureas and imidazolinones is that, due to differential metabolism among various plant species, it is possible to identify compounds that only particular crop species are able to detoxify (Shaner and Singh, 1997). The sulfonylureas and imidazolinones vary in their manners of absorption and translocation as well as the degree of AHAS inhibition within plants, however these three mechanisms contribute very little to the widely variable effects on different plants (Shaner and Singh, 1997). The most diverse effects of these inhibitors on plants are due to differential metabolism across assorted species (Shaner and Singh, 1997). For example, detoxification of the herbicides can be achieved by dealkylation, ring hydroxylation, glucose conjugation, or ring cleavage (Shaner and Singh, 1997). In this way, it is possible for selected plants, such as the crop of interest, to completely inactivate the compound within a few hours following application (Shaner and Singh, 1997). Alternatively, rather than selecting the herbicide to suit the crop, it has become popular to develop crops which are resistant to the herbicides (Tan et al., 2005).

The general structure for the classic sulfonylureas and five examples of these are shown in Fig. 20, **Ia**–**VIa**. Although the structures of sulfonylureas can vary considerably, most consist of an *ortho*-substituted (R_1) aromatic ring linked to either a *meta* di-substituted triazine or pyr-

imidine ring through a sulfonylurea bridge. The *ortho* substituent of the aromatic ring varies from methyl or ethyl carboxyl esters to much larger groups such as trifluoropropane (prosulfuron); however, one of the more potent sulfonylureas, CS has a single chlorine atom in this position (Fig. 20, **IIIa**). Typically, the sulfonylurea bridge is as shown in Fig. 20, **Ia**, and is unsubstituted in the R_2 position. However, slight elongation of the bridge by the addition of a methylene group (bensulfuron methyl) or an oxygen atom (ethoxysulfuron) adjacent to the sulfonyl group is tolerated. Tribenuron methyl (TB) (Fig. 20, **Va**) is an example of a sulfonylurea with a bridge substituted at R_2. The heterocycle is usually di-substituted with smaller methoxy and/or methyl groups at R_3 and R_4. One of the original and most potent sulfonylureas, chlorimuron ethyl (CE, Fig. 20, **IIa**), has both a methoxy group and a chlorine atom at R_3/R_4. The structures of the imidazolinones (Fig. 20, **Ib**–**VIb**) are much less variable than the sulfonylureas. In general (Fig. 20, **Ib**), most of the commercial imidazolinones consist of a carboxylated pyridine ring, which may be substituted at R_1 and/or R_2. The pyridine ring can also be replaced with a benzene ring (X=CH) (imazamethabenz methyl) or a quinoline ring (IQ) (Fig. 20, **VIb**). The best herbicidal activity is obtained with a dihydroimidazolone ring that is substituted with methyl and isopropyl groups as shown (Fig. 20, **Ib**); both the *S* and *R* configurations are active, though the *R* isomer is ten-fold more effective as an herbicide (Los, 1984; Stidham and Singh, 1991).

Both the sulfonylureas and the imidazolinones inhibit AHAS in a time-dependent manner (LaRossa and Schloss, 1984; Ray, 1984; Muhitch et al., 1987; Chang and Duggleby, 1997; Hill and Duggleby, 1998). Both phases of inhibition are dependent upon the concentration of inhibitor added and tight-binding effects are apparent when the concentrations of the enzyme and inhibitor are approximately equal (Hill and Duggleby, 1998). The sulfonylureas have been reported to be mixed (Durner and Böger, 1988; Durner et al., 1991; Babczinski and Zelinski, 1991; Hill et al., 1997), uncompetitive (Xing and Whitman, 1987) and nearly competitive inhibitors with respect to pyruvate (Schloss, 1984, 1990; Ahan et al., 1992). The imidazolinones have been described as either mixed (Schloss et al., 1988; Ahan et al., 1992) or uncompetitive (Shaner et al., 1984; Durner et al., 1991; Babczinski and Zelinski, 1991; Chang and Duggleby, 1997) inhibitors of AHAS. In general, the imidazolinones inhibit plant AHAS in the μM range, while the sulfonylureas are more potent inhibitors of the plant enzyme, with K_i^{app} values in the nM range (Chang and Duggleby, 1998).

2.5.2 The herbicide-binding site of AHAS

The crystal structures of CE, CS, TB, sulfometuron methyl (SM) (Fig. 20, **VIa**), and metsulfuron methyl (MM) (Fig. 20, **IVa**), in complex with both *S. cerevisiae* AHAS (Pang et al., 2003; McCourt et al., 2005) and *A. thaliana* AHAS (McCourt et al., 2006), as well as IQ in complex with *A. thaliana* AHAS (McCourt et al., 2006) have been determined. Both classes of herbicide bind within the tunnel leading to the active site thereby blocking substrate access (Fig. 21).

The constellation of amino acid residues which make up the sulfonylurea binding-pocket in *S. cerevisiae* AHAS and *A. thaliana* AHAS are almost identical (refer to Table 2 for equivalent residues involved in herbicide binding). In all ten structures the sulfonylureas are in a conformation in which the aromatic ring of the herbicide is rotated away from the axis of the sulfonylurea bridge so that larger substituents of the aromatic ring, such as the ethyl carboxy ester group of CE, aligns parallel with atoms of the sulfonylurea bridge (Fig. 21a). With a few exceptions, most of the residues (Val196′, Pro197′, Met200′, Ala205′, and Asp376) that are involved in anchoring the aromatic ring of the sulfonylureas make the same, or similar, contacts in AHAS from both organisms. Likewise, the dimethylbenzene ring of FAD always has a hydrophobic interaction with the methoxy substituent on the heterocyclic ring of CE, CS, MM, and TB. In contrast, the interactions of the five sulfonylureas with Gly121′, Phe206′, Lys256′, Met351, Met570, and Val571 of either *S. cerevisiae* AHAS or *A. thaliana* AHAS are quite variable. With the exception of Lys256′, which is hydrogen-bonded to either the nitrogen or oxygen atoms of the sulfonylurea bridge in some of the complexes, all of these residues make hydrophobic contacts with either the substituents on the heterocyclic ring or the pyrimidine ring. In addition, Phe206′ often makes close contacts with *ortho* carboxy ester substituents of the aromatic ring. Although the herbicide binding pocket is quite hydrophobic, in almost all cases, there is at least one water molecule hydrogen-bonded to either nitrogen or oxygen atoms within the sulfonylurea bridge, and/or to a nitrogen atom within the heterocyclic ring. The only contact for Ala122′ is with the terminal methyl group of the carboxy ester substituent on CE in AHAS from both organisms. The only substantial difference in the sulfonylurea binding sites for the two enzymes is that Ser653 is close to the sulfonylureas in *A. thaliana* AHAS. In the plant enzyme this residue makes a hydrogen bond with one or more of the oxygen atoms in the sulfonylurea bridge, whereas the equivalent residue in

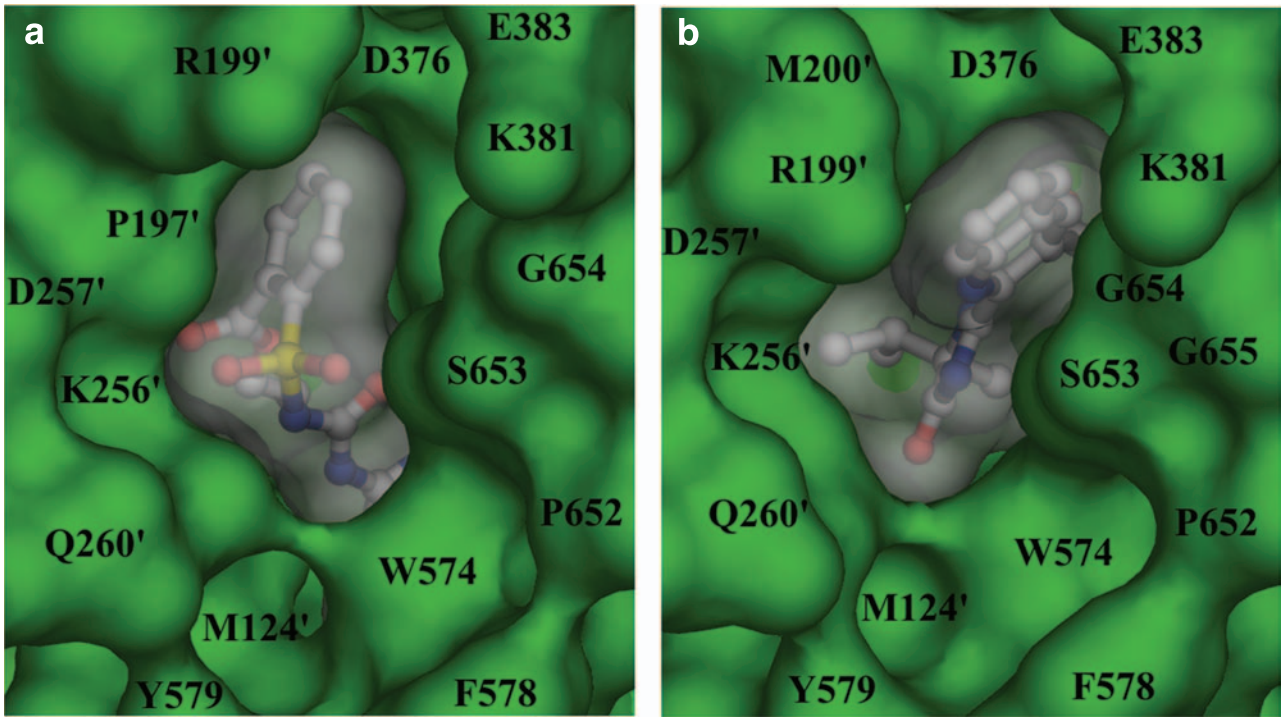

Fig. 21. CE and IQ blocking access to the active site of *A. thaliana* AHAS. A Connolly surface representation of *A. thaliana* AHAS (green) is shown for the CE (**a**) and IQ (**b**) complexes. Both herbicides are represented as ball and stick models with transparent surfaces. Carbon is grey, nitrogen is blue, oxygen is red, and sulfur is yellow. The prime symbol (′) is used to differentiate residues from the two different monomers

S. cerevisiae AHAS, Gly657, lies outside of the herbicide binding pocket.

Two of the most important residues that bind all five sulfonylureas are Trp574 and Arg377, both of which play a critical role in catalysis (Tittmann et al., 2005b). Trp574 is believed to be involved in recognition of the second substrate, and mutation of this residue, which will be discussed later, gives rise to strong resistance against both the sulfonylureas and the imidazolinones. Arg377 is believed to be responsible for substrate recognition by binding the carboxylate moiety of 2-ketoacids (Engel et al., 2004b; Tittmann et al., 2005b). It is therefore interesting to note that the terminal nitrogen atoms of Arg377 are always hydrogen-bonded to one or more of the sulfonyl oxygen atoms, one of the nitrogen atoms of the heterocyclic ring and, if present, the oxygen atom of the meth-

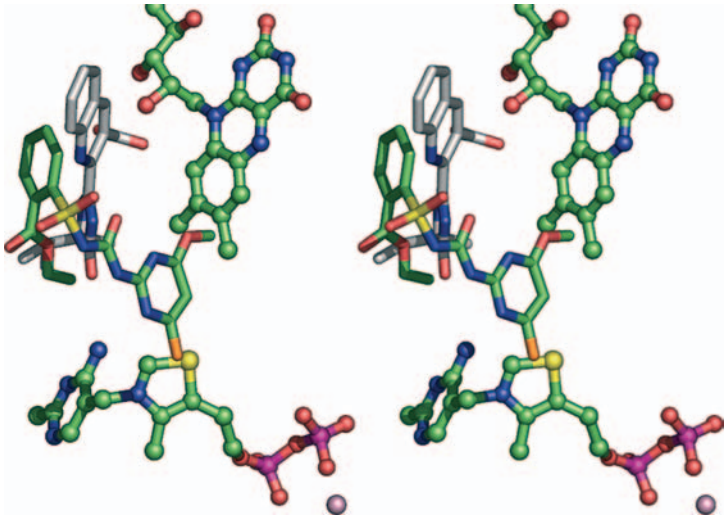

Fig. 22. Stereo view of overlapping sulfonylurea and imidazolinone binding sites in *A. thaliana* AHAS. The CE-AHAS complex has been superimposed onto the IQ-AHAS complex. ThDP and FAD are both represented as ball and stick models, CE and IQ as stick models and Mg^{2+} as a pink sphere. Carbon is grey for IQ, green for CE, ThDP, and FAD. Nitrogen is blue, oxygen red, sulfur yellow, chlorine orange, and phosphorus magenta

oxy substituent on the heterocylic ring. These interactions give further support to the waiting room concept mentioned in Section 2.3.2.

The molecule of IQ bound within the channel leading to the active site is in the *R* configuration and positioned so that the dihydroimidazolone ring is directed toward the C2 centre of ThDP while the quinoline ring protrudes out toward the surface of the protein (Fig. 21b). If the *A. thaliana* AHAS-CE complex is superimposed onto the IQ complex, it is apparent that the two herbicides are overlapping (Fig. 22). However, only the dihydroimidazolone ring and part of the quinoline ring of IQ share part of the sulfonylurea binding site. Of the ten residues involved in securing IQ to the protein, all but two of these, Gly654 and Arg199′, also function to bind sulfonylureas. It is therefore impossible that both herbicides could effectively bind and inhibit AHAS at the same time.

IQ is held in place by 18 hydrophobic interactions, and by a salt bridge between the carboxylic acid substitution and one of the terminal nitrogen atoms of Arg377. The quinoline ring is held in place by Met200′, Asp376, Arg377, Ser653, and Gly654. Three of these contacts, one with Gly654 and two with Met200′, are with the benzene ring of the quinoline, which is absent in imazapyr (IP) (Fig. 20, **IIIb**), and replaced with an ethyl group in imazethapyr (IT) (Fig. 20, **IIb**). These extra contacts may help to explain the order of potency towards *A. thaliana* AHAS (Chang and Duggleby, 1998) for IQ ($K_i^{app} = 3.0\,\mu M$), IT ($K_i^{app} = 9.0\,\mu M$) and IP ($K_i^{app} = 16.7\,\mu M$). The dihydroimidazolone ring itself interacts with Lys256′ and Trp574, while the methyl and isopropyl substituents, which are required for high herbicidal activity (Los, 1984; Stidham and Singh, 1991), interact with the α carbon of Ala122′ and the side-chains of Ala122′, Phe206′, Gln207′, Lys256′, and Trp574. Although the exocyclic oxygen substitution on the dihydroimidazolone ring is absolutely necessary for herbicidal activity, it does not make any contacts with *A. thaliana* AHAS. As mentioned earlier, Ser653 of *A. thaliana* AHAS interacts with the sulfonylureas and IQ, whereas, at least for the sulfonylureas, the equivalent Gly657 of *S. cerevisiae* AHAS does not. This contact undoubtedly contributes to the very much more potent inhibition by imidazolinones of *A. thaliana* compared to *S. cerevisiae* AHAS (Chang and Duggleby, 1998; Duggleby et al., 2003). It is well established that mutating Ser653 renders plant AHAS strongly resistant to imidazolinones (Sathasivan et al., 1991; Hattori et al., 1992; Chang and Duggleby, 1998; Lee et al., 1999; Chong and Choi, 2001).

In addition to the imidazolinone molecule bound within the channel leading to the active site of *A. thaliana* AHAS (Fig. 21b), there is another located in a cleft ∼20 Å away next to a molecule of CHES buffer. We attribute this second, extraneous IQ molecule, to the high concentration of IQ in the crystallization liquor (Pang et al., 2004b) and, since the surrounding residues have never been implicated in herbicide resistance, do not expect it to contribute to the herbicidal activity of IQ. Nevertheless, this second molecule makes several contacts with AHAS. There are fifteen hydrophobic interactions with Gly245, Gly275, Tyr276, Arg279, Pro281, and Asp297. In addition, the exocyclic oxygen of the imidazole ring makes two hydrogen bonds with the terminal nitrogen atom of Lys220 and the backbone nitrogen atom of Arg246.

2.5.3 Mechanism of inhibition

Despite the availability of the sulfonylurea- and imidazolinone-bound AHAS crystal structures, the mechanism of inhibition by these herbicides is still not very well understood. For example, the underlying basis for slow-binding inhibition remains unclear. Most reports have suggested that these herbicides bind tightly to the enzyme following formation of the L-ThDP intermediate (LaRossa and Schloss, 1984; Schloss et al., 1988; Schloss and Van Dyk, 1988; Schloss and Aulabaugh, 1988; Schloss, 1990; Durner et al., 1991; Stidham and Singh, 1991; Delfourne et al., 1994; Southan and Copeland, 1996), which implies that inhibition requires turnover conditions. This finding is consistent with the proposal mentioned earlier that herbicides occupy the waiting room where the second substrate normally binds. However, from the crystal structures (Pang et al., 2003; McCourt et al., 2005, 2006) and other studies (LaRossa and Schloss, 1984; Schloss et al., 1988) it is clear that sulfonylureas are capable of binding to AHAS in the absence of substrate and inactivating the enzyme (Ortega et al., 1996; McCourt, 2004). Interestingly, Ortega et al. (1996) found that ThDP-Mg^{2+} is absolutely required for thifensulfuron methyl-mediated inactivation of *E. coli* AHASII, and they therefore suggested that herbicide-induced inactivation may correspond to a change in enzyme conformation that disfavors the V conformation of ThDP required for catalysis. Since they discovered that the affinity for ThDP may vary considerably among enzymes from different species, they further suggested that failure to remove this cofactor would explain why many reports concerning the irreversibility of herbicide-induced inactivation of AHAS are conflicting. Indeed, in studies where removal of the inhibitor was verified, only the activity of

bacterial AHAS (LaRossa and Schloss, 1984), but not *H. vulgare* AHAS (Durner et al., 1991), which binds ThDP with a much higher affinity than bacterial AHAS (Ortega et al., 1996), could be recovered. Moreover, in the case of the bacterial enzyme which was incubated for several hours in the presence of EDTA, it is more likely that ThDP and Mg^{2+} were separated from the enzyme.

In 1985, Schloss and coworkers purified and characterized *S. typhimurium* AHASII and found that under normal assay conditions the enzyme slowly loses activity with a half time of ~1.5 hours at 37 °C. Interestingly they found that enzyme lability is at least party mediated by ThDP and can be reversed by extended dialysis with EDTA. Recently, studies in our laboratory with *E. coli* AHASII (McCourt, 2004), *S. cerevisiae* AHAS, and PDC (unpublished results) have shown that during the course of catalysis, ThDP is slowly destroyed. Furthermore, in the presence of herbicides this process is somewhat enhanced in AHAS (McCourt, 2004). A possible related observation was reported for pyruvate dehydrogenase (Strumilo et al., 2004) in which it appears that ThDP can be dephosphorylated.

Accordingly, with the exception of one molecule of ThDP in the *S. cerevisiae* AHAS-CE complex (Pang et al., 2003), there is broken electron density in the region of the thiazole and pyrimidine rings for all of the sulfonylurea-bound AHAS structures (McCourt et al., 2005, 2006). In all cases the contour of broken electron density not only differs among *A. thaliana* AHAS-sulfonylurea complexes (PDB codes 1YBH, 1YHY, 1YHZ, 1YI0, and 1YI1, McCourt et al., 2006), but also from the fragmented ThDP molecules in *S. cerevisiae* AHAS-sulfonylurea complexes (PDB codes 1N0H, Pang et al., 2003; 1T9A-D, McCourt et al., 2005). We have suggested possible structures for some of these fragments (McCourt et al., 2005), although we cannot provide a chemical mechanism to explain the fragmentation at this time. Interestingly, there is complete electron density for ThDP in the IQ complex and the contacts which ThDP makes with the enzyme are similar to those for the intact ThDP molecule found in one monomer of the *S. cerevisiae* AHAS-CE complex (Pang et al., 2003) and only slightly different than those for ThDP in the uninhibited complex (PDB code 1JSC, Pang et al., 2002). However, it may be significant that in this AHAS-IQ complex the coordination geometry is distorted around the Mg^{2+} that links the diphosphate tail of ThDP to the protein. Although it will be necessary to conduct further studies to characterize this process, the original idea that herbicides inactivate AHAS by forcing ThDP into an unfavourable conformation (Ortega et al., 1996) is feasible. Deformation of ThDP perturbs the Mg^{2+} coordination geometry in the IQ complex and disrupts one or both rings of the cofactor in the sulfonylurea complexes. Since the conformation of enzyme-bound ThDP is suspected to protect the cofactor from fragmentation (Moore and Kluger, 2002) it is a possibility that modification of this structure may subject the cofactor to intramolecular attack by either the highly reactive carbanionic HE-ThDP intermediate (in the presence of substrate) or by the ylide (in the absence of substrate).

2.5.4 Herbicide-resistant AHAS mutants

There are now more plants resistant to AHAS inhibitors than any other herbicide class and the numbers are rising (Tranel and Wright, 2002). One of the reasons for this high level of tolerance is that resistance is transmitted by a single dominant nuclear-encoded gene (Newhouse et al., 1991) which, on the molecular level, usually results in a single amino acid change in AHAS (Tranel and Wright, 2002). In light of the recent, detailed reviews of herbicide resistance provided by Duggleby and Pang (2000) and Tranel and Wright (2002), our discussion will be brief. Mutations within AHAS which result in herbicide resistance have been studied extensively and many of these have been deliberately introduced using site-directed mutagenesis approaches (for example, Falco et al., 1989; Chang and Duggleby, 1998; Duggleby et al., 2003). The four most common naturally occurring mutations are at amino acids Ala122 (Bernasconi et al., 1995; Tranel and Wright, 2002), Pro197 (Lee et al., 1988; Mourad et al., 1995; Sibony et al., 2001), Trp574 (Lee et al., 1988; Bernasconi et al., 1995; Hattori et al., 1995) and Ser653 (Hattori et al., 1992; Tranel and Wright, 2002). With the exception of one report (Sibony et al., 2001), all mutations of Pro197 give rise to either strong sulfonylurea (Haughn et al., 1988) or triazolopyrimidine resistance (Mourad and King, 1992). Mutations of Ala122 impart strong resistance to imidazolinones, and mutations of Ser653 have been reported to result in resistance to both the imidazolinones (Hattori et al., 1992) and the pyrimidinylsalicylic acids (Mourad and King, 1992). Finally, cross tolerance among sulfonylureas, imidazolinones, pyrimidylsalicylic acids, and triazolopyrimidines is observed with mutations of Trp574 (Bernasconi et al., 1995). With the information available from the crystal structures of AHAS in complex with the sulfonylureas (Pang et al., 2003; McCourt et al., 2005, 2006) and an imidazolinone (McCourt et al., 2006), it has been possible to offer explanations as to why some mutations result in resistance to one class of herbicide, but

not the other (McCourt et al., 2006). For instance, it is now known that most residues which bind the imidazolinones also bind the sulfonylureas; however, there are several additional residues comprising the sulfonylurea binding site which do not interact with imidazolinones. Although the crystal structures of AHAS in complex with pyrimidinylsalicylic acids and triazolopyrimidines are yet to be solved, it is expected that these two classes of herbicide bind to the same sites within AHAS. Based on the cross-resistance data it appears that pyrimidinylsalicylic acids bind in a site that closely overlaps that of the imidazolinones while the triazolopyrimidines occupy the same site as the sulfonylureas.

2.5.5 Other inhibitors of AHAS

Other compounds that were developed to act as inhibitors of AHAS but, as far as we are aware, are not currently on the market as herbicides include sulfonylamide azines, pyrimidylmandelic acids, benzenesulfonyl carboxamides, sulfonylimino-triazinyl heteroazoles, substituted sulfonyldiamides (Babczinski and Zelinski, 1991), sulfonylcarboxamides (Stidham, 1991), vinylogous sulfonylureas (McFadden et al., 1993), 4,6-dimethoxypyrimidines (Fig. 23, **Ia** and **IIa**, Table 5, Shim et al., 1995), carbamoylpyrazolines (Fig. 23 **Ib**, Table 5, Babczinski and Zelinski, 1991), acetyl phosphinate (Table 5, Abell et al., 1995), N-phthalylanilides and dicarboximide derivatives of valyl anilide (Table 5, Huppatz and Casida, 1985). In some cases the fact that these compounds are not commercial herbicides is undoubtedly because they are not specific for AHAS and could be toxic to animals. For example acetyl phosphinate inhibits pyruvate dehydrogenase (Schonbrunn-Hanebeck et al., 1990), an enzyme that is essential for oxidative carbohydrate metabolism in many organisms. In other cases, the inhibitor may not readily reach its target in a plant due to poor uptake or metabolic detoxification. Furthermore, even if a compound is a specific and effective herbicide, it must compete in the market with sulfonylureas and imidazolinones, which are cheap, effective and safe.

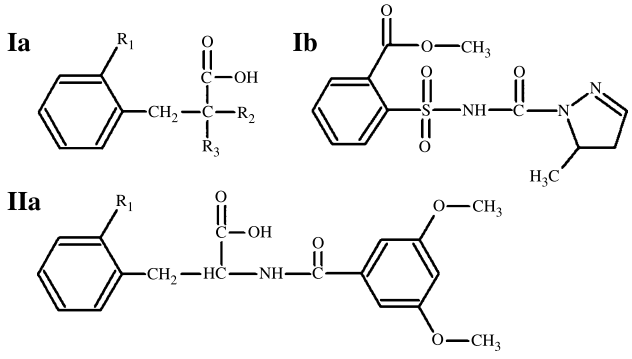

Fig. 23. The general structure of 4,6-dimethyoxypyrimidines (**Ia**), the structure of K11570, a 4,6-dimethoxypyrimidine (**IIa**), and of carbamoylpyrazolinone (**Ib**)

AHAS is also inhibited by the ThDP analog thiamin thiazolone diphosphate (TThDP) (Table 5, Schloss, 1991; Roux et al., 1996), ubiquinone-0 and ubiquinone-5 (Fig. 24, Table 5, Schloss et al., 1988), hydroxypyruvate, which is a suicidal inhibitor of *E. coli* AHASII (Duggleby, 2005), and gliotoxin from the fungus *Aspergillus flavus* (Haraguchi et al., 1996).

Until recently, there has been little interest in the development of AHAS inhibitors as antimicrobial agents because most organisms would be able to overcome the effects of these inhibitors by obtaining the BCAAs from

Table 5. Properties of some AHAS inhibitors

Inhibitor	Enzyme	Inhibitory concentration (μM)	Inhibition type[a]
N-phthalyl-L-valine anilide	*Z. mays*[b]	2.3[c]	ND
1-cyclohexene-1,2-dicarboximide derivative of valine anilide	*Z. mays*[b]	3.5[c]	ND
Ubiquinone-0	*S. typhimurium* II[d]	110[e], 150[f]	Noncompetitive
Ubiquinone-5	*S. typhimurium* II[d]	660[e], 400[f]	Noncompetitive
TThDP	*Z. mays*[g]	0.3	ND
acetylphosphinate	Bacterial II[h]	15	competitive
4,6-dimethyoxypyrimidine	*H. vulgare*[i]	0.2[b], 1.1[f], 2.2[e]	mixed
carbamoylpyrazoline	*C. roseus*[j]	2.9[c]	mixed

The inhibitory concentrations are expressed as K_i^{app} unless otherwise noted. For slow, tight-binding inhibitors (carbamoylpyrazoline, TThDP, ubiquinone-0, ubiquinone-5) these values are calculated from initial velocities. [a] Type of inhibition with respect to pyruvate. [b] Huppatz and Casida (1985). [c] IC_{50}. [d] Schloss et al. (1988). [e] K_{is}. [f] K_{ii}, [g] Roux et al. (1996). [h] Abell et al. (1995). [i] Shim et al. (1995). [j] Babczinski and Zelinski (1991). ND, not determined

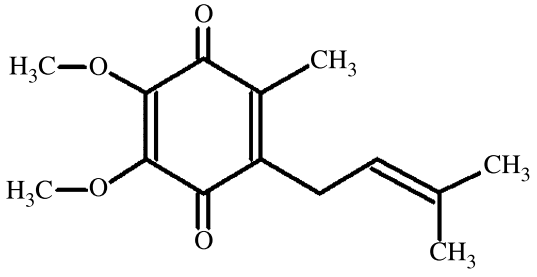

Fig. 24. Ubiquinone-5

their environment. However, the mycobacteria are better targets for amino acid synthesis inhibitors than other bacteria because they replicate within phagocytes, such as macrophages, where the availability of certain amino acids may be limited. In 1998, Grandoni and colleagues demonstrated that selected sulfonylurea herbicides are effective at inhibiting the growth of several *M. tuberculosis* strains. Sulfometuron methyl and metsulfuron methyl inhibited the growth of *M. tuberculosis* at concentrations <20 μM which is 100-fold less potent than two of the drugs (isoniazid and rifampicin) currently used to treat the disease. The sulfonylureas are also moderately good inhibitors of *M. avium* AHAS with the lowest K_i^{app} values ranging from 13.5 μM–215 μM (Zohar et al., 2003). Interestingly, in both studies not all of the sulfonylureas tested were effective and the imidazolinones showed little or no inhibitory activity at all (Grandioni et al., 1998; Zohar et al., 2003).

The incidence of tuberculosis has reached uncontrollable levels especially in several third world countries in recent years and there are now drug resistance problems which complicate its treatment (Okeke et al., 2005). New measures, such as the development of novel drugs, are required to control the spread of disease and to treat infected patients. In the past year, Choi and colleagues (2005) purified and characterized recombinant AHAS catalytic and regulatory subunits from *M. tuberculosis*. Using a chemical library they screened thousands of compounds and identified four that inhibit >90% of the *M. tuberculosis* AHAS activity at a concentration of 40 μM. The two most active compounds, KHG20612 and KHG20614 with IC_{50} values of 1.77 μM and 1.99 μM, respectively, are shown in Fig. 25. With the exception of pyrazosulfuron, all four compounds are better inhibitors than each of ten sulfonylureas tested. The development of this new class of inhibitors is an exciting prospect for the future of antituberculosis agents.

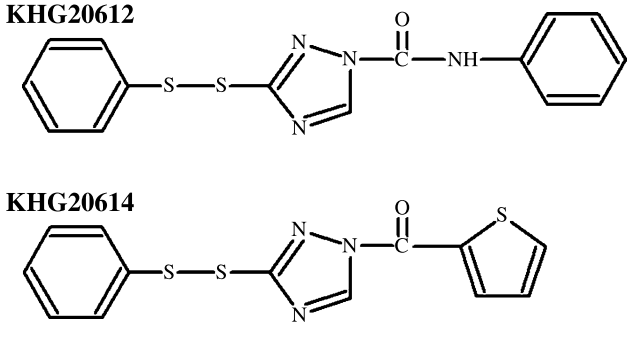

Fig. 25. Inhibitors of *M. tuberculosis* AHAS

3. Concluding remarks

Structural biology is approaching the stage where it is reasonable to expect that the structures will be solved for all enzymes in any given biochemical pathway. In the case of BCAA biosynthesis, this point has nearly been reached; the only enzyme for which there are no crystal structures available is DHAD. Also, for both AHAS and bacterial 3-IPMD, only one of the two subunits remain to be solved. This structural information will cast light upon the way in which this pathway evolved and, in addition, will provide new opportunities for the rational design of bioactive compounds. To date, the only bioactive compounds that target this pathway are the various AHAS-inhibiting herbicides and these were all, without exception, developed by classical biological screening and synthetic chemistry. While the herbicides used currently are undoubtedly highly successful, resistance is becoming a problem and eventually new herbicides will need to be developed. Moreover, targeting AHAS or other enzymes in this pathway may lead to new antimicrobial agents. There has been a small amount of research in this area, and undoubtedly there will be more in the future.

While herbicide resistance can reduce the value of current compounds for weed control, it also opens up the opportunity of tailoring resistance in chosen crops. The introduction of such genetically modified plants does raise several ethical and environmental concerns but there are also clear benefits that should not be overlooked. The better these genetically modified crops are understood, the greater is the likelihood that the drawbacks can be minimized.

Finally, understanding the enzymes in this pathway will extend the possibilities for chemoenzymatic syntheses of various compounds on an industrial scale. Again, studies using AHAS are leading the way but there is certainly the potential to use other enzymes in the pathway for this purpose.

Note added in proof

The structure of the RSU of *E. coli* AHASIII has now been solved (Kaplun et al. (2006), J Mol Biol 357: 951–963).

Acknowledgements

This work supported in part by the Australian Research Council, grant number DP0450275. We thank Dr. Rajiv Tyagi for providing the impetus for us to write this review. Figures were drawn with Chemsketch (ACD labs, Toronto, Canada), and PyMol (DeLano Scientific, LLC).

References

Abell LM, Hanna WS, Kunitsky KJ, Kerschen JA (1995) Active site inhibitors of acetohydroxyacid synthase. Pesticide Sci 44: 89–92

Abell LM, Schloss JV (1991) Oxygenase side reactions of acetolactate synthase and other carbanion-forming enzymes. Biochemistry 30: 7883–7887

Ahan TW, Kim DW, Choi JD (1992) Inhibition of acetohydroxyacid synthase by sulfonylureas and imidazolinones. Korean Biochem J 25: 636–641

Ahn HJ, Eom SJ, Yoon H-J, Lee B-I, Cho H, Suh SW (2003) Crystal structure of Class I acetohydroxy acid isomeroreductase from *Pseudomonas aeruginosa*. J Mol Biol 328: 505–515

Altmiller DH, Wagner RP (1970) Purification and properties of dihydroxy acid dehydratase from soluble and mitochondrial fractions of *Neurospora crassa*. Arch Biochem Biophys 138: 160–170

Alvarez FJ, Ermer J, Huebner G, Schellenberger A, Schowen RL (1991) Catalytic power of pyruvate decarboxylase. Rate-limiting events and microscopic rate constants from primary carbon and secondary hydrogen isotope effects. J Am Chem Soc 113: 8402–8409

Andrews CO, Fischer JH (1994) Gabapentin: a new agent for the management of epilepsy. Ann Pharmacother 28: 1188–1196

Arfin SM (1969) Evidence for an enol intermediate in the enzymatic conversion of alpha, beta-dihydroxyisovalerate to alpha-ketoisovalerate. J Biol Chem 244: 2250–2251

Arfin SM, Koziell DA (1973a) Acetolactate synthase of *Pseudomonas aeruginosa* I. Purification and allosteric properties. Biochim Biophys Acta 321: 348–355

Arfin SM, Koziell DA (1973b) Acetolactate synthase of *Pseudomonas aeruginosa* II. Evidence for the presence of two nonidentical subunits. Biochim Biophys Acta 321: 365–360

Aulabaugh A, Schloss JV (1990) Oxalyl hydroxamates as reaction-intermediate analogues for ketol-acid reductoisomerase. Biochemistry 29: 2824–2830

Babczinski P, Zelinski T (1991) Mode of action of herbicidal ALS-inhibitors on acetolactate synthase from green plant cell cultures, yeast and *Escherichia coli.* Pestic Sci 31: 305–323

Barak Z, Calvo JM, Schloss JV (1988) Acetolactate synthase Isozyme III from *Escherichia coli*. Methods Enzymol 166: 455–458

Barak Z, Chipman DM, Gollop N (1987) Physiological implications of the specificity of acetohydroxy acid synthase isozymes of enteric bacteria. J Bacteriol 169: 3750–3756

Barger G, Bergel F, Todd AR (1935) Über das Thiochrom aus Vitamin B_1 (Antineurin). Chem Ber 68: 2257–2262

Bar-Ilan A, Balan V, Tittmann K, Golbik R, Vyazmensky M, Hübner G, Barak Z, Chipman DM (2001) Binding and activation of thiamin diphosphate in acetohydroxyacid synthase. Biochemistry 40: 11946–11954

Bauerle RH, Freundlich M, Størmer FC, Umbarger HE (1964) Control of isoleucine, valine and leucine biosynthesis: II. End-product inhibition by valine of acetohydroxy acid synthetase in *Salmonella typhimurium*. Biochim Biophys Acta 92: 142–149

Bekkaoui F, Schorr P, Crosby WL (1993) Acetolactate synthase from *Brassica napus*: Immunological characterization and quaternary structure of the native enzyme. Physiol Plant 88: 475–484

Bernasconi P, Woodworth AR, Rosen BA, Subramanian MV (1995) A naturally occurring point mutation confers broad range tolerance to herbicides that target acetolactate synthase. J Biol Chem 270: 17381–17385

Berthold CL, Moussatche P, Richards NGJ, Lindqvist Y (2005) Structural basis for activation of the thiamin diphosphate-dependent enzyme oxalyl-CoA decarboxylase by adenosine diphosphate. J Biol Chem 280: 41645–41654

Bhardwaj G (2006) From pioneering invention to sustained innovation: The story of sulfonylurea herbicides. Chem Herit (in press)

Bigelis R, Umbarger HE (1976) Yeast alpha-isopropylmalate isomerase. Factors affecting stability and enzyme activity. J Biol Chem 251: 3545–3552

Biou V, Dumas R, Cohen-Addad C, Douce R, Job D, Pebay-Peyroula E (1997) The crystal structure of plant acetohydroxy acid isomeroreductase complexed with NADPH, two magnesium ions and a herbicidal transition state analog determined at 1.65 Å resolution. EMBO J 16: 3405–3415

Blatt JM, Pledger WJ, Umbarger HE (1972) Isoleucine and valine metabolism in *Escherichia coli*. XX. Multiple forms of acetohydroxy acid synthetase. Biochem Biophys Res Commun 48: 444–450

Bode R, Birnbaum D (1991) Some properties of the leucine-biosynthesizing enzymes from *Candida maltosa*. J Basic Microbiol 31: 21–26

Bode R, Schult I, Birnbaum D (1986) Purification and some properties of L-threonine dehydratase from *Candida maltosa.* J Basic Microbiol 26: 443–451

Bourgin JP, Goujaud J, Missonier C, Pethe C (1985) Valine-resistance, a potential marker in plant cell genetics. I. Distinction between two types of valine-resistant tobacco mutants isolated from protoplast-derived cultures. Genetics 109: 393–407

Bowen TL, Union J, Tumbula DL, Whitman WB (1997) Cloning and phylogenetic analysis of the genes encoding acetohydroxyacid synthase from the archaeon *Methanococcus aeolicus*. Gene 188: 77–84

Breslow RB (1958) On the mechanism of thiamin enzymes. IV. Evidence from studies on model systems. J Am Chem Soc 80: 3719–3726

Burns RO, Calvo J, Margolin P, Umbarger HE (1966) Expression of the leucine operon. J Bacteriol 96: 1570–1576

Caines ME, Elkins JM, Hewitson KS, Schofield CJ (2004) Crystal structure and mechanistic implications of N_2-(2-carboxyethyl)arginine synthase, the first enzyme in the clavulanic acid biosynthesis pathway. J Biol Chem 279: 5685–5692

Carroll NM, Sheehan D, Cogan TM (1995) Purification of alpha-acetolactate synthase from *Leuconostoc lactis* NCW1. Biochem Soc Trans 23: 366S

Cassady WE, Leiter EH, Bergquist A, Wagner RP (1972) Separation of mitochondrial membranes of *Neurospora crassa* II. Submitochondrial localization of the isoleucine-valine biosynthetic pathway. J Cell Biol 53: 66–72

Chaleff RS, Mauvais CJ (1984) Acetolactate synthase is the site action of two sulfonylurea herbicides in higher plants. Science 224: 1443–1445

Chanchaem W, Palittapongarnpim P (2002) A variable number of tandem repeats result in polymorphic alpha-isopropylmalate synthase in *Mycobacterium tuberculosis.* Tuberculosis (Edinb) 82: 1–6

Chang AK, Duggleby RG (1997) Expression, purification and characterization of *Arabidopsis thaliana* acetohydroxyacid synthase. Biochem J 327: 161–169

Chang AK, Duggleby RG (1998) Herbicide-resistant forms of *Arabidopsis thaliana* acetohydroxyacid synthase: Characterization of the catalytic properties and sensitivity to inhibitors of four defined mutants. Biochem J 333: 765–777

Chang S-I, Kang M-K, Choi J-D, Namgoong S-K (1997) Soluble over expression in *Escherichia coli*, and purification and characterization of

wild-type recombinant tobacco acetolactate synthase. Biochem Biophys Res Commun 234: 549–553

Chang Y-Y, Cronan JE Jr (1988) Common ancestry of *Escherichia coli* pyruvate oxidase and the acetohydroxy acid synthases of the branched-chain amino acid biosynthetic pathway. J Bacteriol 170: 3937–3945

Chipman D, Barak Z, Schloss JV (1998) Biosynthesis of 2-aceto-2-hydroxy acids: acetolactate synthases and acetohydroxyacid synthases. Biochim Biophys Acta 1385: 401–419

Chipman DM, Duggleby RG, Tittmann K (2005) Mechanisms of acetohydroxyacid synthases. Curr Opin Chem Biol 9: 475–481

Choi KJ, Yu YG, Hahn HG, Choi JD, Yoon MY (2005) Characterization of acetohydroxyacid synthase from *Mycobacterium tuberculosis* and the identification of its new inhibitor from the screening of a chemical library. FEBS Lett 579: 4903–4910

Chong C-K, Choi J-D (2000) Amino acid residues conferring herbicide tolerance in tobacco acetolactate synthase. Biochem Biophys Res Commun 279: 462–467

Chong C-K, Shin H-J, Chang S-I, Choi J-D (1999) Role of tryptophanyl residues in tobacco acetolactate synthase. Biochem Biophys Res Commun 259: 136–140

Cromartie TH, Walsh CT (1976) *Escherichia coli* glyoxylate carboligase. Properties and reconstitution with 5-deaza FAD and 1,5-dihydrodeaza $FADH_2$. J Biol Chem 251: 329–333

Crout DHG, Lee ER, Rathbone DL (1990) Absolute configuration of the product of the acetolactate synthase reaction by a novel method of analysis using acetolactate decarboxylase. J Chem Soc Perkin Trans I 1: 1367–1369

Dailey FE, Cronan JE Jr (1986) Acetohydroxy acid synthase I, a required enzyme for isoleucine and valine biosynthesis in *Escherichia coli* K-12 during growth on acetate as the sole carbon source. J Bacteriol 165: 453–460

de Carvalho LP, Argyrou A, Blanchard JS (2005) Slow-onset feedback inhibition: inhibition of *Mycobacterium tuberculosis* alpha-isopropylmalate synthase by L-leucine. J Am Chem Soc 27: 10004–10005

Delfourne E, Bastide J, Badon R, Rachon A, Genix P (1994) Specificity of plant acetohydroxyacid synthase: Formation of products and inhibition by herbicides. Plant Physiol 32: 473–477

Donadini R, Copeland L (2000) Acetohydroxy acid reductoisomerase of wheat. Aust J Plant Physiol 27: 417–423

Duggleby RG (1997) Identification of an acetolactate synthase small subunit gene in two eukaryotes. Gene 190: 245–249

Duggleby RG (2005) Suicide inhibition of acetohydroxyacid synthase by hydroxypyruvate. J Enzyme Inhib Med Chem 20: 1–4

Duggleby RG, Guddat LW, Pang SS (2004) Structure and properties of acetohydroxyacid synthase. In: Jordan F, Patel MS (eds) Thiamine: catalytic mechanisms in normal and disease states. Marcel Dekker, New York, pp 251–274

Duggleby RG, Kartikasari AER, Wunsch RM, Lee Y-T, Kil M-W, Shin J-Y, Chang S-I (2000) Expression in *Escherichia coli* of a putative human acetohydroxyacid synthase. J Biochem Mol Biol 33: 195–201

Duggleby RG, Pang SS (2000) Acetohydroxyacid synthase. J Biochem Mol Biol 33: 1–36

Duggleby RG, Pang SS, Yu H, Guddat LW (2003) Systematic characterization of mutations in yeast acetohydroxyacid synthase: interpretation of herbicide-resistance data. Eur J Biochem 270: 2895–2904

Dumas R, Biou V, Halgand F, Douce R, Duggleby RG (2001) Enzymology, structure, and dynamics of acetohydroxy acid isomeroreductase. Acc Chem Res 34: 399–408

Durner J, Böger P (1988) Acetolactate synthase from barley (*Hordeum vulgare* L.): Purification and partial characterization. Z Naturforsch 43C: 850–856

Durner J, Böger P (1990) Oligomeric forms of plant acetolactate synthase depend on flavin adenine dinucleotide. Plant Physiol 93: 1027–1031

Durner J, Gailus V, Böger P (1991) New aspects on inhibition of plant acetolactate synthase by chlorsulfuron and imazaquin. Plant Physiol 95: 1144–1149

Durner J, Gailus V, Böger P (1994) The oxygenase reaction of acetolactate synthase detected by chemiluminescence. FEBS Lett 354: 71–73

Durner J, Knorzer OC, Böger P (1993) Ketol-acid reductoisomerase from barley (*Hordeum vulgare*) (Purification, properties, and specific inhibition). Plant Physiol 103: 903–910

Dyda F, Furey W, Swaminathan S, Sax M, Farrenkopf B, Jordan F (1993) Catalytic centers in the thiamin diphosphate dependent enzyme pyruvate decarboxylase at 2.4-Å resolution. Biochemistry 32: 6165–6170

Eggeling I, Cordes C, Eggeling L, Sahm H (1987) Regulation of acetohydroxyacid synthase in *Corynebacterium glutamicum* during fermentation of alfa-ketobutyrate to L-isoleucine. Appl Microbiol Biotechnol 25: 346–351

Elišáková V, Patek M, Holatko J, Nesvera J, Leyval D, Goergen JL, Delaunay S (2005) Feedback-resistant acetohydroxy acid synthase increases valine production in *Corynebacterium glutamicum*. Appl Environ Microbiol 71: 207–213

Engel S, Vyazmensky M, Berkovich D, Barak Z, Chipman DM (2004a) Substrate range of acetohydroxy acid synthase I from *Escherichia coli* in the stereoselective synthesis of alpha-hydroxy ketones. Biotechnol Bioeng 88: 825–831

Engel S, Vyazmensky M, Berkovich D, Barak Z, Merchuk J, Chipman DM (2005) Column flow reactor using acetohydroxyacid synthase I from *Escherichia coli* as catalyst in continuous synthesis of *R*-phenylacetyl carbinol. Biotechnol Bioeng 89: 733–740

Engel S, Vyazmensky M, Geresh S, Barak Z, Chipman D (2003) Acetohydroxyacid synthase: a new enzyme for chiral synthesis of *R*-phenylacetylcarbinol. Biotechnol Bioeng 83: 833–840

Engel S, Vyazmensky M, Vinogradov M, Berkovich D, Bar-Ilan A, Qimron U, Rosiansky Y, Barak Z, Chipman D (2004b) Role of a conserved arginine in the mechanism of acetohydroxyacid synthase. J Biol Chem 279: 24803–24812

Eom SJ, Ahn HJ, Yoon HJ, Lee BI, Bae SH, Baek SH, Suh SW (2002) Crystallization and preliminary X-ray crystallographic analysis of acetohydroxy acid isomeroreductase from *Pseudomonas aeruginosa*. Acta Crystallogr D58: 2145–2146

Eoyang L, Silverman PM (1988) Purification and assays of acetolactate synthase I from *Escherichia coli* K12. Methods Enzymol 166: 435–445

Eoyang L, Silverman PM (1986) Role of small subunit (*ilv*N polypeptide) of acetohydroxyacid synthase I from *Escherichia coli* K-12 in sensitivity of the enzyme to valine inhibition. J Bacteriol 166: 901–904

Eoyang L, Silverman PM (1984) Purification and subunit composition of acetohydroxyacid synthase I from *Escherichia coli* K-12. J Bacteriol 157: 184–189

Falco SC, McDevitt RE, Chui C-F, Hartnett ME, Knowlton S, Mauvais CJ, Smith JK, Mazur BJ (1989) Engineering herbicide-resistant acetolactate synthase. Dev Ind Microbiol 30: 187–194

Feng DF, Doolittle RE (1987) Progressive sequence alignment as a prerequisite to correct phylogenetic trees. J Mol Evol 25: 351–360

Flint DH, Emptage MH, Finnegan MG, Fu W, Johnson MK (1993a) The role and properties of the iron-sulfur cluster in *Escherichia coli* dihydroxy-acid dehydratase. J Biol Chem 268: 14732–14742

Flint DH, Smyk-Randall E, Tuminello JF, Draczynska-Lusiak B, Brown OR (1993b) The inactivation of dihydroxy-acid dehydratase in *Escherichia coli* treated with hyperbaric oxygen occurs because of the destruction of its Fe-S cluster, but the enzyme remains in the cell in a form that can be reactivated. J Biol Chem 268: 25547–25552

Flint DH, Emptage MH (1988) Dihydroxy acid dehydratase from spinach contains a [2Fe–2S] cluster. J Biol Chem 263: 3558–3564

Forlani G, Riccardi G, DeRossi E, DeFelice M (1991) Biochemical evidence for multiple forms of acetohydroxy acid synthase in *Spirulina platensis*. Arch Microbiol 155: 298–302

Foulon V, Antonenkov VD, Croes K, Waelkens E, Mannaerts GP, Van Veldhoven PP, Casteels M (1999) Purification, molecular cloning, and expression of 2-hydroxyphytanoyl-CoA lyase, a peroxisomal thiamine pyrophosphate-dependent enzyme that catalyzes the carbon-carbon bond cleavage during – oxidation of 3-methyl-branched fatty acids. Proc Natl Acad Sci USA 96: 10039–10044

Frank RA, Titman CM, Pratap JV, Luisi BF, Perham RN (2004) A molecular switch and proton wire synchronize the active sites in thiamine enzymes. Science 306: 872–876

Fultz PN, Kemper J (1981) Wild-type isopropylmalate isomerase in *Salmonella typhimurium* is composed of two different subunits. J Bacteriol 148: 210–219

Funke RP, Kovar JL, Logsdon JM Jr, Corrette-Bennett JC, Straus DR, Weeks DP (1999) Nucleus-encoded, plastid-targeted acetolactate synthase genes in two closely related chlorophytes, *Chlamydomonas reinhardtii* and *Volvox carteri* phylogenetic origins and recent insertion of introns. Mol Gen Genet 262: 12–21

Gallagher DT, Gilliland GL, Xiao G, Zondlo J, Fisher KE, Chinchilla D, Eisenstein E (1998) Structure and control of pyridoxal phosphate dependent allosteric threonine deaminase. Structure 6: 465–475

Geier PW, Stahlman PW, Hargett JG (2001) Dose response of weeds and winter wheat to MKH 6561. Weed Sci 49: 788–791

Gerwick BC, Mireles LC, Eilers RJ (1993) Rapid diagnosis of ALS/AHAS-resistant weeds. Weed Technol 7: 519–524

Gerwick BC, Subermanian VI, Loney-Gallant VI, Chander DP (1990) Mechanism of action of the 1,2,4-triazolo (1,5-a) pyrimidines. Pestic Sci 29: 357–364

Glatzer L, Eakin E, Wagner RP (1972) Acetohydroxy acid synthetase with a pH optimum of 7.5 from *Neurospora crassa* mitochondria: characterization and partial purification. J Bacteriol 112: 453–464

Gollop N, Damri B, Barak Z, Chipman DM (1989) Kinetics and mechanism of acetohydroxyacid synthase isozyme III from *Escherichia coli*. Biochemistry 28: 6310–6317

Goto M, Miyahara I, Hirotsu K, Conway M, Yennawar N, Islam MM, Hutson SM (2005) Structural determinants for branched-chain aminotransferase isozyme specific inhibition by the anticonvulsant drug gabapentin. J Biol Chem 280: 37246–37256

Goto M, Miyahara I, Hayashi H, Kagamiyama H, Hirotsu K (2003) Crystal structures of branched-chain amino acid aminotransferase complexed with glutamate and glutarate: true reaction intermediate and double substrate recognition of the enzyme. Biochemistry 42: 3725–3733

Grabau C, Cronan JE Jr (1986) Nucleotide sequence and deduced amino acid sequence of *Escherichia coli* pyruvate oxidase, a lipid-activated flavoprotein. Nucleic Acids Res 14: 5449–5460

Grandoni JA, Marta PT, Schloss JV (1998) Inhibitors of branched-chain amino acid biosynthesis as potential antituberculosis agents. J Antimicrob Chemother 42: 475–482

Grimminger H, Umbarger HE (1979) Acetohydroxy acid synthase I of *Escherichia coli*: purification and properties. J Bacteriol 137: 846–853

Gross SR (1970) Isopropylmalate isomerase (*Neurospora*). Methods Enzymol 17A: 786–790

Gross SR, Burns RO, Umbarger HE (1963) The biosynthesis of leucine. II. The enzymatic isomerization of β-carboxy-β-hydroxyisocaproate and α-hydroxy-β-carboxyisocaproate. Biochemistry 2: 1046–1052

Guardiola J, De Felice M, Iaccarino M (1974) Mutant of *Escherichia coli* K-12 missing acetolactate synthase activity. J Bacteriol 120: 536–538

Hagelstein P, Schulz G (1993) Leucine synthesis in spinach chloroplasts: partial characterization of 2-isopropylmalate synthase. Biol Chem Hoppe Seyler 374: 1105–1108

Halgand F, Wessel PM, Laprevote O, Dumas R (2002) Biochemical and mass spectrometric evidence for quaternary structure modifications of plant threonine deaminase induced by isoleucine. Biochemistry 41: 13767–13773

Halgand F, Vives F, Dumas R, Biou V, Andersen J, Andrieu J-P, Cantegril R, Gagnon J, Douce R, Forest E, Job D (1998) Kinetic and mass spectrophotometric analyses of the interactions between plant acetohydroxy acid isomeroreductase and thiadiazole derivatives. Biochemistry 37: 4773–4781

Haraguchi H, Hamatani Y, Hamada M, Fujii-Tachuno A (1996) Effects of gliotoxin on growth and branched-chain amino acid biosynthesis in plants. Phytochemistry 42: 645–648

Hasson MS, Muscate A, McLeish MJ, Polovnikova LS, Gerlt JA, Kenyon GL, Petsko GA, Ringe D (1998) The crystal structure of benzoylformate decarboxylase at 1.6 Å resolution: diversity of catalytic residues in thiamin diphosphate-dependent enzymes. Biochemistry 37: 9918–9930

Hattori J, Brown D, Mourad G, Labbé H, Ouellet T, Sunohara G, Rutledge R, King J, Miki B (1995) An acetohydroxy acid synthase mutant reveals a single site incolved in multiple herbicide resistance. Mol Gen Genet 246: 419–425

Hattori J, Rutledge R, Labbé H, Brown D, Sunohara G, Miki B (1992) Multiple resistance to sulfonylureas and imidazolinones conferred by and acetohydroxyacid synthase gene with separate mutations for selective resistance. Mol Gen Genet 232: 167–173

Haughn GW, Smith J, Mazur B, Somerville C (1988) Transformation with a mutant *Arabidopsis* acetolactate synthase gene renders tobacco resistant to sulfonylurea herbicides. Mol Gen Genet 211: 266–271

Hawkes TR, Cox JM, Fraser EM, Lewis T (1993) A herbicidal inhibitor of isopropylmalate isomerase. Z Naturforsch 48: 364–368

Hayashi-Iwasaki Y, Oshima T (2000) Purification and characterization of recombinant 3-isopropylmalate dehydrogenases from *Thermus thermophilus* and other microorganisms. Methods Enzymol 324: 301–322

Hershey HP, Schwartz LJ, Gale JP, Abell LM (1999) Cloning and functional expression of the small subunit of acetolactate synthase from *Nicotiana plumbaginifolia*. Plant Mol Biol 40: 795–806

Hervieu F, Vaucheret H (1996) A single amino acid change in acetolactate synthase confers resistance to valine in tobacco. Mol Gen Genet 251: 220–224

Hill CM, Duggleby RG (1998) Mutagenesis of *Escherichia coli* acetohydroxyacid synthase isoenzyme II and characterization of three herbicide-insensitive forms. Biochem J 335: 653–661

Hill CM, Pang SS, Duggleby RG (1997) Purification of *Escherichia coli* acetohydroxyacid synthase isoenzyme II and reconstitution of active enzyme from its individual pure subunits. Biochem J 327: 891–898

Hill RK, Yan S, Arfin SM (1973) Enzymatic discrimination between diastereotopic enol faces in the dehydrase step of valine biosynthesis. J Am Chem Soc 95: 7857–7859

Holzer H, Goedde HW, Goeggel KH, Ulrich B (1960) Identification of alpha-hydroxyethyl thiamine pyrophosphate (“active acetaldehyde”) as an intermediate in the oxidation of pyruvate by pyruvic oxidase from yeast mitochondria. Biochem Biophys Res Commun 3: 599–602

Hsu YP, Kohlhaw GB (1980) Leucine biosynthesis in *Saccharomyces cerevisiae* Purification and characterization of beta-isopropylmalate dehydrogenase. J Biol Chem 255: 7255–7260

Hu Z, Poulton JE (1999) Molecular analysis of (R)-(+)-Mandelonitrile lyase microheterogeneity in black cherry. Plant Physiol 119: 1535–1546

Hurley JH, Dean AM (1994) Structure of 3-isopropylmalate dehydrogenase in complex with NAD+: ligand-induced loop closing and mechanism for cofactor specificity. Structure 2: 1007–1016

Huppatz JL, Casida JE (1985) Acetohydroxyacid synthase inhibitors: N-phthalyl valine anilide and related compounds. Z Naturforsch 40c: 652–656

Ibdah M, Bar-Ilan A, Livnah O, Schloss JV, Barak Z, Chipman DM (1996) Homology modeling of the structure of bacterial acetohydroxy acid synthase and examination of the active site by site-directed mutagenesis. Biochemistry 35: 16282–16291

Imada K, Inagaki K, Matsunami H, Kawaguchi H, Tanaka H, Tanaka N, Namba K (1998) Structure of 3-isopropylmalate dehydrogenase

in complex with 3-isopropylmalate at 2.0 Å resolution: the role of Glu88 in the unique substrate-recognition mechanism. Structure 6: 971–982

Imada K, Sato M, Tanaka N, Katsube Y, Matsuura Y, Oshima T (1991) Three-dimensional structure of a highly thermostable enzyme, 3-isopropylmalate dehydrogenase of *Thermus thermophilus* at 2.2 Å resolution. J Mol Biol 222: 725–738

Jordan F (2003) Current mechanistic understanding of thiamin diphosphate-dependent enzymatic reactions. Nat Prod Rep 20: 184–201

Jordan F, Zhang Z, Sergienko E (2002) Spectroscopic evidence for participation of the 1′,4′-imino tautomer of thiamin diphosphate in catalysis by yeast pyruvate decarboxylase. Bioorg Chem 30: 188–198

Jordan F, Li H, Brown A (1999) Remarkable stabilization of zwitterionic intermediates may account for a billion-fold rate acceleration by thiamin diphosphate-dependent decarboxylases. Biochemistry 38: 6369–6373

Jordan F, Mariam YF (1978) N1′-Methylthiaminium diiodide. Model study on the effect of a coenzyme bound positive charge on reaction mechanisms requiring thiamin pyrophosphate. J Am Chem Soc 100: 2534–2541

Joutel A, Ducros A, Alamowitch S, Cruaud C, Domenga V, Marechal E, Vahedi K, Chabriat H, Bousser MG, Tournier-Lasserve E (1996) A human homolog of bacterial acetolactate synthase genes maps within the CADASIL critical region. Genomics 38: 192–198

Kern D, Kern G, Neef H, Tittmann K, Killenberg-Jabs M, Wickner C, Schneider G, Hübner G (1997) How thiamine diphosphate is activated in enzymes. Science 275: 67–69

Kiritani K, Narise S, Wagner RP (1966) The reductoisomerase of *Neurospora crassa*. J Biol Chem 241: 2047–2051

Kleschick WA, Gerwick BC, Carson CM, Monte WT, Snider SW (1992) DE-498, a new acetolactate synthase inhibiting herbicide with multicrop selectivity. J Agric Food Chem 40: 1083–1085

Kohlhaw GB (1988a) Isopropylmalate dehydratase from yeast. Methods Enzymol 166: 423–429

Kohlhaw GB (1988b) Isopropylmalate synthase from yeast. Methods Enzymol 166: 414–423

Kohlhaw GB (2003) Leucine biosynthesis in fungi: entering metabolism through the backdoor. Microbiol Mol Biol Rev 67: 1–15

Koon N, Squire CJ, Baker EN (2004a) Crystallization and preliminary X-ray analysis of alpha-isopropylmalate synthase from *Mycobacterium tuberculosis*. Acta Crystallogr D 60: 1167–1169

Koon N, Squire CJ, Baker EN (2004b) Crystal structure of LeuA from *Mycobacterium tuberculosis*, a key enzyme in leucine biosynthesis. Proc Natl Acad Sci USA 101: 8295–8300

Kopecký J, Janata J, Pospisil S, Felsberg J, Spizek J (1999) Mutations in 2 distinct regions of acetolactate synthase regulatory subunit from *Streptomyces cinnamonensis* result in the lack of sensitivity to end-product inhibition. Biochem Biophys Res Commun 266: 162–166

Landstein D, Chipman DM, Arad SM, Barak Z (1990) Acetohydroxy acid synthase activity in *Chlorella emersonii* under auto- and heterotrophic growth conditions. Plant Physiol 94: 614–620

LaRossa RA, Schloss JV (1984) The sulfonylurea herbicide sulfometuron methyl is an extremely potent and selective inhibitor of acetolactate synthase in *Salmonella typhimurium*. J Biol Chem 259: 8753–8757

Lawther RP, Calhoun DH, Adams CW, Hauser CA, Gray J, Hatfield W (1981) Molecular basis of valine resistance in *Escherichia coli* K-12. Proc Natl Acad Sci USA 78: 922–925

Lawther RP, Wek RC, Lopes JM, Pereira R, Taillon BE, Hatfield GW (1987) The complete nucleotide sequence of the *ilv*GMEDA operon of *Escherichia coli* K-12. Nucleic Acids Res 15: 2137–2155

Le DT, Yoon MY, Kim YT, Choi JD (2004) Homology modeling of the structure of tobacco acetohydroxy acid synthase and examination of the active site by site-directed mutagenesis. Biochem Biophys Res Commun 317: 930–938

Le DT, Yoon MY, Kim YT, Choi JD (2005) Roles of three well-conserved arginine residues in mediating the catalytic activity of tobacco acetohydroxy acid synthase. J Biochem (Tokyo) 138: 35–40

Lee KY, Townsend J, Tepperman J, Black M, Chui CF, Mazur B, Bunsmuir P, Bedbrook J (1988) The molecular basis of sulfonylurea herbicide resistance in tobacco. EMBO J 7: 1241–1248

Lee Y-T, Duggleby RG (2001) Identification of the regulatory subunit of *Arabidopsis thaliana* acetohydroxyacid synthase and reconstitution with its catalytic subunit. Biochemistry 40: 6836–6844

Lee Y-T, Duggleby RG (2002) Regulatory interactions in *Arabidopsis thaliana* acetohydroxyacid synthase. FEBS Lett 512: 180–184

Lee Y-T, Duggleby RG (2006) Mutations in the regulatory subunit of yeast acetohydroxyacid synthase affect its activation by MgATP. Biochem J 395: 331–336

Lee Y-T, Ta HT, Duggleby RG (2005) Cyclopropane-1,1-dicarboxylate is a slow-, tight-binding inhibitor of rice ketol-acid reductoisomerase. Plant Sci 168: 1035–1040

Lee Y-T, Chang AK, Duggleby RG (1999) Effect of mutagenesis at serine 653 of *Arabidopsis thaliana* acetohydroxyacid synthase on the sensitivity to imidazolinone and sulfonylurea herbicides. FEBS Lett 452: 341–345

Lee-Peng FC, Hermodson MA, Kohlhaw GB (1979) Transaminase B from *Escherichia coli*: quaternary structure, amino-terminal sequence, substrate specificity, and absence of a separate valine-alpha-ketoglutarate activity. J Bacteriol 139: 339–345

Levitt G (1978) Herbicidal sulfonamides. US Patent 4127405

Leyval D, Uy D, Delaunay S, Goergen JL, Engasser JM (2003) Characterisation of the enzyme activities involved in the valine biosynthetic pathway in a valine-producing strain of *Corynebacterium glutamicum*. J Biotechnol 104: 241–252

Lie MA, Celik L, Jørgensen KA, Schiøtt B (2005) Cofactor activation and substrate binding in pyruvate decarboxylase. Insights into the reaction mechanism from molecular dynamics simulations. Biochemistry 44: 14792–14806

Los M (1984) o-(5-oxo-2-imidazolin-2-yl)arylcarboxylates: A new class of herbicides. In: Magee PS, Kohn GK, Menn JJ (eds) Pesticide synthesis through rational approaches. American Chemical Society, New York, pp 29–44

Magee PT, deRobichon-Szulmajster H (1968) The regulation of isoleucine-valine biosynthesis in *Saccharomyces cerevisiae* 3. Properties and regulation of the activity of acetohydroxyacid synthetase. Eur J Biochem 3: 507–511

Mazur BJ, Chui C-K, Smith JK (1987) Isolation and characterization of plant genes coding for acetolactate synthase, the target enzyme for two classes of herbicides. Plant Physiol 85: 1110–1117

McCourt JA (2004) Structural and mechanistic studies on acetohydroxyacid synthase and related enzymes. PhD thesis, The University of Queensland, Brisbane, Australia

McCourt JA, Duggleby RG (2005) How an enzyme answers multiple choice questions. Trends Biochem Sci 30: 222–225

McCourt JA, Pang SS, Duggleby RG, Guddat LW (2005) Elucidating the specificity of binding of sulfonylurea herbicides to acetohydroxyacid synthase. Biochemistry 44: 2330–2338

McCourt JA, Pang SS, King-Scott J, Duggleby RG, Guddat LW (2006) Herbicide binding sites revealed in the structure of plant acetohydroxyacid synthase. Proc Natl Acad Sci USA 103: 569–573

McFadden HG, Huppatz JL, Kennard CHL (1993) Vinylogous sulfonylureas: a new class of acetohydroxyacid synthase inhibitors incorporating a large bridging moiety. Z Naturforsch 48c: 356–363

Mendel S, Elkayam T, Sella C, Vinogradov V, Vyazmensky M, Chipman DM, Barak Z (2001) Acetohydroxyacid synthase: A proposed structure for regulatory subunits supported by evidence from mutagenesis. J Mol Biol 307: 465–477

Mendel S, Vinogradov M, Vyazmensky M, Chipman DM, Barak Z (2003) The N-terminal domain of the regulatory subunit is sufficient for

complete activation of acetohydroxyacid synthase III from *Escherichia coli*. J Mol Biol 325: 275–284

Miflin BJ (1971) Cooperative feedback control of barley acetohydroxyacid synthetase by leucine, isoleucine, and valine. Arch Biochem Biophys 146: 542–550

Milano A, De Rossi E, Zanaria E, Barbierato L, Ciferri O, Riccardi G (1992) Molecular characterization of the genes encoding acetohydroxy acid synthase in the cyanobacterium *Spirulina platensis*. J Gen Microbiol 138: 1399–1408

Moore IF, Kluger R (2002) Substituent effects in carbon-nitrogen cleavage of thiamin derivatives. Fragmentation pathways and enzymic avoidance of cofactor destruction. J Am Chem Soc 124: 1669–1673

Mourad G, King J (1992) Effect of four classes of herbicides on growth and acetolactate-synthase activity in several variants of *Arabidopsis thaliana*. Planta 188: 491–497

Mourad G, Williams D, King J (1995) A double mutant allele, *csr1-4*, of *Arabidopsis thaliana* encodes an acetolactate synthase with altered kinetics. Planta 196: 64–68

Mrachko GT, Chunduru SK, Calvo KC (1992) The pH dependence of the kinetic parameters of ketol acid reductoisomerase indicates a proton shuttle mechanism for alkyl migration. Arch Biochem Biophys 294: 446–453

Muhitch MJ, Shaner DL, Stidham M (1987) Imidazolinones and acetohydroxyacid synthase from higher plants. Plant Physiol 83: 451–456

Müller YA, Schulz GE (1993) Structure of the thiamine-and flavin-dependent enzyme pyruvate oxidase. Science 259: 965–967

Müller YA, Schumacher G, Rudolph R, Schulz G (1994) The refined structures of a stabilized and of wild-type pyruvate oxidase from *Lactobacillus plantarum.* J Mol Biol 237: 315–335

Muramatsu N, Nosoh Y (1976) Some catalytic and molecular properties of threonine deaminase from *Bacillus stearothermophilus*. J Biochem 80: 485–490

Namgoong SK, Lee HJ, Kim YS, Shin J-H, Che J-K, Jang DY, Kim G-S, Yoo JW, Kange M-K, Kil M-W, Choi J-D, Chang S-I (1999) Synthesis of quinoline-linked triazolopyrimidine analogues and their interactions with the recombinant tobacco acetolactate synthase. Biochem Biophys Res Commun 258: 797–801

Nemeria N, Baykal A, Joseph E, Zhang S, Yan Y, Furey W, Jordan F (2004) Tetrahedral intermediates in thiamin diphosphate-dependent decarboxylations exist as a 1′,4′-imino tautomeric form of the coenzyme, unlike the Michaelis complex or the free coenzyme. Biochemistry 43: 6565–6575

Newhouse K, Singh B, Shaner D, Stidham M (1991) Mutations in corn (*Zea mays* L.) conferring resistance to imidazolinone herbicides. Theor Appl Genet 83: 65–70

Oda Y, Nakano Y, Kitaoka S (1982) Properties and regulation of valine-sensitive acetolactate synthase from mitochondria of *Euglena gracilis*. J Gen Microbiol 128: 1211–1216

Oh K-J, Park E-J, Yoon M-Y, Han T-R, Choi J-D (2001) Roles of histidine residues in tobacco acetolactate synthase. Biochem Biophys Res Commun 282: 1237–1243

Okada K, Hirotsu K, Hayashi H, Kagamiyama H (2001) Structures of *Escherichia coli* branched-chain amino acid aminotransferase and its complexes with 4-methylvalerate and 2-methylleucine: induced fit and substrate recognition of the enzyme. Biochemistry 40: 7453–7463

Okada K, Hirotsu K, Sato M, Hayashi H, Kagamiyama H (1997) Three-dimensional structure of Escherichia coli branched-chain amino acid aminotransferase at 2.5 Å resolution. J Biochem (Tokyo) 121: 637–641

Okeke IN, Laxminarayan R, Bhutta ZA, Duse AG, Jenkins P, O'Brien TF, Pablos-Mendez A, Klugman KP (2005) Antimicrobial resistance in developing countries. Part I: recent trends and current status. Lancet Infect Dis 5: 568–580

Ortega F, Bastide J, Hawkes TR (1996) Comparison between thifensulfuron methyl-induced inactivation of barley acetohydroxyacid synthase and Escherichia coli acetohydroxyacid synthase isozyme II. Pestic Biochem Physiol 56: 231–242

Ott KH, Kwagh J-G, Stockton GW, Sidorov V, Kakefuda G (1996) Rational molecular design and genetic engineering of herbicide resistant crops by structure modeling and site-directed mutagenesis of acetohydroxyacid synthase. J Mol Biol 263: 359–368

Pang SS, Duggleby RG (1999) Expression, purification, characterization, and reconstitution of the large and small subunits of yeast acetohydroxyacid synthase. Biochemistry 38: 5222–5231

Pang SS, Duggleby RG (2001) Regulation of yeast acetohydroxyacid synthase by valine and ATP. Biochem J 357: 749–757

Pang SS, Duggleby RG, Guddat LW (2002) Crystal structure of yeast acetohydroxyacid synthase: A target for herbicidal inhibitors. J Mol Biol 317: 249–262

Pang SS, Duggleby RG, Schowen RL, Guddat LW (2004a) The crystal structures of *Klebsiella pneumoniae* acetolactate synthase with enzyme-bound cofactor and with an unusual intermediate. J Biol Chem 279: 2242–2253

Pang SS, Guddat LW, Duggleby RG (2001) Crystallization of the catalytic subunit of *Saccharomyces cerevisiae* acetohydroxyacid synthase. Acta Crystallogr D57: 1321–1323

Pang SS, Guddat LW, Duggleby RG (2003) Molecular basis of sulfonylurea herbicide inhibition of acetohydroxyacid synthase. J Biol Chem 278: 7639–7644

Pang SS, Guddat LW, Duggleby RG (2004b) Crystallization of *Arabidopsis thaliana* acetohydroxyacid synthase in complex with the sulfonylurea herbicide chlorimuron ethyl. Acta Crystallogr D60: 1153–1555

Pátek M, Krumbach K, Eggeling L, Sahm H (1994) Leucine synthesis in *Corynebacterium glutamicum*: enzyme activities, structure of leuA, and effect of leuA inactivation on lysine synthesis. Appl Environ Microbiol 60: 133–140

Phalip V, Schmitt P, Divies C (1995) Purification and characterization of the catabolic alpha-acetolactate synthase from *Leuconostoc mesenteroides* subsp. *cremonis*. Curr Microbiol 31: 316–321

Pletcher J, Sax M (1972) Crystal and molecular structure of thiamine pyrophosphate hydrochloride. J Am Chem Soc 94: 3998–4005

Polaina J (1984) Cloning of the *ilv*2, *ilv*3 and *ilv*5 genes of *Saccharomyces cerevisiae*. Carlsberg Res Commun 49: 577–584

Porat I, Vinogradov M, Vyazmensky M, Chung-Dar L, Chipman DM, Abdelal AT, Barak Z (2004) Cloning and characterization of acetohydroxyacid synthase from *Bacillus stearothermophilus*. J Bacteriol 186: 570–574

Poulsen C, Stougaard P (1989) Purification and properties of *Saccharomyces cerevisiae* acetolactate synthase from recombinant *Escherichia coli*. Eur J Biochem 185: 433–439

Proteau G, Silver M (1991) Acetohydroxyacid synthetase of *Thiobacillus acidophilus*. Biomed Lett 46: 121–127

Radhakrishnan AN, Snell EE (1960) Biosynthesis of valine and isoleucine II. Formation of α-acetolactate and α-aceto-α-hydroxybutyrate in *Neurospora crassa* and *Escherichia coli*. J Biol Chem 235: 2316–2321

Rathinasabapathi B, Williams D, King J (1990) Altered feedback sensitivity to valine, leucine and isoleucine of acetolactate synthase from herbicide-resistant variants of *Datura innoxia*. Plant Sci 67: 1–6

Ray T (1984) Site of action of chlorsulfuron. Plant Physiol 75: 827–831

Reith M, Munholland J (1993) Two amino-acid biosynthetic genes are encoded on the plastid genome of the red alga *Porphyra umbilicalis*. Curr Genet 23: 59–65

Relton JM, Wallsgrove RM, Bourgin J-P, Bright SWJ (1986) Altered feedback sensitivity of acetohydroxyacid synthase from valine-resistant mutants of tobacco (*Nicotiana tabacum L.*). Planta 169: 46–50

Riccardi G, DeRossi E, Nielsen E, DeFelice M (1988) Detection and characterization of acetohydroxy acid synthase in *Spirulina platensis*. FEMS Microbiol Lett 49: 13–17

Roux C, Delfourne E, Bastide J (1996) Activation and inhibition of maize acetohydroxyacid synthase by thiamine analogues. Plant Physiol Biochem 34: 293–299

Rutledge RG, Ouellet T, Hattori J, Miki BL (1991) Molecular characterization and genetic origin of the *Brassica napus* acetohydroxyacid synthase multigene family. Mol Gen Genet 229: 31–40

Sathasivan K, Haughn GW, Murai N (1991) Molecular basis of imidazolinone herbicide resistance in *Arabidopsis thaliana* var Columbia. Plant Physiol 97: 1044–1050

Satyanarayana T, Umbarger HE, Lindegren G (1968) Biosynthesis of branched-chain amino acids in yeast: correlation of biochemical blocks and genetic lesions in leucine auxotrophs. J Bacteriol 96: 2012–2017

Schloss JV (1984) Interaction of the herbicide sulfometuron methyl with acetolactate synthase: a slow binding inhibitor. In: Bray RC, Engel PC, Mayhew SG (eds) Flavins and flavoproteins. Walter de Gruyter, Berlin, pp 737–740

Schloss JV (1990) Acetolactate synthase, mechanism of action and its herbicide binding site. Pestic Sci 29: 283–292

Schloss JV (1991) Acetolactate synthase. In: Müller F (ed) Chemistry and biochemistry of flavoenzymes vol III. CRC Press, Boca Raton, pp 531–542

Schloss JV, Aulabaugh A (1988) Acetolactate synthase and ketol-acid reductoisomerase: a search for a reason and a reason for search. In: Barak Z, Chipman DM, Schloss JV (eds) Biosynthesis of branched chain amino acids. VCH Press, Weinheim, pp 329–356

Schloss JV, Ciskanik M, Van Dyk DE (1988) Origin of the herbicide binding site of acetolactate synthase. Nature 331: 360–362

Schloss JV, Van Dyk DE (1988) Acetolactate synthase isozyme II from *Salmonella typhimurium*. Methods Enzymol 166: 445–454

Schloss JV, Van Dyk DE, Vasta JF, Kutny RM (1985) Purification and properties of *Salmonella typhimurium* acetolactate synthase isozyme II from *Escherichia coli* HB101/pDU9. Biochemistry 24: 4952–4959

Schonbrunn-Hanebeck E, Laber B, Amrhein N (1990) Slow-binding inhibition of the *Escherichia coli* pyruvate dehydrogenase multienzyme complex by acetylphosphinate. Biochemistry 29: 4880–4885

Schulz A, Sponemann P, Kocher H, Wengenmayer F (1988) The herbicidally active experimental compound Hoe 704 is a potent inhibitor of the enzyme acetolactate reductoisomerase. FEBS Lett 238: 375–378

Shaner DL, Anderson PC, Stidham MA (1984) Imidazolinones: potent inhibitors of acetohydroxyacid synthase. Plant Physiol 76: 545–546

Shaner DL, Singh BK (1997) Acetohydroxyacid synthase inhibitors. In: Roe M, Burton JD, Kuhr RJ (eds) Herbicide activity: Toxicology, biochemistry and molecular biology. IOS Press, Amsterdam, pp 69–110

Shim H-O, Kim D-W, Chang S-I, Choi JD (1995) The interaction of barley acetolactate synthase with 4,6-dimethoxypyrimidine inhibitors. J Biochem Mol Biol 28: 471–476

Shin H-J, Chong C-K, Chang S-K, Choi J-D (2000) Structural and functional role of cysteinyl residues in tobacco acetolactate synthase. Biochem Biophys Res Commun 271: 801–806

Shimizu T, Nakayama I, Nakao T, Nezu Y, Abe H (1994a) Inhibition of plant acetolactate synthase by herbicides, pyrimidinylsalicylic acids. J Pestic Sci 19: 59–67

Shimizu T, Nakayama I, Wada N, Nakao T, Abe H (1994b) Kinetic studies on the inhibition of acetolactate synthase by pyrimidinylsalicylic acids. J Pestic Sci 19: 257–266

Sibony M, Michel A, Haas HU, Rubin B, Hurle K (2001) Sulfometuron-resistant *Amaranthus retroflexus*: cross resistance and molecular basis for resistance to acetolactate synthase-inhibiting herbicides. Weed Res 41: 509–522

Singh BK, Shaner DL (1995) Biosynthesis of branched chain amino acids: from test tube to field. Plant Cell 7: 935–944

Singh B, Schmitt G, Lillis M, Hand JM, Misra R (1991) Overexpression of acetohydroxyacid synthase from *Arabidopsis* as an inducible fusion protein in *Escherichia coli*. Plant Physiol 97: 657–662

Singh BK, Stidham MA, Shaner DL (1988) Separation and characterization of two forms of acetohydroxyacid synthase from Black Mexican Sweet Corn cells. J Chrom 444: 251–261

Singh BK, Kefala G, Janowski R, Mueller-Dieckmann C, von Kries JP, Weiss MS (2005) The high-resolution structure of LeuB (Rv2995c) from *Mycobacterium tuberculosis*. J Mol Biol 346: 1–11

Singh B, Szamosi I, Hand M, Mistra R (1992) *Arabidopsis* acetohydroxyacid synthase expressed in *Escherichia coli* is insensitive to the feedback inhibitors. Plant Physiol 99: 821–816

Snoep JL, Teixeira de Mattos MJ, Starrenburg MJC, Hugenholtz J (1992) Isolation, characterization, and physiological role of the pyruvate dehydrogenase complex and alpha-acetolactate synthase of *Lactococcus lactis* subsp. *lactis* bv. Diacetylactis. J Bacteriol 174: 4838–4841

Southan MD, Copeland L (1996) Physical and kinetic properties of acetohydroxyacid synthase from wheat leaves. Physiol Plant 98: 824–832

Squires CH, DeFelice M, Devereux J, Calvo JM (1983) Molecular structure of *ilv*H and its evolutionary relationship to *ilv*G in *Escherichia coli* K12. Nucleic Acids Res 15: 5299–5313

Stidham MA (1991) Herbicidal inhibitors of branched chain amino acid biosynthesis. In: Baker NR, Percival MP (eds) Herbicides. Elsevier, Amsterdam, pp 247–266

Stidham MA, Singh BK (1991) Imidazolinone-acetohydroxyacid synthase interactions. In: Shaner DL, O'Connor SL (eds) The imidazolinone herbicides. CRC Press, Boca Raton, pp 71–90

Størmer FC, Umbarger HE (1964) The requirement for flavine adenine dinucleotide in the formation of acetolactate by *Salmonella typhimurium* extracts. Biochem Biophys Res Commun 17: 587–592

Strumilo S, Dobrzyn P, Czerniecki J, Tylicki A (2004) Suicidal dephosphorylation of thiamine pyrophosphate coupled with pyruvate dehydrogenase complex. Ital J Biochem 53: 131–134

Subramanian MV, Loney-Gallant V, Dias JM, Mireles LC (1991) Acetolactate synthase inhibiting herbicides bind to the regulatory site. Plant Physiol 96: 310–313

Takenaka S, Kuwana H (1972) Control of acetohydroxy acid synthetase in *Neurospora crassa*. J Biochem (Tokyo) 72: 1139–1145

Taylor WR (2000) A deeply knotted protein structure and how it might fold. Nature 406: 916–919

Thomazeau K, Dumas R, Halgand F, Forest E, Douce R, Biou V (2000) Structure of spinach acetohydroxyacid isomeroreductase complexed with its reaction product dihydroxymethylvalerate, manganese and (phospho)-ADP-ribose. Acta Crystallogr D56: 389–397

Tittmann K, Golbik R, Ghisla S, Hübner G (2000) Mechanism of elementary catalytic steps of pyruvate oxidase from *Lactobacillus plantarum*. Biochemistry 39: 10747–10754

Tittmann K, Golbik R, Uhlemann K, Khailova L, Schneider G, Patel M, Jordan F, Chipman DM, Duggleby RG, Hübner G (2003) NMR analysis of covalent intermediates in thiamin diphosphate enzymes. Biochemistry 42: 7885–7891

Tittmann K, Neef H, Golbik R, Hübner G, Kern D (2005a) Kinetic control of thiamin diphosphate activation in enzymes studied by proton-nitrogen correlated NMR spectroscopy. Biochemistry 44: 8697–8700

Tittmann K, Schröder K, Golbik R, McCourt J, Kaplun A, Duggleby RG, Barak Z, Chipman DM, Hübner G (2004) Electron transfer in acetohydroxy acid synthase as a side reaction of catalysis. Implications for the reactivity and partitioning of the carbanion/enamine form of (alpha-hydroxyethyl)thiamin diphosphate in a "nonredox" flavoenzyme. Biochemistry 43: 8652–8661

Tittmann K, Vyazmensky M, Hübner G, Barak Z, Chipman DM (2005b) The carboligation reaction of acetohydroxyacid synthase II: steady-

state intermediate distributions in wild type and mutants by NMR. Proc Natl Acad Sci USA 102: 553–558

Tranel PJ, Wright TR (2002) Resistance to ALS-inhibiting herbicides: what have we learned? Weed Sci 50: 700–712

Tsuchiya D, Sekiguchi T, Takenaka A (1997) Crystal structure of 3-isopropylmalate dehydrogenase from the moderate facultative thermophile, *Bacillus coagulans*: two strategies for thermostabilization of protein structures. J Biochem (Tokyo) 122: 1092–1104

Tyagi R, Duquerroy S, Navaza J, Guddat LW, Duggleby RG (2005a) The crystal structure of a bacterial Class II ketol-acid reductoisomerase: domain conservation and evolution. Prot Sci 14: 3089–3100

Tyagi R, Lee Y-T, Guddat LW, Duggleby RG (2005b) Probing the mechanism of the bifunctional enzyme ketol-acid reductoisomerase by site-directed mutagenesis of the active site. FEBS J 272: 593–602

Umbarger HE (1996) Biosynthesis of the branched chain amino acids. In: Neidhardt FC, Curtiss R III, Ingraham JL, Lin ECC, Low KB, Magasanik B, Reznikokk WS, Riley M, Schaechter M, Umbarger HE (eds) *Escherichia coli* and *Salmonella*: cellular and molecular biology. American Society for Microbiology, Washington DC, pp 442–457

Umbarger HE, Brown B (1958) Isoleucine and valine metabolism in *Escherichia coli*. VIII. The formation of acetolactate. J Biol Chem 233: 1156–1160

Vyazmensky M, Barak Z, Chipman DM, Eichler J (2000) Characterization of acetohydroxyacid synthase activity in the archaeon *Haloferax volcanii*. Comp Biochem Physiol B Biochem Mol Biol 125: 205–210

Vyazmensky M, Sella C, Barak Z, Chipman DM (1996) Isolation and characterization of subunits of acetohydroxy acid synthase isozyme III and reconstitution of the holoenzyme. Biochemistry 35: 10339–10346

Wallon G, Kryger G, Lovett ST, Oshima T, Ringe D, Petsko GA (1997a) Crystal structures of *Escherichia coli* and *Salmonella typhimurium* 3-isopropylmalate dehydrogenase and comparison with their thermophilic counterpart from *Thermus thermophilus*. J Mol Biol 266: 1016–1031

Wallon G, Yamamoto K, Kirino H, Yamagishi A, Lovett ST, Petsko GA, Oshima T (1997b) Purification, catalytic properties and thermostability of 3-isopropylmalate dehydrogenase from *Escherichia coli*. Biochim Biophys Acta 1337: 105–112

Washabaugh MW, Jencks WP (1988) Thiazolium C(2)-proton exchange: structure-reactivity correlations and the pKa of thiamin C(2)–H revisited. Biochemistry 27: 5044–5053

Washabaugh MW, Yang CC, Hollenbach AD, Chen P (1993) Hydrolysis of thiamin: evidence for rate-limiting breakdown of the tricyclic dihydrothiachromine intermediate in neutral aqueous solution. Bioorg Chem 21: 170–191

Weinstock O, Sella C, Chipman DM, Barak Z (1992) Properties of subcloned subunits of bacterial acetohydroxy acid synthases. J Bacteriol 174: 5560–5566

Wek RC, Hauser CA, Hatfield WH (1985) The nucleotide sequence homologies of the acetohydroxy acid synthase isozymes. Nucleic Acids Res 13: 3995–4010

Wessel PM, Graciet E, Douce R, Dumas R (2000) Evidence for two distinct effector-binding sites in threonine deaminase by site-directed mutagenesis, kinetic, and binding experiments. Biochemistry 39: 15136–15143

Wiersma PA, Hachey JE, Crosby WL, Moloney MM (1990) Specific truncations of an acetolactate synthase gene from *Brassica napus* efficiently complement *ilv*B/*ilv*G mutants of *Salmonella typhimurium*. Mol Gen Genet 224: 155–159

Wittenbach VA, Teaney PW, Hanna WS, Rayner DR, Schloss JV (1994) Herbicidal activity of an isopropylmalate dehydrogenase inhibitor. Plant Physiol 106: 321–328

Wu K, Mourad G, King J (1994) A valine-resistant mutant of *Arabidopsis thaliana* displays an acetolactate synthase with altered feedback control. Planta 192: 249–255

Xing R, Whitman WB (1994) Purification and characterization of the oxygen-sensitive acetohydro*xy* acid synthase from the archaebacterium *Methanococcus aeolicus*. J Bacteriol 176: 1207–1213

Xing RY, Whitman WB (1987) Sulfometuron methyl-sensitive and -resistant acetolactate synthases of the achaebacteria Methanococcus spp. J Bacteriol 169: 4486–4492

Xing RY, Whitman WB (1991) Characterization of enzymes of the branched-chain amino acid biosynthetic pathway in *Methanococcus* spp. J Bacteriol 173: 2086–2092

Xing RY, Whitman WB (1992) Characterization of amino acid aminotransferases of *Methanococcus aeolicus*. J Bacteriol 174: 541–548

Yang JH, Kim SS (1993) Purification and characterization of the valine sensitive acetolactate synthase from *Serratia marcescens* ATCC 25419. Biochim Biophys Acta 1157: 178–184

Yasutake Y, Yao M, Sakai N, Kirita T, Tanaka I (2004) Crystal structure of the *Pyrococcus horikoshii* isopropylmalate isomerase small subunit provides insight into the dual substrate specificity of the enzyme. J Mol Biol 344: 325–333

Yennawar NH, Conway ME, Yennawar HP, Farber GK, Hutson SM (2002) Crystal structures of human mitochondrial branched chain aminotransferase reaction intermediates: ketimine and pyridoxamine phosphate forms. Biochemistry 41: 11592–11601

Yennawar N, Dunbar J, Conway M, Hutson S, Farber G (2001) The structure of human mitochondrial branched-chain aminotransferase. Acta Crystallogr D57: 506–515

Yoon T-Y, Chung S-M, Chang S-I, Yoon M-Y, Hahn T-R, Choi J-D (2002) Roles of lysine 219 and 255 residues in tobacco acetolactate synthase. Biochem Biophys Res Commun 293: 433–439

Zhang S, Zhou L, Nemeria N, Yan Y, Zhang Z, Zhou Y, Jordan F (2005) Evidence for dramatic acceleration of a C–H bond ionization rate in thiamin diphosphate enzymes by the protein environment. Biochemistry 44: 2237–2243

Zohar Y, Einav U, Chipman DM, Barak Z (2003) Acetohydroxyacid synthase *Mycobacterium avium* and its inhibition by sulfonylureas and imidazolinones. Biochem Biophys Acta 1649: 97–105

Author's address: Dr. Ronald G. Duggleby, School of Molecular and Microbial Sciences, University of Queensland, Brisbane, Qld 4072, Australia,
Fax: +61-7 3365 4699, E-mail: ronald.duggleby@uq.edu.au

Verleger: Springer-Verlag GmbH, Sachsenplatz 4–6, 1201 Wien, Austria – Herausgeber: Prof. Dr. Gert Lubec, Universitäts-Kinderklinik, Währinger Gürtel 18–20, 1090 Wien, Austria – Redaktion: Sachsenplatz 4–6, 1201 Wien, Austria – Hersteller: Satz und Umbruch: Thomson Press (India) Ltd., Chennai; Offsetdruck: Novographic Druck G.m.b.H., Sagedergasse 29, 1120 Wien, Austria – Verlagsort: Wien – Herstellungsort Wien – Printed in Austria.